Aspects of Neutrino Physics in the Early Universe

Ph.D. Thesis

Steen Hannestad

Institute of Physics and Astronomy
University of Aarhus

October 1997

Contents

Preface

The present thesis is a summation of the work carried out during my Ph.D. study. The bulk of the work has been performed in collaboration with my supervisor Jes Madsen at the Institute of Physics and Astronomy at the University of Aarhus. However, some of the work has been done during a six month stay at the Max Planck Institut für Physik in Munich during the spring and summer of 1997, where I also had the pleasure of collaborating with Georg Raffelt in the field of supernova neutrino physics.

Chapters 1-4 contain an introduction to various key issues connected with neutrino physics and Big Bang nucleosynthesis. Chapters 5-8 are essentially reprints of papers as described below.

Finally there is a thesis conclusion in Chapter 9 and an outlook to possible future work in Chapter 10. There are three appendices at the end, appendices A and B contain various mathematical details and Appendix C contains a brief summary of the thesis work.

Note that throughout I use natural units where $c = \hbar = k_B = 1$.

List of Publications

I) S. Hannestad and J. Madsen, *Neutrino Decoupling in the Early Universe*, Published in Phys. Rev. D **52**, 1764 (1995).

II) S. Hannestad and J. Madsen, *Nucleosynthesis and the Mass of the Tau-Neutrino*, Published in Phys. Rev. Lett. **76**, 2848 (1996). Erratum published in Phys. Rev. Lett. **77**, 5148 (1996).

III) S. Hannestad and J. Madsen, *Nucleosynthesis and the Mass of the Tau-Neutrino Revisited*, Published in Phys. Rev. D **54**, 7894 (1996).

IV) S. Hannestad and J. Madsen, *A Cosmological Three Level Neutrino Laser*, Published in Phys. Rev. D **55**, 4571 (1997).

V) S. Hannestad, *Tau Neutrino Decays and Big Bang Nucleosynthesis*, accepted for publication in Phys. Rev. D.

VI) S. Hannestad, *Can Neutrinos be Majorana Particles?*, hep-ph/9701216 (not intended for publication).

VII) S. Hannestad and G. Raffelt, *Supernova Neutrino Opacity from Inverse Nucleon-Nucleon Bremsstrahlung*, in preparation.

The contents of paper I have been described in detail in Chapter 5, papers II and III have been summarised in Chapter 6, paper IV is contained in Chapter 7 and, finally, Chapter 8 describes paper V. Some of the contents of paper VI have been included in Chapter 4. Note that paper VII about supernova neutrino physics has not been included in the thesis. The field it covers is somewhat disjoint from that of the thesis and for this reason I have left it out.

Chapter I

Introduction

One of the most succesful areas of modern physics is the interface between particle physics and astrophysics. This field includes such phenomena as supernovae, active galactic nuclei and, perhaps most notably, the early Universe. It is also a relatively new field that has only existed for less than 50 years, so that there are still big "white spots" left on the map, making it a very interesting field of research.

The present thesis deals with different aspects of the physics of the particles called neutrinos in the early Universe, especially in connection with the formation of light elements.

1.1 Neutrinos

Neutrinos are chargeless spin-1/2 fermions belonging to the family of leptons. There are three known species of neutrinos corresponding to the three known charged leptons. They are grouped together in three generations

$$\begin{pmatrix} \nu_e \\ e \end{pmatrix} \qquad \begin{pmatrix} \nu_\mu \\ \mu \end{pmatrix} \qquad \begin{pmatrix} \nu_\tau \\ \tau \end{pmatrix},$$

with corresponding antiparticles. These three generations correspond to the three quark generations

$$\begin{pmatrix} u \\ d \end{pmatrix} \qquad \begin{pmatrix} c \\ s \end{pmatrix} \qquad \begin{pmatrix} t \\ b \end{pmatrix}.$$

It is not known whether there are additional generations of fermions, but since the fermion masses increase with generation any new generation would likely be extremely heavy. In any case they would have to be so in order not to have been detected in accelerator experiments.

Neutrinos are unique among the known fermions in that they do not possess electric charge, meaning that they have no electromagnetic interactions at tree level. The only interactions that neutrinos have are weak interactions and since

the weak coupling constant $G_{\rm F}$ is very small, neutrinos interact only very weakly with the other fermions.

Neutrinos can be produced on earth for example in nuclear reactors. However, the most constant neutrino source we have is the Sun, where electron neutrinos are produced by the nuclear burning of hydrogen via the reaction

$$4p \rightarrow {}^4\mathrm{He} + 2e^+ + 2\nu_e, \tag{1.1}$$

yielding a neutrino flux of more than 10^{10} cm^{-2}s^{-1} on earth. The most powerful neutrino sources known are the core collapse (type II) supernovae. They emit a burst of neutrinos from the neutronisation reaction

$$p + e \rightarrow n + \nu_e, \tag{1.2}$$

lasting a few seconds. During this period roughly 10^{53} ergs are emitted in neutrino radiation, giving the supernova a neutrino luminosity comparable to the optical luminosity of the whole visible Universe.

Even though neutrinos are so abundant in the Universe their very weak interactions mean that they are extremely difficult to detect in the laboratory. Typically one needs many tons of detection material to achieve a detection rate of a few per day, even with the huge neutrino flux coming from the Sun.

For the same reason very little is known about the properties of neutrinos. In the standard model of particle physics neutrinos are strictly massless. However, there is no *a priori* reason why this should be so, and in many extensions of the standard model neutrinos do indeed have mass. A great number of experiments have been made in order to constrain fundamental parameters like mass and magnetic moment of the different neutrino species. However, most of these experiments are inefficient because of the very low counting statistics, and this is where indirect experiments enter the picture. Neutrinos are thought to be of fundamental importance in triggering the supernova explosions for example. Therefore observations of supernovae yield important information on neutrino properties. The other "laboratory" where fundamental neutrino physics can be probed is the early Universe. Here neutrinos are roughly as abundant as photons and should therefore contribute significantly to for example the cosmic energy density. This in turn leads to stringent limits on parameters like neutrino mass. Neutrinos are also of fundamental importance in the formation of light elements in the early Universe. Constraints on neutrino properties coming from the study of light element formation form the bulk part of the present work and will be described in much more detail later.

1.2 Primordial Nucleosynthesis

For many years cosmology was a research field strongly lacking in observational input. However, during the last decade numerous improvements have been made on this. For example the cosmic microwave anisotropies were discovered in 1992 by the COBE satellite [1] and small scale anisotropies are expected

to be observed by the next generation of satellites expected to fly within 5-10 years time. This has opened up a completely new window on the physics of the early Universe since the physical composition of the Universe at the time of creation of the background radiation is imprinted in these anisotropies. Thus, a new precision determination of such essential parameters as the cosmological density parameter, Ω, and the Hubble parameter, H, can be expected.

Another field under rapid development is that of large scale galaxy redshift surveys [2]. This is primarily due to new telescope technology and observational techniques that automate the processes that earlier had to be done manually. In this way redshifts of millions of galaxies can be obtained and the physical structure of the Universe mapped out. This again tells something about the matter content of the Universe because that affects the way structures form. If the content of the Universe is mainly in the form of very light ($m \simeq$ eV) particles, all imhomogeneities on small scales will have been smeared out by the free streaming of these particles. This means that the first structures to form are very large, roughly on the size of superclusters of galaxies. Only subsequently will these huge structures fragment to form galaxies. This type of scenario is called *hot dark matter* (HDM). The other possibility is that the matter content is mainly in the form of very heavy particles. These are almost at rest so that no free streaming takes place and therefore the first structures to form are of subgalactic size. From these subgalactic size initial structures larger and larger structures are build. This type of scenario is called hierarchical clustering or *cold dark matter* (CDM). In Chapter 8 we will go into a closer discussion of these different models.

Both the above techniques use the inhomogeneity and structure in our Universe to say something about its composition. There is a completely different type of probe that can be used for this purpose, namely that of Big Bang nucleosynthesis. These last few years have also seen strong improvements on the determination of different nuclear abundances in the Universe, and these precision measurements have had a strong impact on Big Bang nucleosynthesis. Historically, Big Bang nucleosynthesis was first discussed by Gamow in 1946 [3]. His idea was that as the Universe cools down and expands, nuclear reactions would proceed to build up abundances of the different nuclei. Gamow proposed that essentially all the nuclei observed today originated in the Big Bang, but it later became clear that this is not possible. The reason is that there exist no stable elements with mass numbers 5 and 8 and that heavier elements therefore must originate from three body reactions like the triple alpha process that occurs in stars. It turns out, however, that the number density of particles at the time of nucleosynthesis is much too low for such reactions to be effective and that therefore essentially no nuclei heavier than $A = 7$ are formed. All the heavy elements must therefore have been formed subsequently in stars and supernovae. However, we also know that almost all of the helium in the Universe today must have been formed in the primordial nucleosynthesis phase, as it turns out that only a very small fraction can have been produced in stars later on.

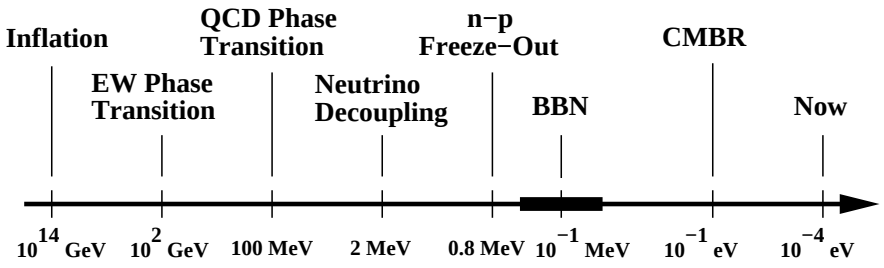

Figure 1.1: Timeline showing different important events during the evolution of our Universe. The scale shown is the temperature of the photon plasma, the drawing is not to scale.

The predicted abundances of light elements depend strongly on the physical composition of the Universe at the epoch of nucleosynthesis, meaning that if the primordial abundances can be somehow determined observationally we can probe the Universe at very early times.

In Fig. 1.1 we show a timeline marking some of the important events during the evolution of the Universe, and in the following we try go give a brief sketch of the event taking place during the epoch of primordial nucleosynthesis [4]. At a temperature of roughly 100 MeV the plasma of quarks and gluons undergoes a phase transition to a gas consisting of hadrons. Since there is some degree of baryon asymmetry in the Universe, some protons and neutrons remain of this gas even at temperatures much lower than the transition temperature. These protons and neutrons are kept in thermodynamic equilibrium via the β reactions until a temperature of roughly 1 MeV and, since the time-temperature relation is roughly

$$t[\mathrm{s}] \simeq T[\mathrm{MeV}]^{-2}, \tag{1.3}$$

this corresponds to a time of roughly 1 s. During this period the neutron to proton ratio is determined by their mass difference alone through the Boltzmann factor

$$\frac{n}{p} \propto e^{-(m_n - m_p)/T}. \tag{1.4}$$

When the temperature drops below 1 MeV, however, the weak reactions are too slow to maintain equilibrium and the proton-neutron fraction remains fixed except for the free decay of neutrons. At roughly the same time the weak reactions keeping neutrinos in equilibrium with the cosmic plasma of photons, electrons and positrons freeze out and the neutrinos become sterile.

As the temperature drops to 0.2 MeV the free nucleons start forming light nuclei in abundance. Deuterium is formed first, but is quickly processed into ^{4}He and the end result is that roughly 25% of the baryons are in ^{4}He and a much smaller fraction (on the $10^{-5} - 10^{-4}$ level) is in the form of nuclei like D, ^{3}He and ^{7}Li. When the temperature reaches 10^{-2} MeV nuclear reactions freeze out because the number densities become too small and primordial nucleosynthesis finishes.

A theoretical calculation of the expected yields of different nuclei from Big Bang nucleosynthesis is rather easily done once the input physics is known. The basic input that is needed to calculate the nucleosynthesis scenario is a specification of the content of the Universe as a function of time or temperature. By "content" we mean all particle species present and their relative abundance as well as such more exotic components as vacuum energy etc.

Then, if it is possible to determine somehow the primordial abundances from observations, this will put strong limits on the possible configuration of the Universe during nucleosynthesis. Unfortunately the main problem with using nucleosynthesis as a probe lies exactly in the observations. What is observable today is primarily the element abundances in stellar atmospheres, interstellar clouds etc. This means that the observations are performed in the local Universe which has an age of roughly 10^{10} years. If one wants to relate the values observed locally to the primordial values one has to take into account possible chemical evolution since primordial nucleosynthesis took place. The element composition changes with time because of nuclear burning in stars, supernovae, cosmic ray processes etc., and therefore it is usually extremely difficult to pin down the primordial values by observations.

With the introduction of a new generation of telescopes like the American Keck telescope and the Hubble Space Telescope is has become possible to study light element abundances in much more distant systems. Until now these observations have concentrated on observing deuterium in what is called QSO absorption systems. These are huge clouds of gas lying in the line of sight to a distant quasar. When light from the quasar passes through such a system, absorption lines are produced by the material in the clouds, and these can be used to determine element abundances in the absorbing cloud. The advantage of this is that the clouds lie at redshifts larger than $z = 1$ so that they are observed at an earlier epoch than the present Universe. Furthermore these absorption systems are thought to be systems that have not yet collapsed to form galaxies and that there has therefore been very little chemical processing in them. This gives rise to the hope that the abundances observed in such systems reflect the primordial much more closely than those observed locally. In Fig. 1.2 we show an example of a spectrum obtained from this type of observation, reproduced from Ref. [5]. Unfortunately the results that have hitherto been obtained are quite controversial and do not agree with each other. The main conclusion must be that this type of observations is an extremely promising technique, but that it is at present too early to use the results at face value. Hopefully the coming few years will resolve the issue.

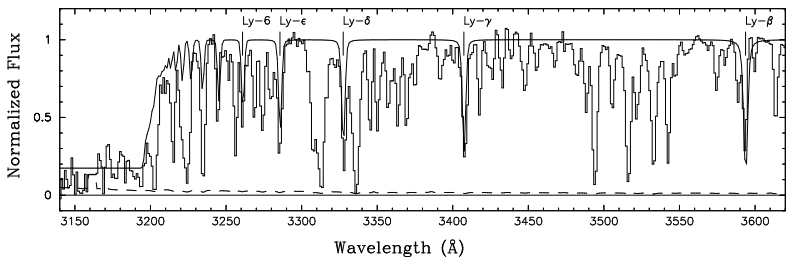

Figure 1.2: Spectrum obtained by Burles and Tytler at the Lick observatory of an absorber at redshift $z = 2.504$. The strong dip to the left is the Lyman limit. This figure was reprinted from Ref. [5].

Now, the standard model of particle physics, together with the theory of general relativity and the so-called cosmological principle, stating that the Universe should be homogeneous and isotropic on large scales, constitute what is known as the standard model of cosmology. Although there are still things that cannot be explained by this model, like the initial density perturbations needed to seed galaxy formation and the asymmetry between particles and anti-particles, it does account for almost all the observed features of the physical Universe. At the time of nucleosynthesis the standard model is that of a plasma of photons, electrons and positrons in complete thermodynamic equilibrium together with three massless neutrino species that have completely decoupled from the electromagnetically interacting plasma. In addition to this there is a small amount of baryons present, but since the exact amount is unknown the baryon content is usually expressed in terms of an adjustable parameter

$$\eta \equiv \frac{n_B - n_{\overline{B}}}{n_\gamma}, \tag{1.5}$$

where the value of η is roughly $10^{-10} - 10^{-9}$.

One of the amazing things about Big Bang nucleosynthesis is that the predicted yields are actually very close to the observed abundances of light nuclei. This can be taken as evidence that the standard model is at least fundamentally correct. It also puts very strong bounds of any physics beyond the standard model during nucleosynthesis and gives us an opportunity to constrain such new physics by means that are complementary to laboratory experiments. One example is the limit to the number of massless neutrino species present during nucleosynthesis. Here, observations are able to give the constraint [6]

$$N_\nu \leq 4, \tag{1.6}$$

whereas the number of light neutrinos measured at LEP from the decay of Z^0 is [7]

$$N_\nu = 2.991 \pm 0.016. \tag{1.7}$$

There are numerous other such constraints coming from nucleosynthesis and some of them will be discussed in more detail in Chapters 5-8. A classic example is the possibility for a heavy τ neutrino, where the mass constraints from nucleosynthesis can be used to complement the accelerator limits. This is very important to experimentalists trying to measure directly the mass and lifetime of the τ neutrino, because the nucleosynthesis constraints can be used to exclude large mass-lifetime intervals, thus making direct searches easier.

Recently there has been added a twist to this standard picture of primordial nucleosynthesis. As the observations have gradually improved over the years there has been growing evidence that something may not be quite right after all. The trouble is that it appears that the amount of helium predicted by BBN calculations is somewhat larger than what is observed [8]. This has led some to the conclusion that standard BBN is wrong and that some new element must be added. However, there still seems to be quite large systematic uncertainties in the helium observations so that it may after all turn out that the discrepancy is due to some observational feature rather than new physics. Still, it may also turn out that there is indeed such a nucleosynthesis crisis. Therefore it is of considerable interest to explore ways of changing the primordial abundances relative to the standard value. One such possibility is the decay of a heavy tau neutrino during nucleosynthesis; a possibility discussed in more detail in Chapter 7.

1.3 Thesis Outline

The remainder of the thesis is structured in the following way. Chapter 2 contains a review of the dynamics of an expanding Universe as well as a discussion of the Boltzmann equation that describes particle interactions between different species. Chapter 3 deals with the concepts of Big Bang nucleosynthesis theory. Furthermore it contains a discussion of the observational aspects. In Chapter 4 we review the definition of Dirac and Majorana neutrinos and discuss the different possible interactions of neutrinos, from the standard weak interactions to

neutrino decays. Armed with the basic physical concepts introduced in Chapter 2-4 we proceed in Chapters 5-8 to apply the formalism to actual problems. Chapter 5 is about neutrino freeze-out in the standard model. Chapter 6 deals with massive, but stable neutrinos in connection with primordial nucleosynthesis. By use of nucleosynthesis arguments, the tau neutrino mass is constrained to be below roughly 0.2 MeV if it is stable during nucleosynthesis. In Chapter 7 we go one step further to deal with possible neutrino decays during Big Bang nucleosynthesis. It is shown that such decays can lead to significant changes in the primordial abundances. Chapter 8 deals with a somewhat different aspect of neutrino physics in the early Universe, namely that of neutrino lasing. This effect comes from the out-of-equilibrium decay of neutrinos to a final state that contains bosons. Due to the stimulated emission factors in the phase-space integrals for bosons such decays can produce large amounts of very cold bosons, resembling a condensate. Chapters 9 and 10 contain a thesis conclusion and an outlook to possible future research respectively. Finally there are three appendices, the first two containing mathematical detail, and the third containing an english resumé of the thesis work.

Chapter II

Particle Dynamics in the Expanding Universe

2.1 Global Evolution Equations

Our present understanding of the evolution of our Universe is based on what is called the Standard Hot Big Bang model. There are two essential assumptions that go into this model, namely that

1) Einsteins theory of general relativity is correct,

2) The Universe is homogeneous and isotropic on large scales ($R \geq 100$Mpc). This is usually referred to as the cosmological principle.

The most general structure of the line element ds^2 then has the well known Robertson-Walker shape

$$ds^2 = R^2(t)\left[\frac{dr^2}{1-kr^2} + r^2 d\theta^2 + r^2 \sin^2\theta d\phi^2\right] - dt^2, \tag{2.1}$$

where R is a quantity with dimension $[l]$. R is usually referred to as the scale factor and it is a measure of the expansion of the Universe. The quantity k measures the sign of gaussian curvature of the Universe so that it can take the values $k = 0, \pm 1$. The global evolution of a homogeneous and isotropic Universe is therefore described in terms of R and k alone.

Using the two above assumptions the Einstein equation

$$G^{\mu\nu} = 8\pi G T^{\mu\nu} \tag{2.2}$$

reduces to two scalar equations in R and k, the $0-0$ component giving the Friedmann equation

$$\frac{\dot{R}^2}{R^2} + \frac{k}{R^2} = \frac{8\pi G}{3}\rho, \tag{2.3}$$

and the $i-i$ component giving the equation

$$2\frac{\ddot{R}}{R}+\frac{\dot{R}^2}{R^2}+\frac{k}{R^2}=-8\pi GP. \tag{2.4}$$

The two equations, Eqs. (2.3) and (2.4), assume a perfect fluid form of the stress-energy tensor

$$T^{\mu\nu}=\rho U^\mu U^\nu+P(g^{\mu\nu}+U^\mu U^\nu), \tag{2.5}$$

where ρ and P are the cosmic energy density and the pressure respectively.

The second of the two above equations, Eq. (2.4), involves the second derivative of the scale factor R. It would be of interest to find instead an equation involving only the first derivative. There are basically two ways to establish the relation between time, temperature and scale factor in the early Universe during the epoch of nucleosynthesis, using only first order equations. The simplest way to do it is via entropy conservation.

As long as there is thermodynamic equilibrium or all distribution functions are described by equilibrium distributions (as in the case of totally decoupled massless neutrinos), entropy is conserved [9].

This means that

$$dS=0=d\left(\frac{(\rho+P)R^3}{T}\right), \tag{2.6}$$

where ρ and P are the total energy density and pressure contributions from all particle species present. This conservation equation can be used to calculate the relation between the scale factor and the photon temperature.

In the following we shall assume that the neutrinos are completely decoupled from the electromagnetic plasma long before the electrons and positrons annihilate. This only introduces a small error in the final results. An error that can be quantified by use of the more correct equation of energy conservation that is described below.

We can then rewrite the entropy conservation equation in the following way. Without loss of generality we can put $R(t_0)=1$, where t_0 is the starting point of the calculation. By using $T_\nu \propto R^{-1}$ we then get

$$R^3\left(\frac{\rho_e+P_e}{T_\gamma}+\frac{4}{3}\frac{\pi^2}{15}T_\gamma^3+3\frac{7}{8}\frac{4}{3}\frac{\pi^2}{15}T_\nu^3(t_0)R^{-3}\right)=Constant, \tag{2.7}$$

where the constant can be determined at the initial time [1] . Thus we now have the scale factor as a function of photon temperature, but in order to calculate it as a function of time, we parametrise it as $R(t)=f(t)t^{1/2}$, where $f(t)$ is the deviation from the standard expansion of a radiation dominated Universe. We

[1] Eq. (2.7) can be used to calculate the final temperature of completely decoupled neutrinos. The result is $T_\nu/T_\gamma=(4/11)^{1/3}$. If Boltzmann statistics is used for all particle species, Eq. (2.7) reads $R^3\left(\frac{\rho_e+P_e}{T_\gamma}+\frac{4}{3}\frac{\pi^2}{15}T_\gamma^3+3\frac{4}{3}\frac{\pi^2}{15}T_\nu^3(t_0)R^{-3}\right)=Constant$, and the result is $T_\nu/T_\gamma=(1/3)^{1/3}$.

make the following (good) approximation $f^{-1}df/dt \ll \frac{1}{2}t^{-1}$, and the Friedmann equation, Eq. (2.3), then takes the form

$$\left(\frac{dR}{dt}\frac{1}{R}\right)^2 = \frac{1}{4}t^{-2} = \frac{8\pi G\rho}{3}. \tag{2.8}$$

This means that we can calculate $t(T_\gamma)$ and thus $R(t)$. We have now established a relationship between time, temperature and scale factor.

However, although the approximations made are very good for massless neutrinos this is not necessarily the case for massive neutrinos. In this case there can be significant deviations from the above equations.

A procedure that does not involve any approximations on this level is to use energy conservation. From the conservation of stress-energy

$$T^{\mu\nu}_{;\nu} = 0, \tag{2.9}$$

one finds the following equation if one assumes a perfect fluid form of the stress-energy tensor,

$$\frac{d}{dt}(\rho R^3) + p\frac{d}{dt}(R^3) = 0, \tag{2.10}$$

where again ρ and P are the total energy density and pressure contributions of all particles. This equation is an expanding Universe equivalent of the 1st law of thermodynamics.

However, we are not necessarily dealing with a perfect fluid. Only if all particle distributions are described by equilibrium distribution functions or all particle species are either massless or completely non-relativistic (not a mix of relativistic and non-relativistic particles) will the fluid be perfect. Since we are considering the possibility of non-equilibrium processes with semi-relativistic particles, there is no reason to assume that the perfect fluid approximation should be valid.

Phenomena such as heat conduction, shear viscosity and bulk viscosity may occur in such a scenario. However, Weinberg [10] has shown that in a homogeneous and isotropic Universe, only the bulk viscosity can be non-zero.

Now, in all that follows, we shall assume that all particle species are describable by single particle distribution functions. This approach of course assumes that the particles do not interact apart from instantaneous collisions, so that a single particle distribution function makes sense at all. However, we shall always use this approach in the present work. For massless neutrinos it is definitely justified, but for massive neutrinos that can oscillate this is not necessarily the case [11]. Furthermore, we shall assume that all phase space distributions are homogeneous in coordinate space and isotropic in phase space

$$f(\mathbf{x}, \mathbf{p}, t) = f(p, t). \tag{2.11}$$

To see the effect of bulk viscosity, we proceed in the following way. We write the distribution functions as [9]

$$f_i = f_{0i}(1 + \phi_i). \tag{2.12}$$

f_{0i} is an equilibrium distribution of the normal form

$$f_{0i} = \frac{1}{\exp\left(\frac{E-\mu_i}{T_i}\right) \pm 1} \tag{2.13}$$

and ϕ_i parametrises the deviation from equilibrium. There is, however, an ambiguity in the definition of f_{0i} as there are two unknown parameters, μ_i and T_i. These are usually fixed by letting

$$\int f_{0i}\phi_i d^3p = \int f_{0i}\phi_i E d^3p = 0, \tag{2.14}$$

so that $\rho_{0i} = \rho_i$ and $n_{0i} = n_i$ [9]. The pressure is not determined by these conditions. We still have

$$P_i = \frac{1}{3}\int f_{0i}(1+\phi_i)\frac{p^2}{E}\frac{d^3p}{(2\pi)^3}. \tag{2.15}$$

Now, if the ϕ_i's are not too large, as would be expected unless some very extreme processes were occuring, the deviation from a perfect fluid can be described by first order term in the stress-energy tensor [2] [10], $T^{\mu\nu}$,

$$\Delta T^{\mu\nu} = -\zeta(g^{\mu\nu} + U^\mu U^\nu)U^\alpha_{;\alpha}, \tag{2.16}$$

where ζ is called the coefficient of bulk viscosity. The total stress-energy tensor must then assume the form [10]

$$\begin{aligned} T^{\mu\nu} &= \rho_0 U^\mu U^\nu + (P_0 - 3\zeta\frac{\dot{R}}{R})(g^{\mu\nu} + U^\mu U^\nu) \\ &= \rho U^\mu U^\nu + (P_0 - 3\zeta\frac{\dot{R}}{R})(g^{\mu\nu} + U^\mu U^\nu). \end{aligned} \tag{2.17}$$

On the other hand, the spatial components of the stress-energy tensor are [9]

$$T^{aa} = \frac{1}{3}\sum_i \int f_{0i}(1+\phi_i)\frac{p^2}{E}\frac{d^3p}{(2\pi)^3} = P_0 + \frac{1}{3}\sum_i \int f_{0i}\phi_i\frac{p^2}{E}\frac{d^3p}{(2\pi)^3}. \tag{2.18}$$

Since we are in a comoving coordinate system, $U^i = 0$ and $U^0 = 1$. This gives

$$T^{aa} = P_0 - 3\zeta\frac{\dot{R}}{R} = P_0 + \frac{1}{3}\sum_i \int f_{0i}\phi_i\frac{p^2}{E}\frac{d^3p}{(2\pi)^3}, \tag{2.19}$$

or

$$\zeta = -\frac{1}{9}\frac{R}{\dot{R}}\sum_i \int f_{0i}\phi_i\frac{p^2}{E}\frac{d^3p}{(2\pi)^3}. \tag{2.20}$$

[2] When dealing with general relativistic tensors, Greek letter denominate all four spacetime components, whereas Roman letters only denominate the three spatial components.

The energy conservation equation with bulk viscosity is then [10]

$$\begin{aligned}\frac{d}{dt}(\rho R^3) &= -3R^2\dot{R}(P_0 - 3\zeta\frac{\dot{R}}{R}) \\ &= -P_{\rm TOT}\frac{d}{dt}(R^3). \end{aligned} \tag{2.21}$$

Altogether then, the energy conservation equation is unchanged if we just use the total pressure, defined as

$$P_{\rm TOT} = \sum_i \int \frac{1}{3} f_i \frac{p^2}{E}\frac{d^3p}{(2\pi)^3}. \tag{2.22}$$

As noted by Fields *et al.* [12], bulk viscosity can be a potentially serious problem if one uses the standard way of solving the Boltzmann equation, namely by assuming complete kinetic equilibrium at all times (that is, working only with distributions of the f_{0i} form). Using our method, bulk viscosity is not a problem because we use the true distribution functions f_i directly without any assumptions. Thus, when we calculate the pressure, P, the bulk viscosity is automatically taken into account. We can then still use the conservation equation (2.10) in our non-equilibrium case.

We now introduce the quantity $r \equiv \ln(R^3)$, in which case the conservation equation can be rewritten as

$$\frac{dr}{dT_\gamma} = -\frac{\frac{d\rho}{dT_\gamma}}{\rho + P} \tag{2.23}$$

In addition to this we again use the Friedmann equation

$$\frac{dR}{dt} = \sqrt{\frac{8\pi G\rho}{3}}R, \tag{2.24}$$

or, in terms of r,

$$\frac{dr}{dt} = \sqrt{24\pi G\rho}. \tag{2.25}$$

Combining the two equations, we get

$$\frac{dT_\gamma}{dt} = \frac{dr/dt}{dr/dT_\gamma} \tag{2.26}$$

We thus have the two fundamental equations (2.25) and (2.26) describing the time evolution of temperature and scale factor without any approximations [3]. One should perhaps also note here that the problem of bulk viscosity does not appear in the Friedmann equation since it only involves the energy density ρ and not the pressure.

[3] Note that we have actually made an approximation by assuming that a first order bulk viscosity term is sufficient. If the distributions deviate largely from kinetic shapes, a first order term might not be adequate. Of course there is also still the approximation of a single particle distribution function which may not be adequate either

2.2 The Boltzmann Equation

The formalism described above describes fully the global expansion of the Universe assuming knowledge of ρ and P as functions of time. For a completely non-interacting plasma these quantities are easy to calculate, but since the early Universe consists of a plasma of different interacting species the situation is not so simple. We need a transport equation that describes the coupling of different particle species so as to calculate their relative abundances etc. Such an equation together with the evolution equations above is enough to, at least in principle, describe the whole evolution of the Universe. The equation needed for this purpose is the Boltzmann transport equation,

$$\mathrm{L}[f] = C_{\mathrm{coll}}[f] + C_{\mathrm{dec}}[f], \tag{2.27}$$

for the evolution of the single particle distribution function, f, of a particle species. In a homogeneous and isotropic Universe the Boltzmann equation assumes a fairly simple form, the left hand side of the above equation is the Liouville operator in an expanding Universe,

$$\mathrm{L}[f] = \frac{\partial f}{\partial t} - \frac{dR}{dt}\frac{1}{R}p\frac{\partial f}{\partial p}. \tag{2.28}$$

The right hand side of Eq. (2.27) involves the specific physics of the decay process as well as possible other collision processes such as elastic scattering and annihilation. This set of equations together with the two equations, Eqs. (2.3) and (2.10), in principle allows us to follow the evolution of all particle species as well as the global expansion of the Universe. However, these equations are usually tremendously difficult to solve, except for a few special cases. For that reason one usually resorts to approximations for the Boltzmann equation. If we look at sufficiently early times where the electromagnetic interaction timescale is very short compared to the expansion timescale of the Universe ($T \geq$ eV) we can always consider electromagnetically interacting particles such as photons and $e^{\pm}$ as being in perfect thermodynamic equilibrium.

For particles that do not interact strongly but are not completely decoupled either, such as neutrinos, the situation is much more complicated. If we restrict ourselves to look only on 2 particle reactions; that is, reactions like pair annihilation $a + \overline{a} \to b + \overline{b}$ or elastic scattering $a + b \to a + b$, the first term on the right hand side, C_{coll} can be written as a 9-dimensional phase-space integral.

$$\begin{aligned} C_{\mathrm{coll}}[f] &= \frac{1}{2E_1}\int d^3\tilde{p}_2 d^3\tilde{p}_3 d^3\tilde{p}_4 \Lambda(f_1,f_2,f_3,f_4) \times \\ &\quad S\,|M|^2_{12\to 34}\,\delta^4(p_1+p_2-p_3-p_4)(2\pi)^4, \end{aligned} \tag{2.29}$$

where $\Lambda(f_1,f_2,f_3,f_4) = (1-f_1)(1-f_2)f_3f_4 - (1-f_3)(1-f_4)f_1f_2$ is the phase space factor, including Pauli blocking of the final states, and $d^3\tilde{p} = d^3p/((2\pi)^3 2E)$. S is a symmetrisation factor of $1/2!$ for each pair of identical particles in initial or final states [13], and $|M|^2$ is the weak interaction

matrix element squared, and appropriately spin summed and averaged. p_i is the four-momentum of particle i. The standard way of simplifying the Boltzmann equation for this case is to assume that elastic scattering reactions are always much more important than number changing reactions. If this is the case one may assume that the given species is in kinetic equilibrium, and that its distribution functions is of equilibrium shape with an added pseudochemical potential. This allows us to look only on the number changing reactions, since the elastic scattering integrals all become zero for distributions in kinetic equilibrium (kinetic equilibrium is sometimes also referred to as scattering equilibrium). If one furthermore assumes Boltzmann statistics for all the particle species present,

$$f(p) = e^{-E/T-z}, \tag{2.30}$$

where z is the pseudochemical potential, it is possible to arrive at a relatively simple set of evolution equations (one for each species present) by integrating the Boltzmann equation,

$$\dot{n_i} + 3Hn_i = \sum_j \langle \sigma v \rangle_{ij} , (n_{i,\mathrm{eq}}^2 - n_i^2). \tag{2.31}$$

where n_{eq} is the thermodynamic equilibrium number density and the sum is over all annihilation channels. $\langle \sigma |v| \rangle$ is the thermally averaged cross section for the number changing reactions [14],

$$\langle \sigma |v| \rangle_{ij} = \frac{1}{8m^4 T K_2^2(m/T)} \int_{4m^2}^{\infty} ds \sqrt{s}(s-4m^2) K_1 \left(\frac{\sqrt{s}}{T} \right) \sigma_{ij}^{CM}(s), \tag{2.32}$$

where it has been assumed that all annihilation products are massless. The K_i's are modified Bessel functions of the second kind and s is defined in the standard way as $s \equiv (p_1 + p_2)^2$, with p_i being the four-momentum of particle i.

A step up from this approach is to relax the assumption of Boltzmann statistics, which was first done by Kainulainen and Dolgov [15], and subsequently developed further by Fields, Kainulainen and Olive [12]. In this case the particle distributions are of the form

$$f(p) = \frac{1}{e^{E/T-z} \pm 1}. \tag{2.33}$$

This step is done at the expense of not being able to write the right hand side of the Boltzmann equation in a simple form. However, since errors induced by using Boltzmann statistics instead of Fermi-Dirac or Bose-Einstein are typically of order 10-20%, it may be necessary to use the full statistics. The Boltzmann equation then takes the form

$$\dot{n}_i + 3Hn_i = \sum C_{ij}. \tag{2.34}$$

In this case, the left hand side is [12]

$$\dot{n_i} + 3Hn_i \quad = \quad \frac{T_i^3}{2\pi^2} \left[H(J_1(x_i, z_i) - x_i^2 J_{-1}(x_i, z_i)) \right. \tag{2.35}$$

$$+\frac{\dot{T}_i}{T_i}J_1(x_i,z_i) - \dot{T}_\gamma J_0(x_i,z_i)\frac{\mathrm{d}z_i}{\mathrm{d}T_\gamma}\Bigg],$$

where $x_i = m_i/T$ and

$$J_n(x,z) = \int_0^\infty dy y^2 (x^2+y^2)^{n/2} \frac{e^{\sqrt{x^2+y^2}+z}}{(1+e^{\sqrt{x^2+y^2}+z})^2}. \tag{2.36}$$

The right hand side is expressed as an integral of the same type as Eq. (2.29), but integrated over momentum space for the incoming particle [12]. This integral must then be evaluated numerically. Even for this more complicated equation the evolution of particle species is relatively easy to follow numerically because one only needs to follow the functions, $z_i(T)$, which are functions of temperature alone.

However, most of the present work deals with possible deviations from these simple equations, Eq. (2.31) and Eq. (2.34). If the distribution functions deviate significantly from kinetic equilibrium one is forced to use the full Boltzmann equation which is numerically rather complicated because one needs to use a grid in momentum space and solve for the distribution function on this grid, meaning that effectively one has to solve a huge number of coupled differential equations. Appendix B is devoted to describing the analytical integration of the collision terms for the case of neutrinos interacting through the weak interaction.

We now return to the original Boltzmann equation and look at the second term on the right hand side, C_{dec}. In general this term will have the same form as the collision term, Eq. (2.29), namely a large phase space integral of the involved matrix element. However, we shall only need to look at the case where the decay is to a two particle final state, $a \to b + c$. We also restrict ourselves to look only at decays isotropic in the rest frame of the parent particle. In this case the collision term can be simplified tremendously because the decay strength is fully described by the rest frame decay lifetime, τ. The decay spectrum is then determined by kinematics alone. To be specific, we look at the decay

$$H \to F + \phi, \tag{2.37}$$

where H and F are both fermions and ϕ is a scalar particle. The decay terms in the Boltzmann equation have been calculated by Starkman, Kaiser and Malaney [16] to be

$$C_{\mathrm{dec}}[f_H] = -\frac{m_H^2}{\tau m_0 E_H p_H}\int_{E_\phi^-}^{E_\phi^+} dE_\phi \Lambda(f_H, f_F, f_\phi), \tag{2.38}$$

$$C_{\mathrm{dec}}[f_F] = \frac{g_H}{g_F}\frac{m_H^2}{\tau m_0 E_F p_F}\int_{E_H^-}^{E_H^+} dE_H \Lambda(f_H, f_F, f_\phi), \tag{2.39}$$

$$C_{\mathrm{dec}}[f_\phi] = \frac{g_H}{g_\phi}\frac{m_H^2}{\tau m_0 E_\phi p_\phi}\int_{E_H^-}^{E_H^+} dE_H \Lambda(f_H, f_F, f_\phi), \tag{2.40}$$

where $\Lambda(f_H, f_F, f_\phi) = f_H(1-f_F)(1+f_\phi) - f_F f_\phi(1-f_H)$ and $m_0^2 = m_H^2 - 2(m_\phi^2 + m_F^2) + (m_\phi^2 - m_F^2)^2/m_H^2$. τ is the lifetime of the heavy neutrino and g is the statistical weight of a given particle. The integration limits are

$$E_H^{\pm}(E_i) = \frac{m_0 m_H}{2m_i^2}[E_i(1+4(m_i/m_0)^2)^{1/2} \pm (E_i^2 - m_i^2)^{1/2}], \tag{2.41}$$

and

$$E_i^{\pm}(E_H) = \frac{m_0}{2m_H}[E_H(1+4(m_i/m_0)^2)^{1/2} \pm p_H], \tag{2.42}$$

where the index $i = F, \phi$.

The formalism presented in this chapter gives us all the equations needed to follow the evolution of neutrinos in the early Universe that will be discussed in Chapters 5-8.

Chapter III

Basic Big Bang Nucleosynthesis

3.1 Theory

At high temperatures, the baryon content of the Universe is in the form of a free quark-gluon plasma. However, at a temperature of $\simeq 100$ MeV this plasma undergoes a phase transition to a gas of bound quark systems. At first, this plasma consists almost solely of pions, but as the temperature drops, the pions disappear and the gas then only consists of neutrons and protons that are "left over" because of the baryon asymmetry of our Universe. These protons and neutrons are kept in thermodynamic equilibrium by the β reactions

$$n + \nu_e \leftrightarrow p + e^-, \tag{3.1}$$
$$n \leftrightarrow p + e^- + \overline{\nu}_e, \tag{3.2}$$
$$n + e^+ \leftrightarrow p + \overline{\nu}_e, \tag{3.3}$$
$$n + e^+ + \nu_e \leftrightarrow p. \tag{3.4}$$

During this era the ratio of protons to neutrons is determined by the Boltzmann factor

$$\frac{n}{p} = \exp(-(m_n - m_p)/T) \tag{3.5}$$

alone. Now, since the rate for these interactions is roughly

$$\Gamma_\beta \simeq G_F^2 T^5 \tag{3.6}$$

and the expansion timescale of the Universe is

$$\tau_H = H^{-1} = \sqrt{\frac{3}{8\pi G\rho}}, \tag{3.7}$$

which is proportional to T^{-2} in a radiation dominated Universe, one arrives at the relation

$$\frac{\Gamma_\beta}{\tau_H^{-1}} \simeq (T/0.8\text{MeV})^3, \tag{3.8}$$

so that, at a temperature of roughly 1 MeV the average time for $n-p$ conversion will be longer than the expansion time of the Universe. At this point the conversions can no longer maintain equilibrium and the neutron to proton fraction freezes out. From this point on the ratio of neutrons to protons remains constant except for the change due to free neutron decays. However, shortly after this freeze-out occurs all free neutrons are bound in nuclei thereby preventing further neutron decay.

Because of the high entropy of the Universe free nucleons are preferred down to very low temperatures, only at $T \simeq 0.2$ MeV does deuterium production commence. This deuterium is quickly processed into ^{4}He, but at higher A very little happens. The reason for this is easy to understand. Because formation of nuclei is suppressed down to very low temperatures the number density is very low, so that triple reactions are unlikely. Furthermore the Coulomb barrier against nuclear reactions is typically very high compared with typical thermal energies, and there exist no stable $A = 5$ and $A = 8$ nuclei. Small amounts of Li, Be and B are produced, but beyond this essentially nothing. In Fig. 3.1 we show the primary reaction network for primordial nucleosynthesis and in Fig. 3.2 we show the build-up of light nuclei as the temperature drops.

The final abundances stemming from BBN depend sensitively on the baryon-to-photon ratio,

$$\eta \equiv \frac{n_B - n_{\overline{B}}}{n_\gamma}. \tag{3.9}$$

Therefore BBN in principle allows us to determine η if the primordial abundances can somehow be determined. Furthermore, the outcome (especially the abundance of ^{4}He) depends on the number of particle species present during nucleosynthesis. The reason can be seen from the Friedmann equation

$$H^2 = \frac{8\pi G\rho}{3}. \tag{3.10}$$

If the number of particle species is increased during nucleosynthesis, this increases ρ and thereby H for given temperature. This again means that Γ_β/H is decreased so that the weak interactions decouple earlier than usual. Thus, increasing ρ during nucleosynthesis has the effect of leaving more neutrons to survive than normally, meaning that in the end more helium is formed. Therefore one can use Big Bang nucleosynthesis to put limits on novel physics by limiting the number of particle species that can be present during nucleosynthesis. In Fig. 3.3 we show the primordial abundances after nucleosynthesis, both as functions of the baryon-to-photon ratio and of the equivalent number of neutrinos, $N_{\nu,\mathrm{eq}}$. This quantity is just a measure of the energy density present in neutrinos and all other non-electromagnetic interacting particles during nucleosynthesis and is defined as

$$N_{\nu,\mathrm{eq}} \equiv \frac{\sum \rho_{\nu+X}}{\rho_{\nu_0}}, \tag{3.11}$$

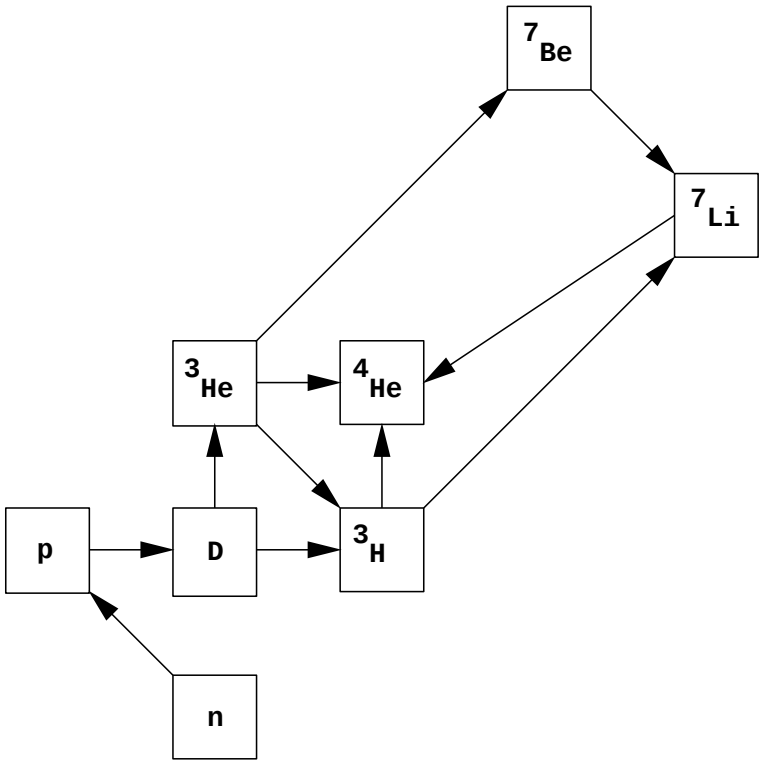

Figure 3.1: The most important reactions for primordial nucleosynthesis.

where ν_0 indicates a standard massless neutrino species. X indicates novel particles from physics beyond the standard model that may be present during nucleosynthesis, such as majorons, axions etc.

Finally it should also be mentioned that nucleosynthesis is very sensitive to the electron neutrino distribution because this enters directly into the β conversion rates through the β process rate integrals of type

$$\Gamma_{n\nu_e\to pe} = \int f_{\nu_e}(E_{\nu_e})(1-f_e(E_e))|M|^2_{n\nu_e\to pe}(2\pi)^{-5} \times\delta^4(p_n+p_{\nu_e}-p_p-p_e)d^3\tilde{p}_{\nu_e}d^3\tilde{p}_e d^3\tilde{p}_n, \quad (3.12)$$

where $d^3\tilde{p}_i = d^3p_i/(2E_i(2\pi)^3)$. Thus, one can also put strong limits on physical processes that change the electron neutrino distribution, such as massive or unstable neutrinos. This is a point we shall return to in more detail later.

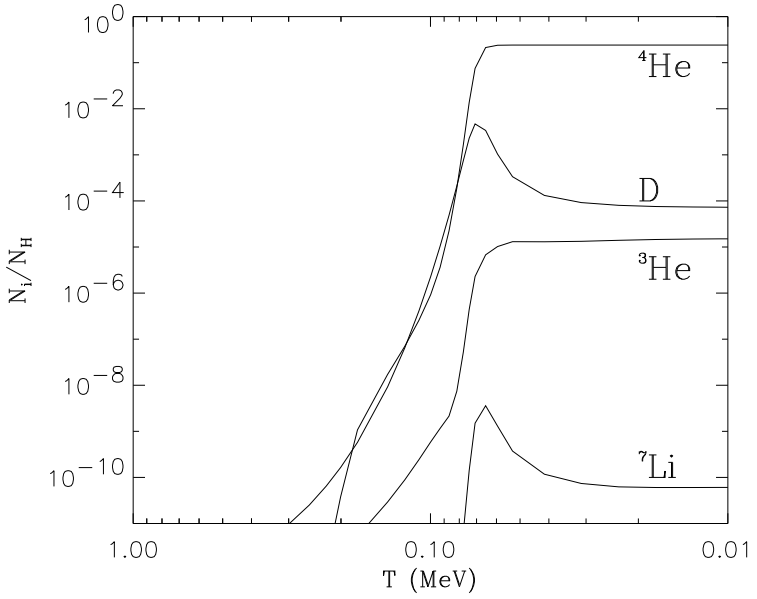

Figure 3.2: The mass fraction of ^{4}He as well as the number densities of different light nuclei relative to H as a function of cosmic temperature.

3.2 Observations

A very important but also very difficult part of this game is the determination of primordial abundances from observations in the present day Universe. The observations are made difficult by the fact that often the abundances of the relevant elements, such as lithium, are extremely small. However, even more difficult is the interpretation of the results. The trouble is that the present day Universe has evolved since the Big Bang. Most of the material in the present day Universe has been processed through stars and supernovae, changing its chemical composition. We will try to give a very brief resumé of the observational status of the most important Big Bang nucleosynthesis elements.

The observation of ^{4}He is relatively easy in the sense that the abundance of ^{4}He is large in all astrophysical systems. However, since the primordial helium abundance is only weakly (logarithmically) dependent on η it is also necessary to pin down the primordial fraction to very high precision if one wants to measure the baryon-to-photon ratio. Since ^{4}He is extremely stable it is very difficult to destroy and one can assume that it is only produced not destroyed. We also know that no elements with $A \geq 8$ are produced in the Big Bang. Therefore

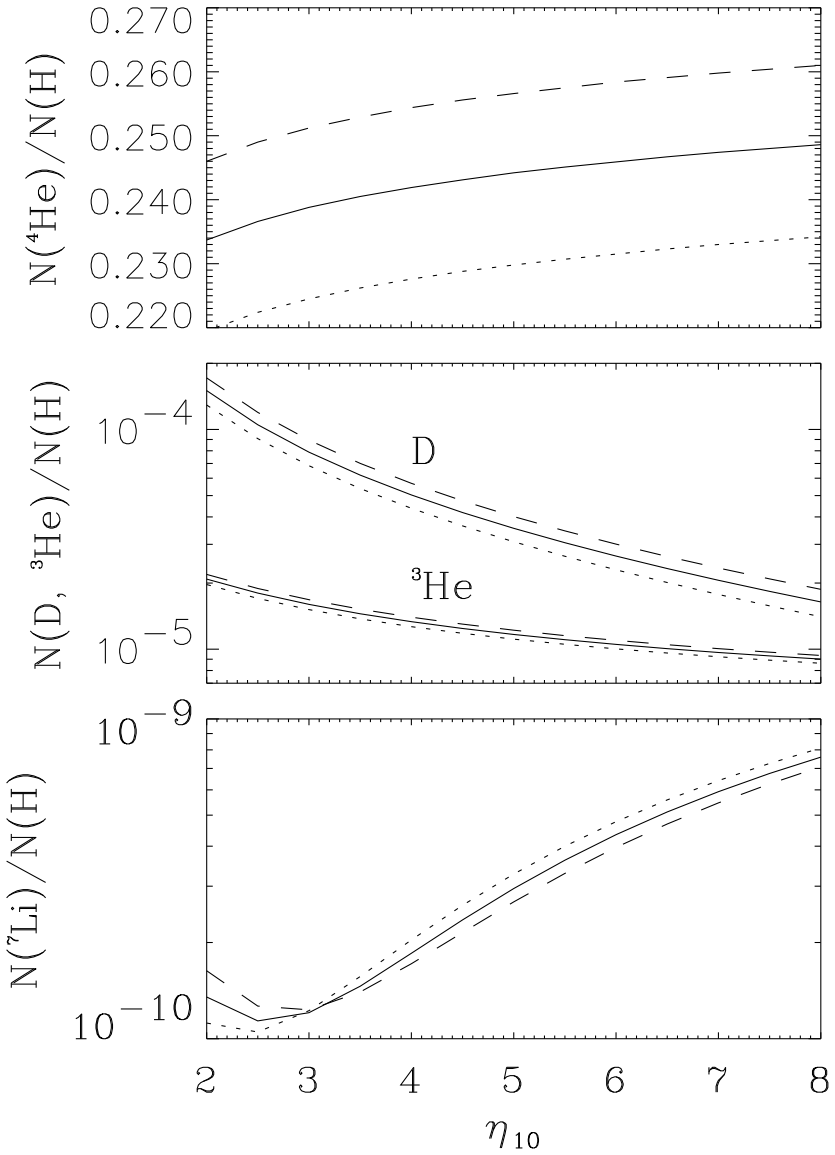

Figure 3.3: Relic abundances of different nuclei as a function of the baryon-to-photon ratio, $\eta_{10} \equiv 10^{10} \times n_B/n_\gamma$, for different values of $N_{\nu,\mathrm{eq}}$. The full lines indicate the standard value $N_\nu = 3$, the dotted ones indicate $N_{\nu,\mathrm{eq}} = 2$ and the dashed ones $N_{\nu,\mathrm{eq}} = 4$.

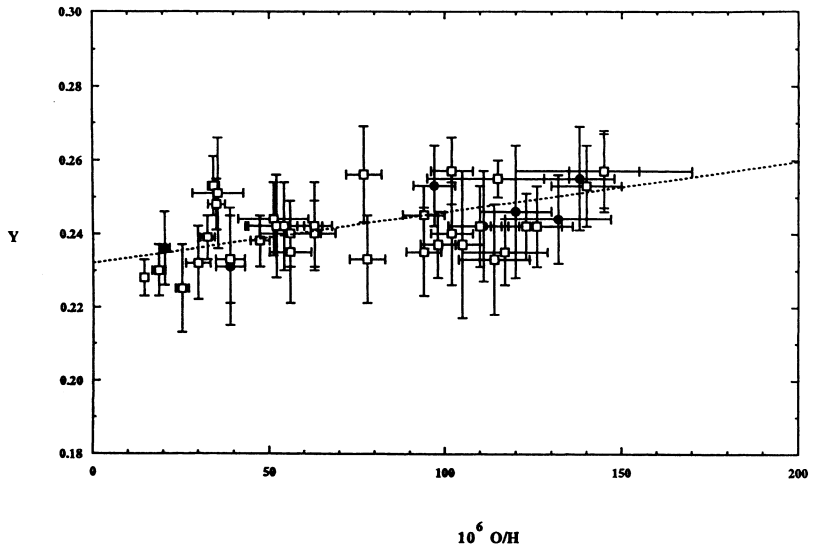

Figure 3.4: Observed abundance of ^{4}He in a number of extragalactic HII regions as a function of metallicity. The figure has been reproduced from Ref. [17].

if one finds a system with very low abundance of these heavy elements relative to the solar values it should indicate that very little processing has taken place and one may hope that the measured helium abundance in these systems reflects the primordial abundance closely. These observations are typically done in large extragalactic HII regions. In Fig. 3.4 we show a typical example of such a set of observations. The difficulties in pinning down the helium mass fraction,

$$Y_P \equiv m(^4\mathrm{He})/m(\mathrm{H}), \tag{3.13}$$

from observations should be obvious looking at the figure. At present there are two papers that reflect the most up to date observational constraints. Unfortunately these two papers do not agree with each other on the value found. First there are the results of Olive and Steigman [17] who analyse existing data from extragalactic HII regions. Doing this they find a primordial helium value of

$$Y_P \equiv 0.232 \pm 0.003 \pm 0.005, \tag{3.14}$$

where the first uncertainty is of purely statistical nature and the second is an estimated systematical uncertainty. The results of Izotov *et al.* [18] predict a much higher value for the primordial helium abundance

$$Y_P \equiv 0.243 \pm 0.003. \tag{3.15}$$

In Fig. 3.5 we show the results of Izotov *et al.* corresponding to those shown in Fig. 3.4.

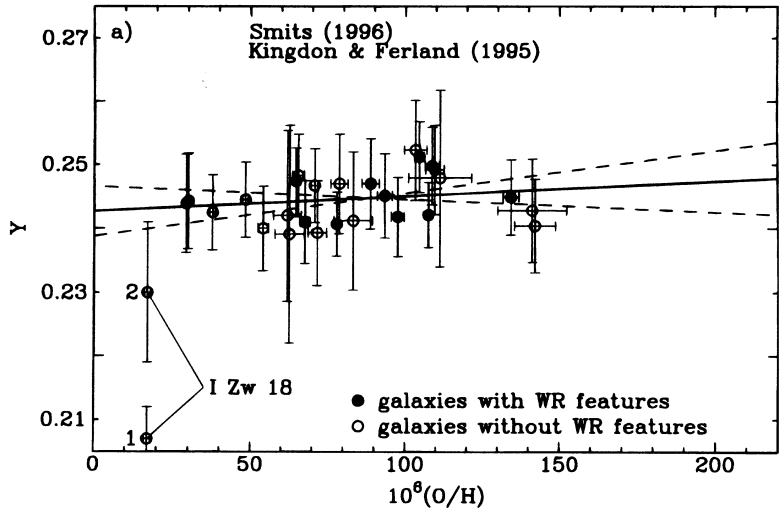

Figure 3.5: The results of Izotov *et al.* [18] for the abundance of helium. The figure has been reproduced from Ref. [18].

There are two problems in both these results. First of all, the usual way of getting the primordial value for helium is to do a linear fit to the observational data and interpret the y-axis crossing point as the primordial abundance. This assumes that a linear fit makes sense at all, which is by no means obvious. The other problem is the lack of very metal poor HII regions. Ideally one should find just one extremely metal poor object and use the value obtained for helium in this system as the primordial one. This would eliminate the need for a linear fit using more metal rich objects, but has unfortunately not been possible so far. Thus, it is not clear what the primordial abundance of helium actually is. Hopefully the coming years will show an increase in the number of metal poor objects known, so that a more precise value can be found. There are several ongoing projects with this goal.

For deuterium the observations used to be done in the solar neighbourhood. However, since D is very fragile and no known process can produce significant amounts of deuterium, these observations give a lower limit to the primordial abundance. The values that have been obtained from such observations are typically [8]

$$\mathrm{D/H} \simeq 1.6 \times 10^{-5}. \tag{3.16}$$

In the last few years it has become possible to observe deuterium in quasar absorption systems at significant redshift. Since these systems have evolved very little since the Big Bang one can hope to pin down the primordial deuterium abundance precisely. Unfortunately the results so far are very controversial. Some of the observations indicate a high deuterium fraction in these clouds

[19–21], around

$$\mathrm{D/H} \simeq 2 \times 10^{-4}. \tag{3.17}$$

However, there are other observations, mainly those by Tytler *et al.* [22], that indicate a relatively low deuterium value

$$\mathrm{D/H} \simeq 3 \times 10^{-5}, \tag{3.18}$$

which is more consistent with the local value. This low value seems more reliable since the analysis by Tytler *et al.* has been extremely careful. Nevertheless, only a few systems have so far been observed and more observations are greatly needed. It also appears that there are problems in accomodating a high primordial deuterium value in models of chemical evolution. At present it thus seems very difficult to draw any conclusions about the primordial value of D. ^{3}He has been used together with D in local observations to put an upper limit on the combined abundance of D and ^{3}He. The argument here is that it seems difficult to destroy D without at the same time producing ^{3}He. However, these results depend strongly on chemical evolution models and therefore seem not too reliable either.

For ^{7}Li the situation is also quite muddy. Until the early 80's it was thought impossible to determine the primordial Li abundance from observations because Li is both produced and destroyed in astrophysical environments. However in 1982 results appeared by Spite and Spite [23], indicating that in a certain group of very old metal poor halo stars, the ^{7}Li abundance is constant and does not depend on metallicity. This abundance is then interpreted as the primordial abundance, subject to rather small evolution effects compared with normal main sequence stars. The most recent published determination of the ^{7}Li abundance gives a value of [24]

$$^7\mathrm{Li/H} = (1.73 \pm 0.05[\mathrm{stat}] \pm 0.2[\mathrm{syst}]) \times 10^{-10}, \tag{3.19}$$

but the systematical uncertainties are, of course, difficult to estimate since they involve chemical evolution. The trouble is that there may still have been significant depletion even in the plateau stars, so that the value observed there is smaller than the primordial value by some unknown factor. It therefore seems premature to use ^{7}Li measurements to say anything about the value of η. In Fig. 3.6 we show a typical measurement of the ^{7}Li abundance in a group of old halo stars. At high masses, almost all Li remains, whereas at lower masses the convection zone extends deep enough to dissociate Li.

In conclusion, there is only one element, namely ^{4}He, whose primordial abundance is known to any real precision. However, the trouble is that even here there is controversy as to the primordial abundance so that a precision determination of η from the observational value of Y is not possible. However, the abundance is still known sufficiently well that one may put rather stringent limits on new physics. At present, one may fairly certainly conclude that [6]

$$N_{\nu,\mathrm{eq}} \leq 4 \tag{3.20}$$

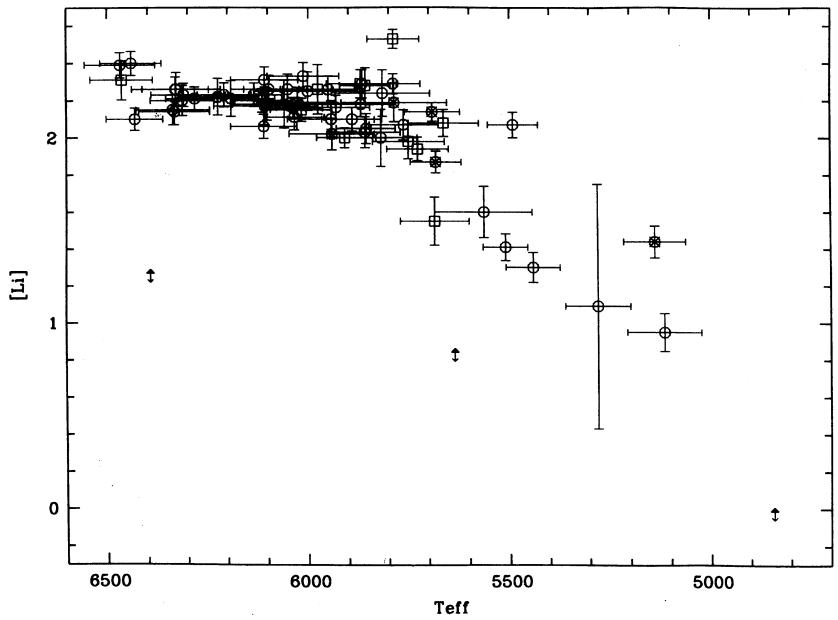

Figure 3.6: The abundance of ^{7}Li in old halo stars shown as a function of surface temperature. The Spite plateau is clearly seen to the left at high surface temperatures. The figure has been reproduced from Ref. [24].

so that only the equivalent of one extra neutrino species may be present during BBN. This bound allows for a fairly large uncertainty in the observational parameters. However, the value of $N_{\nu,\mathrm{eq}}$ favoured is much lower than this, even somewhat below 3 [8]. The reason for the low value is that the primordial helium fraction observed is too low compared to the theoretical predictions. This may point to a coming crisis for standard Big Bang nucleosynthesis, so that new physics like decaying neutrinos must be invoked to bring consistency. At this point, however, it is probably too early to say that there is any real "crisis" for the standard model of primordial nucleosynthesis. Finally, if the primordial value of deuterium is ever determined to within a few tens of percent, this will pin down the value of η very accurately because the predicted D abundance is a very steeply varying function of η. Until then, it is very likely that not much progress will be made in determining the baryon-to-photon ratio using Big Bang nucleosynthesis. Nevertheless, as previously mentioned, there now seems to be some real hope that it will actually be possible to measure the primordial deuterium abundance within the foreseeable future.

Note that in Chapters 5-8 nucleosynthesis limits will be used several times to constrain models of neutrinos. However, for historical reasons the limits used in the different chapters do not necessarily coincide, but rather reflect the

observational status at the time where the specific paper was written. None of the conclusions change in any significant way by using the most up to date observational values.

Chapter IV

Dirac and Majorana Neutrino Interactions

Neutrinos are an integral part of the standard model of particle physics. They are spin-1/2 leptons without electromagnetic charge. As far as we know they are also massless although there is no fundamental reason why this should be so. In fact there are a number of indications that neutrinos have non-zero masses. These all come from the fact that if neutrinos are massive the different flavour states can mix because these flavour states do not necessarily correspond to mass eigenstates.

The first piece of evidence is from the solar neutrinos [25]. Neutrinos emitted from the Sun through the *pp* reaction can be observed on earth using different techniques. A common feature of all these experiments is that fewer neutrinos than expected from standard solar model calculations are seen. It also appears that there is no astrophysical solution to this problem in the sense that no solar models have been able to solve this discrepancy in a satisfactory way. The trouble is that the neutrino emission is very sensitive to the central temperature of the Sun, but if that is changed in order to explain the neutrino flux, other visible effects will occur. The explanation that seems most likely is that the electron neutrinos emitted from the Sun mix with muon neutrinos which are not observed on earth, so that this appears as an apparent deficit in the number of neutrinos emitted.

The second place where evidence for neutrino mass is thought to be seen is the atmospheric neutrinos [26]. These are produced by cosmic rays that interact with nuclei in the atmosphere to produce ν_e, ν_μ and the corresponding antineutrinos. Water Cerenkov detectors like Super-Kamiokande see a strong deficit in the number of the observed $\nu_\mu - \nu_e$ ratio compared with the expected flux and this can again be taken as evidence for neutrino oscillations. The last indication is from the accelerator experiment at the LSND facility [27]. In this case evidence for neutrino oscillations is claimed from a $\overline{\nu}_\mu$ beam.

There has been a large number of terrestrial experiments looking for neutrino masses. For ν_e, the endpoint of the tritium decay spectrum is used to look for a non-zero mass, both because the decay is very simple and the Q value is very low (Q = 14.3 keV) [28]. A small neutrino mass should show up as a deficit

in the electron spectrum near the endpoint energy. However, it turns out that there is apparently a small surplus of electrons in this region corresponding to a negative neutrino mass squared. This mystery has been tried resolved for example by invoking interactions with cosmic background neutrinos, but this effect should be too small by many orders of magnitude to explain the observed effect. So far no good explanation has been produced.

For ν_μ, the pion decay $\pi^+ \to \mu^+\nu_\mu$ has been used to constrain the ν_μ mass. This is done by measuring the decay energy spectrum of the decay product muons [29].

To measure the ν_τ mass, decay of τ leptons is used. The specific decay is $\tau \to 5\pi^\pm\pi^0\nu_\tau$ and the measured quantities are the invariant mass as well as the energy of the hadronic decay products [30]. Altogether, the present upper mass limits are

$$m_{\nu_e} \leq 15\text{eV[7]} \tag{4.1}$$
$$m_{\nu_\mu} \leq 170\text{keV[29]} \tag{4.2}$$
$$m_{\nu_\tau} \leq 24\text{MeV[30]} \tag{4.3}$$

4.1 Definition and Properties of Neutrino Fields [1]

Only two physical neutrino states are known, the left handed neutrino and the right handed anti neutrino. The other fermions are known to be Dirac particles, having both left and right handed particles and antiparticles, but possibly neutrinos are describable in a theory containing only two components. We distinguish between these two fundamental ways of building the theory of neutrinos, the four component Dirac neutrino and the two component Majorana neutrino. Let us start out from the definition of the neutrino fields. The Dirac field is defined in the same way as for the other fermions

$$\psi_D = \int \frac{d^3p}{2E(2\pi)^3} \sum_s \left[f_s u_s e^{-ip\cdot x} + \overline{f}_s^\dagger v_s e^{ip\cdot x} \right], \tag{4.4}$$

where u and v are the plane wave solutions to the Dirac equation for positive and negative energy respectively

$$(\gamma^\mu p_\mu - m)u_s(\mathbf{p}) = 0 \tag{4.5}$$
$$(-\gamma^\mu p_\mu - m)v_s(\mathbf{p}) = 0. \tag{4.6}$$

f_s is the particle annihilation operator and $\overline{f}_s^\dagger$ is the creation operator for antiparticles

$$f_s(\mathbf{p})|\mathbf{p},\mathbf{s}\rangle = |0\rangle \tag{4.7}$$
$$\overline{f}_s^\dagger(\mathbf{p})|\mathbf{0}\rangle = \overline{|\mathbf{p},s\rangle}. \tag{4.8}$$

[1] This section borrows heavily from Ref. [31].

We use the standard normalisation of the Dirac spinors

$$u_s^\dagger(\mathbf{p})u_{s'}(\mathbf{p}) = 2E\delta_{ss'} \quad (4.9)$$
$$v_s^\dagger(\mathbf{p})v_{s'}(\mathbf{p}) = 2E\delta_{ss'} \quad (4.10)$$
$$v_s^\dagger(\mathbf{p})u_{s'}(\mathbf{p}) = 0 \quad (4.11)$$

The Majorana field, on the other hand, is defined using only two components

$$\psi_D = \int \frac{d^3p}{2E(2\pi)^3} \sum_s \left[f_s u_s e^{-ip\cdot x} + \lambda f_s^\dagger v_s e^{ip\cdot x} \right], \quad (4.12)$$

where λ is a phase called the creation phase factor. It can be chosen at will, but it is not always advantageous to choose it as $\lambda = 1$. For this reason it is usually kept as a free parameter to define. The obvious difference between Dirac and Majorana fields is that the Majorana field is defined by only two components. Essentially this must also mean that a Majorana particle is its own antiparticle. To show this we need a few definitions. We start with a spinor field, $\psi(x)$. Under a Lorentz tranformation

$$x'^\mu = x^\mu + \omega^\mu_\nu x^\nu, \quad (4.13)$$

the spinor field transforms as [32]

$$\psi'(x') = \exp\left(\frac{i}{4}\sigma_{\mu\nu}\omega^{\mu\nu}\right)\psi(x), \quad (4.14)$$

where

$$\sigma_{\mu\nu} = \frac{i}{2}[\gamma_\mu, \gamma_\nu]. \quad (4.15)$$

To define a conjugate field that transforms in this way it is not enough to use ψ^*. The reason is that ψ^* does not transform in the same way as ψ under Lorentz transformations, instead it obeys the transformation law

$$\psi^{*'}(x') = \exp\left(-\frac{i}{4}\sigma^*_{\mu\nu}\omega^{\mu\nu}\right)\psi^*, \quad (4.16)$$

which is not the same as Eq. (4.14). We define the conjugate field as

$$\overline{\psi} \equiv C'\gamma_0\psi^*, \quad (4.17)$$

where, by ψ^*, we mean the column vector

$$\psi^* = \begin{pmatrix} \psi_1^\dagger \\ \psi_2^\dagger \\ \psi_3^\dagger \\ \psi_4^\dagger \end{pmatrix}.$$

C' is some operator which will, in a moment, be identified with the charge conjugation operator. For consistency C' must obey the condition

$$-C'\gamma_0\sigma^*_{\mu\nu} = \sigma_{\mu\nu}C'\gamma_0. \tag{4.18}$$

So far we have not discussed things in a specific representation basis, but we now shift to the Dirac representation in which

$$\gamma_0 = \begin{bmatrix} I & 0 \\ 0 & -I \end{bmatrix} \qquad \gamma_i = \begin{bmatrix} 0 & \sigma_i \\ -\sigma_i & 0 \end{bmatrix}, \tag{4.19}$$

where σ_i are the Pauli matrices. In this basis we can choose $C' = i\gamma_2\gamma_0$ so that it obeys the condition, Eq. (4.18). Under the operation of charge conjugation any fermion field transforms as

$$C\psi C^{-1} = \eta^*_C C\gamma_0\psi^*, \tag{4.20}$$

where η_C is a phase factor. Let us now check the effect of using our operator C on the Dirac field to see that we can indeed make the identification $C' = C$. We do this by assuming $C' = C$ and from there show that this identification makes sense. The right hand side of Eq. (4.20) gives

$$\eta^*_C C\gamma_0\psi^* = \eta^*_C i\gamma_2\psi^* \tag{4.21}$$

and, if we use the plane wave expansion,

$$\eta^*_C C\gamma_0\psi^* = \eta^*_C \int \frac{d^3p}{2E(2\pi)^3} \sum_s \left[\overline{f}_s u_s e^{ip\cdot x} + f^\dagger_s v_s e^{-ip\cdot x}\right], \tag{4.22}$$

since

$$\gamma_2 u^* = v \tag{4.23}$$
$$\gamma_2 v^* = u. \tag{4.24}$$

On the other hand, the left hand side gives

$$C\psi^D C^{-1} = \int \frac{d^3p}{2E(2\pi)^3} \sum_s \left[C f_s C^{-1} u_s e^{ip\cdot x} + C\overline{f}^\dagger_s C^{-1} v_s e^{-ip\cdot x}\right]. \tag{4.25}$$

Putting the two equations together we obtain the following relations for the creation and annihilation operators

$$C f_s C^{-1} = \eta^*_C \overline{f}_s \tag{4.26}$$
$$C f^\dagger_s C^{-1} = \eta_C \overline{f}^\dagger_s. \tag{4.27}$$

The effect of C on a state $|\mathbf{p}, s\rangle$ is then

$$C|\mathbf{p}, s\rangle = \eta_C \overline{|\mathbf{p}, s\rangle}. \tag{4.28}$$

Altogether then, this means that the effect of C' is to change a physical state into a corresponding state for the antiparticle, justifying our identification of the operator C' with the charge conjugation operator C.

Finally, we are now ready to apply the same procedure to the Majorana field. Here, one finds that

$$C\psi^M C^{-1} = (\eta_C \lambda)^* \psi^M, \tag{4.29}$$

where we have used our plane wave definition of the Majorana field, Eq. (4.12). The Majorana field is thus, apart from a phase factor, invariant under charge conjugation. In exactly the same way as for the Dirac field one may show that the following relations hold for the creation and annihilation operators,

$$\begin{aligned} C f_s C^{-1} &= \eta_C \lambda f_s & (4.30)\\ C f_s^\dagger C^{-1} &= \eta_C \lambda f_s^\dagger. & (4.31) \end{aligned}$$

If we now apply this to a free Majorana state we get

$$C|\mathbf{p}, s\rangle = \eta_C \lambda |\mathbf{p}, s\rangle, \tag{4.32}$$

so we see that a free Majorana state is an eigenstate of charge conjugation. Similar relations apply for CP and CPT, specifically for CPT one finds the relation

$$CPT|\mathbf{p}, s\rangle = \eta_{CPT} \lambda (-1)^{s-1/2} |\mathbf{p}, -s\rangle, \tag{4.33}$$

where η_{CPT} is again a phase. This indeed means that the left and right handed states are particle and anti particle in the usual sense, since application of the CPT operator on a left handed Majorana state turns it into a right handed state with the same momentum.

4.2 Neutrino Weak Interactions

Let us now look at the interactions of neutrinos to see the difference between Dirac and Majorana neutrinos. At sufficiently low energies, neutrinos interact via a current-current interaction because of the large masses of the gauge bosons ($W^\pm, Z^0$) so that the weak hamiltonian density to lowest order in the coupling constant has the form

$$\mathcal{H}_{\text{weak}} = \frac{G_{\text{F}}}{\sqrt{2}} j_\mu(x) j^\mu(x). \tag{4.34}$$

This interaction is described by the standard $V - A$ theory. In the present work we are only interested in purely leptonic interactions, meaning that the terms we are interested in are the leptonic charged current

$$j_\mu^{CC} = \sum_{e,\mu,\tau} \overline{\psi}_i(x) \gamma_\mu (1 - \gamma_5) \psi_{\nu_i}(x), \tag{4.35}$$

the charged fermion neutral current

$$j_\mu^{NC} = \sum_{e,\mu,\tau} \overline{\psi}_i(x)\gamma_\mu(g_V - g_A\gamma_5)\psi_i(x), \tag{4.36}$$

and the neutrino neutral current

$$j_\mu^{NC} = \sum_{e,\mu,\tau} \overline{\psi}_{\nu_i}(x)\gamma_\mu(1 - \gamma_5)\psi_{\nu_i}(x). \tag{4.37}$$

g_V and g_A are the charged fermion vector and axial vector neutral current couplings respectively. They are given in terms of the Weinberg angle, $\sin^2\Theta_{\rm W} = 0.2325 \pm 0.0008$, as

$$C_V = -\frac{1}{2} + 2\sin^2\Theta_{\rm W} \tag{4.38}$$

$$C_A = -\frac{1}{2}. \tag{4.39}$$

The S matrix is then given by

$$S = 1 - i\int d^4x\mathcal{H}_{\rm weak}, \tag{4.40}$$

and from this all matrix elements are calculable.

There is no *a priori* reason why Dirac and Majorana neutrinos should behave the same under these interactions. However, because of the left handedness of the weak interactions it turns out that interactions that are different for Dirac and Majorana neutrinos always scale as some power of neutrino mass. This means that for massless neutrinos, Dirac and Majorana neutrinos are indistinguishable. However, if neutrinos are massive Dirac and Majorana neutrinos behave differently. For example there is no conserved lepton number if neutrinos are Majorana particles because neutrinos can flip their spin direction and thereby violate lepton number by two units. If we look at Majorana neutrinos, it is straightforward to show that they possess no neutral current vector interactions. This is true because of the relation

$$\overline{\psi^c}\gamma_\mu\psi^c = -\overline{\psi}\gamma_\mu\psi, \tag{4.41}$$

which holds for any fermion field. However, since the majorana field is invariant under C up to a phase this implies that

$$\overline{\psi^M}\gamma_\mu\psi^M = -\overline{\psi^M}\gamma_\mu\psi^M = 0 \tag{4.42}$$

Furthermore, there is the difference that the Majorana field ψ^M can both create and destroy neutrino states as opposed to the Dirac field ψ^M that only contains the annihilation operator for neutrinos.

One should perhaps think that this difference leads to observable effects even for massless neutrinos. However, for massless neutrinos there is no detectable

difference between Majorana and Dirac neutrinos. Neutrinos are either created in pairs via neutral current reactions or as a single neutrino or anti-neutrino via charged current reactions. In the case of neutral current reactions, the neutrino pair is not born with definite helicity. This has nothing to do with lack of vector current interactions but is rather an effect of wave packet superposition, and is independent of whether neutrinos are of Dirac or Majorana type. We now look at the detection of neutrinos created via neutral current reactions. Since the charged current is still left handed even for Majorana neutrinos, if these neutrinos are detected via charged current reactions, only the left handed component will interact and one therefore detects either particles or antiparticles, but not both. The left handedness of the charged current thus "reintroduces" the vector current for Majorana neutrinos, making them behave as Dirac particles. This means that there is absolutely no detectable difference between Dirac and Majorana neutrinos in this case. If they are detected via neutral current reactions, there is no way to measure their helicity anyway and, again, there is no detectable difference. Next, we look at neutrinos created via charged current reactions. These are born with definite helicity and, even if detected by neutral current reactions, still behave as if they do possess vector neutral current interactions because of the definite helicity of their initial state.

Also, of course, the two superfluous states for Dirac neutrinos, the right handed neutrino and the left handed anti neutrino are completely sterile if neutrinos are massless because of the $(1-\gamma_5)$ factor in the weak current. Thus they are not relevant for the massless standard model neutrinos.

This discussion about the possible differences between Dirac and Majorana neutrinos have given rise to some discussion recently [33]. It was claimed that the measurement of the $\nu_\mu - e$ vector neutral current coupling constant by the CHARM II collaboration [35] giving

$$C_V = -0.035 \pm 0.017, \tag{4.43}$$

excludes the neutrino as being a Majorana particle [34]. In light of the discussion above this cannot be the case of course, since the muon neutrinos observed by CHARM II are produced by the charged current decays of charged kaons and pions [35] and therefore they are born with definite helicity. Therefore they are observed as having vector current interactions even if they are Majorana particles.

For massive neutrinos, the situation is much more complex. Here, all the four states for Dirac neutrinos are active so that Majorana and Dirac neutrinos behave differently. Also their weak interaction cross sections are different. In the early Universe it is therefore important to distinguish between Dirac and Majorana neutrinos if their mass sufficiently large. For Dirac neutrinos, if the mass is below roughly 0.2-0.3 MeV the two "sterile" states decouple prior to the QCD phase transition so that their number density is diluted by a large factor because of the entropy release from the phase transition. In this case they do not contribute to the cosmic energy density during nucleosynthesis. Also, the mass is then sufficiently low that the Dirac and Majorana annihilation cross sections

are practically identical until long after they have decoupled. Therefore, at these low masses the two types are again indistinguishable. For higher masses one needs to do a full calculation for all four states of Dirac neutrinos, and one can expect that Dirac and Majorana neutrinos have a completely different impact on nucleosynthesis. In Fig. 4.1 we show the relic number density of massive neutrinos during nucleosynthesis times neutrino mass. This is a good measure of the energy density contributed during BBN by a massive neutrino, either Majorana or Dirac. It is seen that the Dirac neutrino in most of the mass region contributes much more than the corresponding Majorana neutrino because it has four interacting states. For large masses, however, the Majorana annihilation cross section is smaller than the Dirac one so that the Majorana neutrinos actually contribute more to the cosmic energy density. The cross section for annihilation into massless final states is for non-relativistic neutrinos given by

$$\langle\sigma|v|\rangle_{\rm Dirac} = \frac{G_{\rm F}^2 m^2}{2\pi}\sum_i (C_{V,i}^2 + C_{A,i}^2) \tag{4.44}$$

$$\langle\sigma|v|\rangle_{\rm Majorana} = \frac{G_{\rm F}^2 m^2}{2\pi}\sum_i 8\beta^2 (C_{V,i}^2 + C_{A,i}^2)/3 \tag{4.45}$$

where β is the relative velocity of the incoming particles. This shows the strong difference between Dirac and Majorana neutrinos in the non-relativistic limit. The cross section is velocity dependent for Majorana neutrinos whereas it is not for Dirac neutrinos. As the neutrino kinetic energy becomes smaller and smaller relative to the mass the Dirac cross section is increased relative to the Majorana one, and this is the reason why very heavy Majorana neutrinos contribute more than Dirac neutrinos at high mass.

In the remainder of this work we shall only be concerned with Majorana type neutrinos. The good thing about these is that one need only consider the two usual states. Furthermore, since there is very little lepton asymmetry in the early Universe, Majorana neutrinos effectively behave as one single unpolarised particle species. Interaction cross sections and the like are therefore relatively easy to calculate in this case.

4.3 Mixed Neutrinos

If neutrinos are massive they may in principle mix. The reason is that the states produced by the weak interaction are not necessarily mass eigenstates. In general there exists a unitary transformation between the weak interaction (flavour) eigenstates and the mass eigenstates

$$|\nu_f\rangle = U|\nu_m\rangle, \tag{4.46}$$

where U is a unitary matrix. Therefore, if neutrinos have mass, the freely propagating neutrinos may oscillate between different flavours. This is very

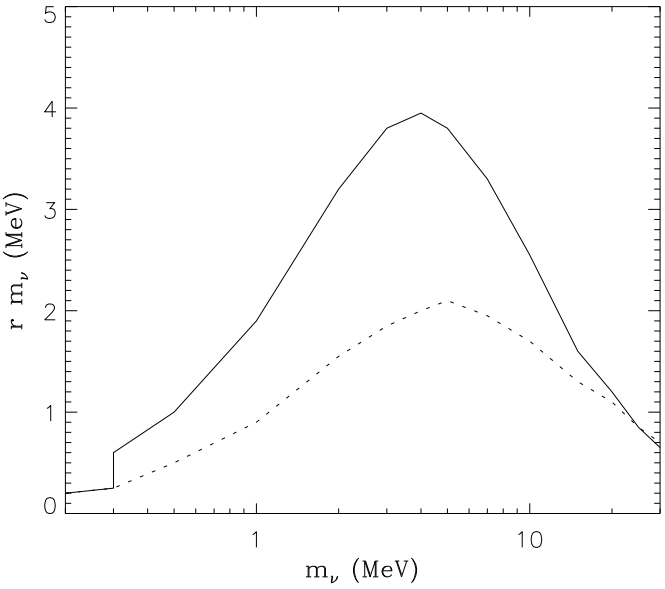

Figure 4.1: The number relic number density times mass of a massive neutrino, defined in units of the number density of a massless neutrino species $rm \equiv n/n(m=0)\times m$. The full line is for Dirac neutrinos and the dotted for Majorana neutrinos. The discontinuity at $m \simeq 0.3$ MeV for Dirac neutrinos indicate that above this mass all four states are in equilibrium below the QCD phase transition temperature. The figure has been reprinted from Ref. [36].

important for our understanding for example of the solar neutrino problem. They are of course potentially very interesting for BBN as well. However in the present work we shall not deal with neutrino oscillations at all. We shall be looking at mixed neutrinos in the context of neutrino decays but neglect the possible oscillations between flavours. This particular area is, however, definitely worthy of further study.

4.4 Decaying Neutrinos

In the standard model neutrinos do not have mass and therefore they are absolutely stable. However, once a mass term is introduced this is no longer so. Also, if the mass is larger than roughly 100 eV for any neutrino it must be unstable with a lifetime shorter than the Hubble expansion time in order not to overclose the Universe [36], but there are many possible decay modes for such

neutrinos. For example within the standard model the decay $\nu_i \to \nu_e e^+ e^-$ is possible at tree level provided that $m_{\nu_i} \geq 2m_e$ and that the mixing amplitude between the two neutrino flavours is different from zero. Another possibility is the neutrino radiative decay $\nu_i \to \nu_j \gamma$ which is mediated by interactions at loop level. If there exists a flavour violating neutral current there is also the decay to a three neutrino final state $\nu_i \to \nu_j \nu_k \overline{\nu}_k$. Further beyond the standard model there are decays like $\nu_i \to \nu_j \phi$ where ϕ is some new particle like the majoron.

There is a large number of models for physics beyond the standard model that predict different neutrino lifetimes to the different decay modes. Our approach will be to discuss the experimental limits to the different decay modes, not so much to go into specific physical models of neutrino decays.

We start out with the simplest possible decay, namely $\nu_i \to \nu_e e^+ e^-$. This decay mode is relatively easy to constrain because the decay products interact electromagnetically. If we restrict ourselves to the three known neutrino generations only the τ neutrino mass is not required to be below the threshold for this decay mode. Within the standard model the decay lifetime is given by [11]

$$\tau^{-1} = 3.5 \times 10^{-5} |U_{e\tau}|^2 m_{\mathrm{MeV}}^5 \Phi(m_{\nu_\tau}^2/m_e^2)\,\mathrm{s}^{-1}, \tag{4.47}$$

where $|U_{e\tau}|$ is the mixing between electron and tau neutrino and Φ is a phase space factor dependent on the tau neutrino mass

$$\begin{aligned} \Phi(q) &= (1-4q)^{1/2}(1-14q-2q^2-12q^3) + \\ &\quad 24q^2(1-q^2)\ln\left(\frac{1+(1-4q)^{1/2}}{1-(1-4q)^{1/2}}\right). \end{aligned} \tag{4.48}$$

Strong limits on this decay come from SN1987A because of the very intense tau neutrino production from this source. Furthermore a tau neutrino with mass in the relevant region should decay sufficiently early that the decay products do not overclose the Universe. These limits have been summarised by Raffelt [11] and effectively this decay mode has been excluded by existing data. In Fig. 4.2 we show the excluded regions for this decay from both SN1987A, cosmological and other constraints.

Next we turn to the radiative decay of heavy neutrinos, $\nu_i \to \nu_j \gamma$. Unless the neutrino possesses a small electromagnetic charge the radiative decay of neutrinos proceed via loop graphs. Therefore the decay lifetime is exceedingly long in all viable models that have so far been constructed. From an argument using the cooling of red giant stars it is possible to constrain severely the charge of neutrinos. The reason is that if neutrinos do possess charge they couple to the photon at tree level and therefore plasma excitations can produce neutrino pairs at a much higher rate than in the standard model. This leads to a very fast cooling of stars, in conflict with observations. From this argument an upper bound of $q_\nu \leq 2 \times 10^{-14} e$ on the neutrino charge can be derived [11]. In conclusion it does not seem possible to construct models that predict neutrino radiative decay lifetimes shorter than the lifetime of the Universe.

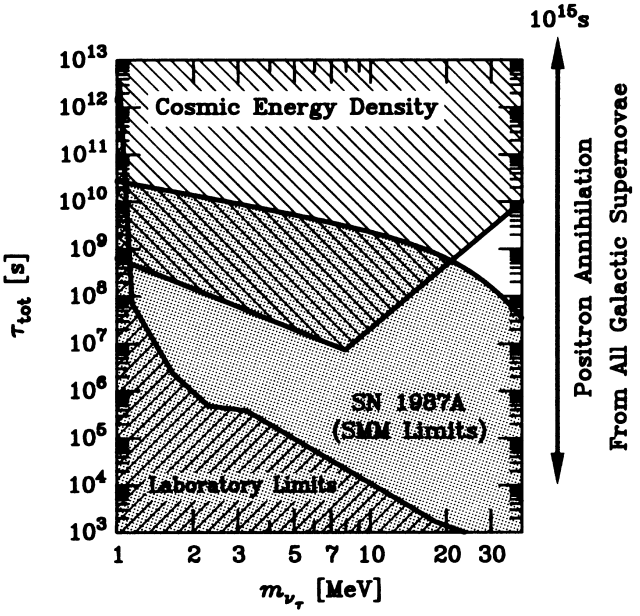

Figure 4.2: Exclusion plot for the decay $\nu_\tau \to \nu_e e^+ e^-$. The excluded region indicated by the arrow to the right is from limits to the galactic positron annihilation line flux. This figure has been reproduced from Ref. [11].

The radiative decay is relatively easy to constrain experimentally because of the emitted photon that interacts electromagnetically. In the most general case the decay rate can be expressed in terms of an effective electromagnetic transition moment, μ_ν, as

$$\tau^{-1} = \mu_\nu^2 \frac{m^3}{8\pi}. \tag{4.49}$$

Bounds can be placed on this transition moment from observations of SN1987A. These come from the gamma ray observations made by the solar maximum mission satellite and have been discussed in great detail by for example Raffelt [11].

However, the most interesting limits come from cosmological considerations, especially from observations of the cosmic microwave background and the diffuse photon background. These mainly concern neutrinos with long lifetime, but since it is probably impossible to construct viable physical models that predict short neutrino lifetimes to radiative decay this is exactly the region we are interested in constraining. The relevant limits have been compiled by for example Kolb and Turner [36]. Fig. 4.3 shows the excluded regions reproduced from

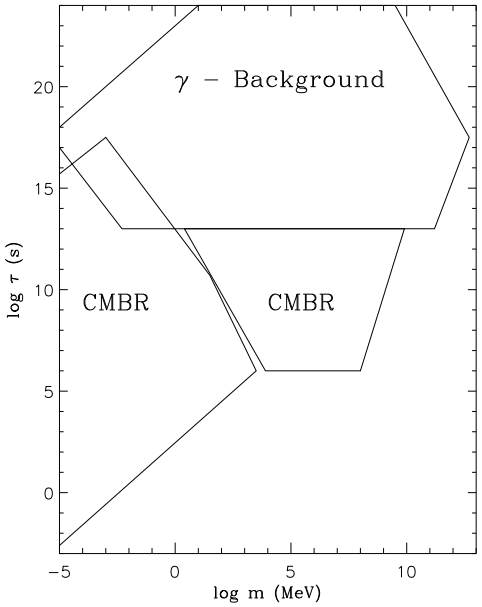

Figure 4.3: Exclusion plot for radiative decay of neutrinos from cosmological considerations. The excluded regions are within the boxes. This figure has been reproduced from Ref. [36].

[36].

If we discard the cosmologically allowed region for low masses on the theoretical grounds discussed above, and use the 24 MeV upper limit on allowed neutrino masses, the only allowed region is in the upper left corner of Fig. 4.3. Thus, the lifetime to radiative decay is constrained to be larger than 10^{18} s, meaning that this particular decay mode is completely uninteresting for BBN. However, such a neutrino may still be interesting for other reasons, for example as an explanation of the Gunn-Peterson effect [37]. Observations indicate that at high redshift a surprisingly small fraction of the hydrogen is in the form of neutral hydrogen and this is what is usually referred to as the Gunn-Peterson effect. This lack of neutral hydrogen indicates some ionising source which may be an early generation of stars. Another explanation could be a massive neutrino with mass just large enough to ionise hydrogen, decaying on a timescale of roughly 10^{23} s [38].

As for the decay to a three neutrino final state, this is very difficult to constrain experimentally because the decay products are invisible. However, it of course requires the existence of a flavour violating neutral current. Such a

current would also give rise to processes like $\mu^- \to e^- e^+ e^-$ which are strongly constrained experimentally [39]. The best constraints on the decay itself come from BBN considerations, the most recent calculation being that of Dodelson, Gyuk and Turner [40]. In general neutrinos with mass in the MeV region are excluded if their lifetime is too long. For very light neutrinos ($m \ll$ MeV) BBN does not in general exclude this type of decay because it only becomes important after BBN has already taken place.

Finally, in the present work we shall only deal with neutrino decays of the type $\nu_i \to \nu_j \phi$. Exactly as for the previous decay mode to three neutrinos this decay mode is of course not easy to constrain since the decay products are invisible. For the class of models called majoron models the above coupling to ϕ also leads to processes like neutrinoless double beta decay and from this some constraints can be put on the possible decay strength. However, these are very weak and at the moment the best constraints come from the BBN considerations discussed in more detail in Chapters 7 and 8.

Chapter V

Neutrino decoupling in the Standard Model

Essentially all of this chapter has appeared as the paper *Neutrino Decoupling in the Early Universe*, Phys. Rev. D **52**, 1764 (1995).

Nonequilibrium thermodynamics is fundamental to the understanding of the early Universe. There are many examples of this, the quark-hadron phase transition, the electroweak phase transition, inflation etc. Another example is the decoupling of neutrinos from the electromagnetic plasma at a temperature of a few MeV. The normal assumption [36] is that neutrinos decouple completely before the temperature approaches the mass of the electron. When the temperature gets below the electron rest mass, the electrons and positrons annihilate and pump energy and entropy into other particles. But since the neutrinos are decoupled they do not share in this transfer. Their final distribution is therefore still described by an equilibrium distribution, but with a lower temperature than the photon temperature, $T_\nu = (4/11)^{1/3} T_\gamma$.

However, this is not the complete story. The fact that the decoupling temperature is of the same order as the electron mass means that neutrinos must, to some degree, share the entropy transfer. This phenomenon is known as neutrino heating. Because it has consequences for Big Bang Nucleosynthesis, it has been investigated many times in the literature [41–45]. All of these investigations have found that the change in neutrino energy density is of the order 1 %, relative to the standard case where total decoupling is assumed. This is too small a change to have any noticeable effect on nucleosynthesis.

One possible problem is, however, that they all assume that Boltzmann statistics is a good approximation for all particle distribution functions. This means that effects that depend on quantum statistics, such as Pauli blocking of final states, are neglected. Furthermore they also neglect the electron mass in the weak interaction matrix elements. This approximation is valid as long as the temperature is high, but possibly not when it is comparable to, or lower than, the electron mass.

Since the neutrino distributions are important both for nucleosynthesis and

structure formation models, it is of considerable interest to see if neutrino heating has any consequences for either.

5.1 Fundamental Equations

As explained in Chapter 2, the equation necessary to describe all the different particle interactions is the Boltzmann equation. Since we are looking at standard weak interactions at low energy, all processes can be calculated using simple V-A theory as explained in Chapter 4. To first order in the weak coupling constant, G_F, all interactions are two-particle scatterings and annihilations and the matrix elements therefore are all of the same type. As an example we show the matrix element for the neutral current process $\nu_i\nu_j \to \nu_i\nu_j$,

$$M = \frac{G_{\rm F}}{\sqrt{2}}\overline{u}_{\nu_i}\gamma_\mu\frac{1-\gamma_5}{2}u_{\nu_i}\overline{u}_{\nu_j}\gamma^\mu\frac{1-\gamma_5}{2}u_{\nu_j}. \tag{5.1}$$

All the possible reactions and their corresponding matrix elements have been summarised in Tables 5.1 and 5.2. Higher order corrections to these matrix elements as well as electromagnetic corrections from plasma processes are neglected. The collision integral on the right hand side of the Boltzmann equation then has the form given in Eq. (2.29). Assuming standard weak interactions as described in Chapter 4, it is possible to analytically integrate this 9 dimensional integral down to two dimensions (Appendix B). This makes the integral much easier to evaluate numerically.

The problem now is to evaluate $R(t)$. This can basically be done in two ways, using either entropy or energy conservation (see Chapter 2). As explained in Ref. [46], the end result is almost the same for massless neutrinos.

5.2 Numerical Results

We have solved the coupled Boltzmann equations together with the entropy conservation equation to obtain numerical results. The equations were solved numerically by using a grid of 35 points in momentum space and a Runge-Kutta integrator to evolve the relevant quantities forward in time. To compare with previous results, we have solved for several different cases: 1. $m_e \neq 0$ and FD statistics; 2. $m_e = 0$ and FD statistics; 3. $m_e \neq 0$ and MB statistics; 4. $m_e = 0$ and MB statistics. In all cases we assume zero chemical potentials for the particles involved at the initial temperature. Case 4 is the approximation used in previous studies. Case 1 is the correct approach.

For each of these scenarios we have calculated the energy density deviation, defined as $\delta\rho_\nu/\rho_\nu = (\rho_\nu - \rho_{\nu_0})/\rho_\nu$, as a function of the photon temperature T_γ. ρ_{ν_0} is the energy density of a neutrino species that has decoupled long before $e^\pm$ annihilation.

For electron neutrinos, the result is shown in Fig. 5.1, whereas Fig. 5.2 shows the result for muon and tau neutrinos. In the limit of MB statistics and zero

Table 5.1: Possible electron neutrino processes and the corresponding matrix elements for massless Dirac neutrinos. 1 is defined equal to the particle for which we calculate $C_{\rm coll}$. 2 is the other incoming particle. 3 is defined as either particle 1 going out (scattering) or the outgoing lepton (annihilation). 4 is defined as either particle 2 going out (scattering) or the outgoing antilepton (annihilation). We have introduced the quantities $C_V = \frac{1}{2} + 2\sin^2\theta_W$ and $C_A = \frac{1}{2}$, where $\sin^2\theta_W \approx 0.23$. p_i is the four-momentum of particle i.

Process	$S \mid M \mid^2$
$\nu_e + \overline{\nu}_e \to \nu_e + \overline{\nu}_e$	$128G_F^2(p_1\cdot p_4)(p_2\cdot p_3)$
$\nu_e + \nu_e \to \nu_e + \nu_e$	$32G_F^2(p_1\cdot p_2)(p_3\cdot p_4)$
$\nu_e + \nu_i \to \nu_e + \nu_i$	$32G_F^2(p_1\cdot p_2)(p_3\cdot p_4)$
$\nu_e + \overline{\nu}_i \to \nu_e + \overline{\nu}_i$	$32G_F^2(p_1\cdot p_4)(p_2\cdot p_3)$
$\nu_e + e^- \to \nu_e + e^-$	$32G_F^2[(C_A+C_V)^2(p_1\cdot p_2)(p_3\cdot p_4)+$ $(C_A-C_V)^2(p_1\cdot p_4)(p_2\cdot p_3)-$ $(C_V^2-C_A^2)m_e^2(p_1\cdot p_3)]$
$\nu_e + e^+ \to \nu_e + e^+$	$32G_F^2[(C_A+C_V)^2(p_1\cdot p_4)(p_2\cdot p_3)+$ $(C_A-C_V)^2(p_1\cdot p_2)(p_3\cdot p_4)-$ $(C_V^2-C_A^2)m_e^2(p_1\cdot p_3)]$
$\nu_e + \overline{\nu}_e \to e^- + e^+$	$32G_F^2[(C_A+C_V)^2(p_1\cdot p_4)(p_2\cdot p_3)+$ $(C_A-C_V)^2(p_1\cdot p_3)(p_2\cdot p_4)+$ $(C_V^2-C_A^2)m_e^2(p_1\cdot p_2)]$
$\nu_e + \overline{\nu}_e \to \nu_i + \overline{\nu}_i$	$32G_F^2(p_1\cdot p_4)(p_2\cdot p_3)$

electron mass (case 4), we reproduce the results of Ref. [41] to within 10-15%. This is quite reassuring, as we use a completely different procedure for solving the Boltzmann equations. Dodelson and Turner [41] used a first order perturbation expansion,

$$f_{\nu_i}(p,t) = f_0(p) + \Delta_{\nu_i}(p,t), \tag{5.2}$$

and

$$T_\gamma = T_\nu(1+\delta(t)). \tag{5.3}$$

They then solved the perturbation equations for $\Delta_{\nu_i}(p,t)$ and $\delta(t)$.

Using the correct quantum statistics and non-zero electron mass (case 1), the final result for the deviation in energy density is roughly

$$\begin{array}{ll} 0.83\% & \text{for } \nu_e \\ 0.41\% & \text{for } \nu_\mu, \nu_\tau \end{array} \tag{5.4}$$

Generally, it is seen that the deviation is smaller if Fermi statistics is used. This is because the Pauli blocking factors in the collision integral, Eq. (2.30), dampen the interactions. Furthermore using the correct electron mass also lessens the deviation because the structure of the matrix elements changes.

Table 5.2: Possible μ, τ neutrino processes and matrix elements. The definition of particle numbers is the same as in table 5.1.

Process	$S \mid M \mid^2$
$\nu_i + \overline{\nu}_i \to \nu_i + \overline{\nu}_i$	$128 G_F^2 (p_1 \cdot p_4)(p_2 \cdot p_3)$
$\nu_i + \overline{\nu}_j \to \nu_i + \overline{\nu}_j$	$32 G_F^2 (p_1 \cdot p_4)(p_2 \cdot p_3)$
$\nu_i + \nu_i \to \nu_i + \nu_i$	$32 G_F^2 (p_1 \cdot p_2)(p_3 \cdot p_4)$
$\nu_i + \nu_j \to \nu_i + \nu_j$	$32 G_F^2 (p_1 \cdot p_2)(p_3 \cdot p_4)$
$\nu_i + \overline{\nu}_e \to \nu_i + \overline{\nu}_e$	$32 G_F^2 (p_1 \cdot p_4)(p_2 \cdot p_3)$
$\nu_i + \nu_e \to \nu_i + \nu_e$	$32 G_F^2 (p_1 \cdot p_2)(p_3 \cdot p_4)$
$\nu_i + e^- \to \nu_i + e^-$	$32 G_F^2 [(C_V + C_A - 2)^2 (p_1 \cdot p_2)(p_3 \cdot p_4) +$ $(C_A - C_V)^2 (p_1 \cdot p_4)(p_2 \cdot p_3) -$ $[(C_V - 1)^2 - (C_A - 1)^2] m_e^2 (p_1 \cdot p_3)]$
$\nu_i + e^+ \to \nu_i + e^+$	$32 G_F^2 [(C_V + C_A - 2)^2 (p_1 \cdot p_4)(p_2 \cdot p_3) +$ $(C_A - C_V)^2 (p_1 \cdot p_2)(p_3 \cdot p_4) -$ $[(C_V - 1)^2 - (C_A - 1)^2] m_e^2 (p_1 \cdot p_3)]$
$\nu_i + \overline{\nu}_i \to e^- + e^+$	$32 G_F^2 [(C_V + C_A - 2)^2 (p_1 \cdot p_4)(p_2 \cdot p_3) +$ $(C_A - C_V)^2 (p_1 \cdot p_3)(p_2 \cdot p_4) +$ $[(C_V - 1)^2 - (C_A - 1)^2] m_e^2 (p_1 \cdot p_2)]$
$\nu_i + \overline{\nu}_i \to \nu_e + \overline{\nu}_e$	$32 G_F^2 (p_1 \cdot p_4)(p_2 \cdot p_3)$
$\nu_i + \overline{\nu}_i \to \nu_j + \overline{\nu}_j$	$32 G_F^2 (p_1 \cdot p_4)(p_2 \cdot p_3)$

Apart from the changes in energy density, the shape of the distribution functions are changed from their equilibrium form. We parametrise this change by using an effective temperature for the neutrino distributions, defined as [41]

$$T_{\rm eff}^{\rm FD}(p) \equiv \frac{p}{\ln(1/f(p) - 1)} \tag{5.5}$$

for Fermi-Dirac statistics and

$$T_{\rm eff}^{\rm MB}(p) \equiv \frac{-p}{\ln f(p)} \tag{5.6}$$

for Maxwell-Boltzmann statistics.

Fig. 5.3 shows the effective temperature using Fermi statistics, both with and without electron mass incorporated. Note that the effective temperature of a completely decoupled neutrino is $T_\nu \simeq 0.714 T_\gamma$. Fig. 5.4 shows the same, but using Boltzmann statistics. Notice the general offset in effective temperature compared to Fig. 5.3. This is because the final effective temperature of a decoupled neutrino is $T_\nu \simeq 0.693 T_\gamma$ if Boltzmann statistics is used (see Chapter 2).

We see that, regardless of the statistics used, the effective temperature rises with momentum for medium and high momentum states. As noted in Refs. [41, 42], this is not surprising, because the weak cross sections are much larger for large momenta. The shape of the effective temperature curve is the same in

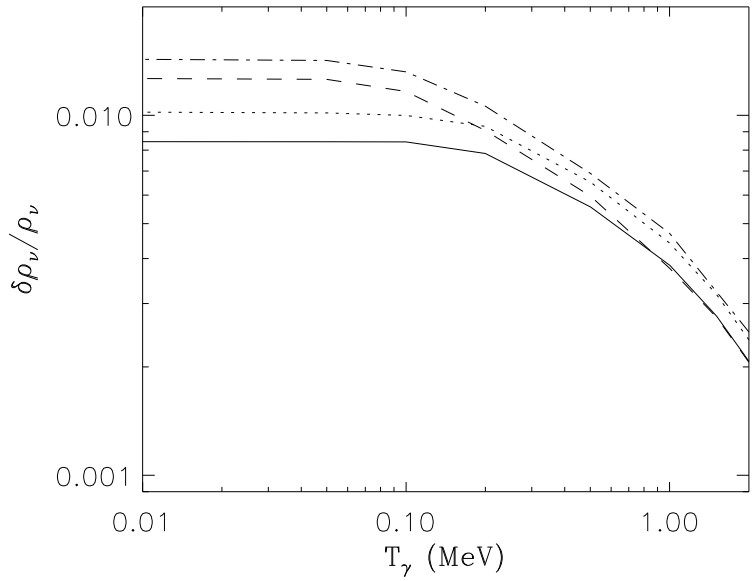

Figure 5.1: The evolution of $\delta\rho_\nu/\rho_\nu$ for electron neutrinos. The solid curve corresponds to case 1, the dashed to case 2, the dotted to case 3, and the dot-dashed to case 4.

all four cases, but the actual numerical values are slightly different, being higher if the electron mass is neglected in $C_{\rm coll}[f]$. This effect reflects that the neutrino energy density is slightly higher for massless electrons, as seen in Fig. 5.1.

5.3 Discussion and Conclusions

We have calculated the decoupling of massless neutrinos in the early Universe by solving the Boltzmann equations. Our method differs from previous studies in that it makes no approximations for the neutrino distribution functions and the weak interaction matrix elements. Although our results do not deviate dramatically from these previous calculations, we show that the inclusion of FD statistics and non-zero electron mass reduce the effect of neutrino heating on the relativistic neutrino energy density by almost 50% for ν_e, compared to the results of Dodelson & Turner [41].

We find that the neutrino distribution after decoupling is non-thermal at the 1% level. This is also in relatively good agreement with previous results [41, 42]. The effective temperature grows with momentum for medium and large

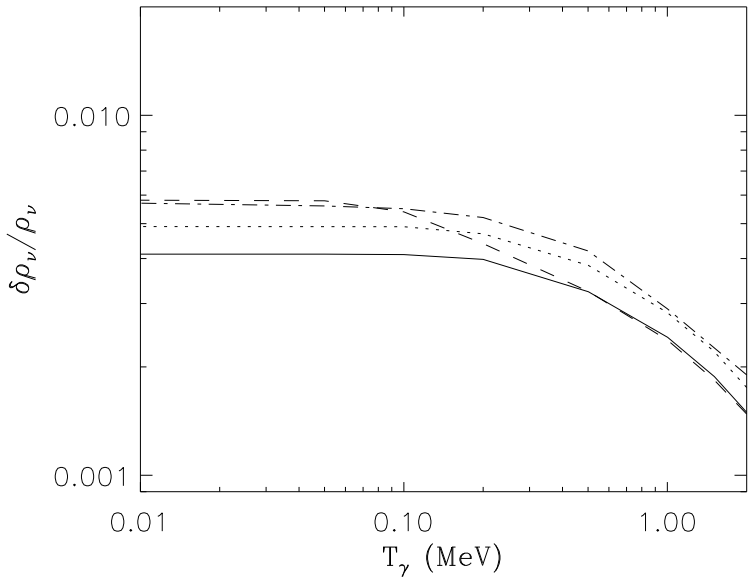

Figure 5.2: The evolution of $\delta\rho_\nu/\rho_\nu$ for muon and tau neutrinos. The curve labels are as in Fig. 1.

momenta, because of the momentum dependence of the weak interactions.

The slight heating of neutrinos relative to the standard scenario has consequences for Big Bang nucleosynthesis. We have changed the nucleosynthesis code of Kawano [47] to include the effect of neutrino heating. As discussed in Ref. [48], there are several effects that combine to change the nucleosynthesis scenario. First of all, the energy density in neutrinos is changed. However, this has the consequence of lowering the energy density in photons and $e^\pm$, because of energy conservation. The result is, if we use FD statistics and non-zero electron mass, that the photon temperature goes up because of $e^\pm$ annihilations by a factor of 1.3998 instead of the usual 1.4010 (a change of -0.09%). Furthermore, the weak rates are changed, because of the different abundances of $e^\pm$ and ν_e. With the relevant changes to the code, we obtain a change in the primordial ^{4}He abundance, Y_P, of $\Delta Y = +1.0 \times 10^{-4}$. This is in good agreement with Ref. [48]. They calculate a change of $+1.5 \times 10^{-4}$, but with a 50% larger neutrino heating. Other authors have found similar values [42, 43]. A change in ^{4}He abundance of $= +1.0 \times 10^{-4}$ is much below current observational accuracies. The systematic uncertainty in the primordial ^{4}He abundance is estimated to be as large as $\Delta Y_{\rm sys} = +0.016/-0.012$ [49], or more than a factor of 100 larger

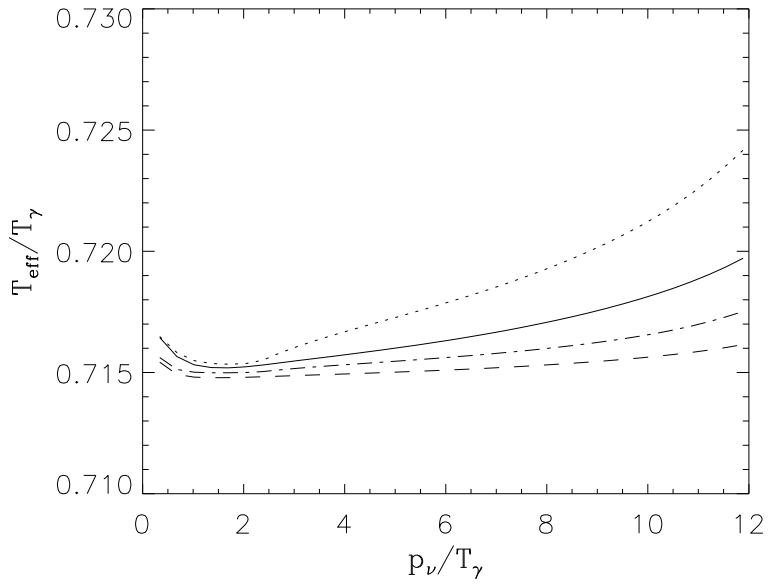

Figure 5.3: The effective neutrino temperature after complete $e^{\pm}$ annihilation, using FD statistics. The solid line is for ν_e and case 1, the dashed is for $\nu_{\mu,\tau}$ also case 1. The dotted is for ν_e and case 2, the dot-dashed for $\nu_{\mu,\tau}$ and case 2.

than the change induced by neutrino heating.

Another consequence of neutrino heating is that it increases the number density of neutrinos. If one of the neutrino species has a mass, it will therefore contribute slightly more than usually expected to Ω, the cosmological density parameter. In general, it is possible to put a mass limit on a light neutrino that is completely decoupled long before $e^{\pm}$ annihilation [50]. The mass density of such a species today is

$$\rho_\nu = n_\nu m_\nu. \tag{5.7}$$

Expressing this in terms of the photon density, $n_\gamma = 2\zeta(3)T_\gamma^3/\pi^2$, one gets

$$\rho_\nu = m_\nu \frac{n_\nu}{n_\gamma}\zeta(3)\frac{2}{\pi^2}T_\gamma^3, \tag{5.8}$$

where $\zeta(x)$ is the Riemann zeta-function. If the neutrinos decouple long before $e^{\pm}$ annihilation, this can be translated into the normal textbook relation

$$\Omega_\nu h^2 = \frac{g_\nu}{2}\frac{m_\nu}{93.03eV}, \tag{5.9}$$

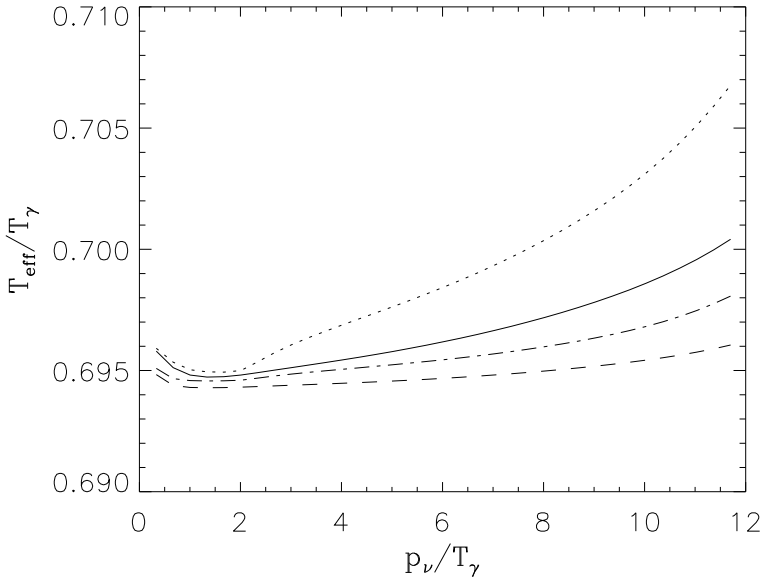

Figure 5.4: The effective neutrino temperature after complete $e^{\pm}$ annihilation, using MB statistics. The solid line is for ν_e and case 3, the dashed is for $\nu_{\mu,\tau}$ also case 3. The dotted is for ν_e and case 4, the dot-dashed for $\nu_{\mu,\tau}$ and case 4.

using a present photon temperature of 2.736 K. h is the dimensionless Hubble constant, and $g_\nu = 2$ for one flavour of neutrino and antineutrino. Since observations demand that $\Omega_\nu h^2 \leq 1$ [36], we have a mass limit on any given light neutrino. Because of neutrino heating, this limit is changed by a small amount. Using FD statistics and non-zero $m_{e^\pm}$, the final number density of neutrinos after decoupling deviates from the standard case by $\delta n_\nu/n_\nu \sim 0.52\%$ for ν_e and $\delta n_\nu/n_\nu \sim 0.25\%$ for $\nu_{\mu,\tau}$. For electron neutrinos this changes Eq. (5.9) to

$$\Omega_{\nu_e} h^2 = \frac{g_{\nu_e}}{2} \frac{m_{\nu_e}}{92.55eV}, \tag{5.10}$$

whereas for muon or tau neutrinos we find

$$\Omega_{\nu_{\mu,\tau}} h^2 = \frac{g_{\nu_{\mu,\tau}}}{2} \frac{m_{\nu_{\mu,\tau}}}{92.80eV}. \tag{5.11}$$

As this is a very small change to the standard value, neutrino heating does not alter the usual conclusion that electron neutrinos can not contribute more than about 0.5 (using the current experimental upper limit to its mass, $m_{\nu_e} \leq 15$ eV [7]) to Ω, whereas muon and tau neutrinos can.

The main conclusion is that it is safe to ignore neutrino heating when doing nucleosynthesis and structure formation calculations. However, one should note that neutrino heating is a non-negligible effect if one wants to construct a high precision BBN code. It should also be noted that since this work was performed new results by Dolgov *et al.* [51] have appeared. They use the same basic approach as ours but with much higher numerical precision and their results confirm ours very nicely. Their results for the neutrino energy density change are $\delta\rho_{\nu_e}/\rho_{\nu_e} = 0.9\%$ and $\delta\rho_{\nu_\mu}/\rho_{\nu_\mu} = 0.4\%$ compared to our result of $\delta\rho_{\nu_e}/\rho_{\nu_e} = 0.83\%$ and $\delta\rho_{\nu_\mu}/\rho_{\nu_\mu} = 0.41\%$. They find a resulting increase in the primordial He production of $\Delta Y = +1.4 \times 10^{-4}$ which is somewhat larger than our result, $\Delta Y = +1.0 \times 10^{-4}$. However, their implementation into the nucleosynthesis code differs from ours to some extent which may explain this small difference.

Chapter VI

Massive Stable Neutrinos in BBN

Essentially all of this chapter has appeared as the paper *Nucleosynthesis and the Mass of the Tau-Neutrino Revisited*, Phys. Rev. D **54**, 7894 (1996).

The possibility of heavy τ neutrinos in the MeV region has been investigated many times in the literature, primarily because such a neutrino could have very interesting consequences for both cosmology and supernovae [52]. In Chapter 4 we discussed the mass limits on the different neutrino species. The best current experimental limit to the τ neutrino mass comes from the ALEPH collaboration [30], and is $m_{\nu_\tau} \leq 24$ MeV with 95 % CL. Primordial nucleosynthesis puts stringent limits on the mass and lifetime of the τ neutrino [12, 40, 53–60]. The bounds are most stringent for neutrinos in the MeV region because their mass is comparable to the weak decoupling temperature. This can be seen from the following argument. As long as massive neutrinos are kept in weak equilibrium with the relativistic species their number density is that of a species in thermodynamic equilibrium. That is, if the mass is much smaller than the temperature, the number density is roughly equivalent to that of a massless species, whereas if the mass is much larger than the temperature, the number density is exponentially suppressed

$$\frac{n}{n_{\rm massless}} \propto \exp(-m/T). \tag{6.1}$$

As soon as the massive neutrinos decouple their number density stays constant relative to that of a massless species. However, their energy density starts growing as the temperature drops because the energy density becomes dominated by the rest mass term. In this case the energy density scales as

$$\rho_{\rm NR} \propto mT^3, \tag{6.2}$$

whereas for relativistic species the energy density scales as

$$\rho_{\rm R} \propto T^4, \tag{6.3}$$

because of the redshift of the particle wavelength. At late times the rest mass term therefore dominates the cosmic energy density completely.

Now, if the rest mass of the neutrino is much smaller than the decoupling temperature its number density after decoupling is roughly that of a massless species. However, since nucleosynthesis takes place not long after weak freeze-out the rest mass term will not have become important at that time and the neutrino behaves effectively as a massless species during nucleosynthesis. On the other hand, if the rest mass is much larger than the freeze-out temperature the number density is exponentially suppressed by a large factor. Therefore, even though the rest mass is large the number density is sufficiently small that such a neutrino does not play a role during nucleosynthesis. If such a neutrino species is one one the three known species we therefore effectively have only 2 neutrino species present during nucleosynthesis. This is the reason why the effect is expected to be strongest for neutrinos with mass $m \sim$ few MeV.

Some of the most recent investigations of the effects of a massive Majorana τ-neutrino in the MeV region on nucleosynthesis, are those of Kolb *et al.* [57], Dolgov and Rothstein [58], and Kawasaki *et al.* [59]. For a standard Majorana neutrino that is stable on the timescale of nucleosynthesis Kolb *et al.* find an excluded mass interval of 0.5-32 MeV, whereas Kawasaki *et al.* find an exclusion interval of 0.1-50 MeV. Combined with the experimental data this means that a massive τ neutrino with mass greater than 0.1-0.5 MeV and lifetime greater than 10^3 s is excluded by nucleosynthesis. However, these calculations, except [59], use the integrated Boltzmann equation. Furthermore, they assume that the distribution functions are kept in kinetic equilibrium at all times by scattering reactions [14, 62]. Kawasaki *et al.* [59] have used the full equations, but assuming only annihilation interactions, no scattering. Furthermore they use Boltzmann statistics. It is therefore important to see how these limits change when we use the full set of Boltzmann equations, with all possible interactions. Below we calculate the relic abundance of a massive Majorana τ neutrino with lifetime longer than the time of nucleosynthesis ($\tau \geq 10^3$ s). We then use nucleosynthesis to put limits on the allowed mass range, and find that the resulting limits are more stringent than those normally obtained from the integrated Boltzmann equation, but less stringent than found from the full Boltzmann equations without inclusion of scattering.

6.1 Numerical Calculations

As discussed in Chapter 2 the fundamental way to go about calculating the relic abundance of massive tau neutrinos is to solve the Boltzmann equation, Eq. (2.27). In addition to this we use the two independent evolution equations for the cosmic expansion, the Friedmann equation, Eq. (2.3) and the equation of energy conservation, Eq. (2.10). Now with respect to the right hand side collision integral, Eq. (2.30) the matrix element for all the weak processes can be calculated using the theory outlined in Chapter 4. Since we are looking at Majorana neutrinos and the lepton asymmetry of the early Universe is very

small, ($L \leq 10^{-9}$), we can, as previously explained, assume these neutrinos to be effectively one single unpolarised species. In this case the interaction matrix elements are rather simple to calculate, and are given in Table 6.1.

Table 6.1: Possible neutrino processes and the corresponding matrix elements. 1 is defined equal to the particle for which we calculate $C_{\rm coll}$. 2 is the other incoming particle. 3 is defined as either particle 1 going out (scattering) or the outgoing lepton (annihilation). 4 is defined as either particle 2 going out (scattering) or the outgoing antilepton (annihilation). We have introduced the quantities C_V and C_A. If $\nu_1 = \nu_e$ then $C_V = \frac{1}{2} + 2\sin^2\theta_W$ and $C_A = \frac{1}{2}$, where $\sin^2\theta_W \approx 0.23$. If $\nu_1 = \nu_{\mu,\tau}$ then $C_V = -\frac{1}{2} + 2\sin^2\theta_W$ and $C_A = -\frac{1}{2}$. For processes involving τ-neutrinos, the parameter $m = m_{\nu_\tau}$; otherwise $m = 0$. p_i is the four-momentum of particle i.

Process	$S \mid M \mid^2$
$\nu_1 + \overline{\nu}_1 \to \nu_1 + \overline{\nu}_1$	$64G_F^2[(p_1\cdot p_2)(p_3\cdot p_4)+$ $(p_1\cdot p_4)(p_2\cdot p_3)+$ $m^2(p_2\cdot p_4)]$
$\nu_1 + \nu_1 \to \nu_1 + \nu_1$	$16G_F^2[(p_1\cdot p_2)(p_3\cdot p_4)+$ $(p_1\cdot p_4)(p_2\cdot p_3)+$ $m^2(p_2\cdot p_4)]$
$\nu_1 + \nu_i \to \nu_1 + \nu_i$	$16G_F^2[(p_1\cdot p_2)(p_3\cdot p_4)+$ $(p_1\cdot p_4)(p_2\cdot p_3)+$ $m^2(p_2\cdot p_4)]$
$\nu_1 + \overline{\nu}_i \to \nu_1 + \overline{\nu}_i$	$16G_F^2[(p_1\cdot p_2)(p_3\cdot p_4)+$ $(p_1\cdot p_4)(p_2\cdot p_3)+$ $m^2(p_2\cdot p_4)]$
$\nu_1 + e^- \to \nu_1 + e^-$	$32G_F^2[\{(p_1\cdot p_2)(p_3\cdot p_4)+$ $(p_1\cdot p_4)(p_2\cdot p_3)+$ $m^2(p_2\cdot p_4)\}(C_V^2 + C_A^2)+$ $(C_V^2 - C_A^2)m_e^2\{-(p_1\cdot p_3) - 2m^2\}]$
$\nu_1 + e^+ \to \nu_1 + e^+$	$32G_F^2[\{(p_1\cdot p_2)(p_3\cdot p_4)+$ $(p_1\cdot p_4)(p_2\cdot p_3)+$ $m^2(p_2\cdot p_4)\}(C_V^2 + C_A^2)+$ $(C_V^2 - C_A^2)m_e^2\{-(p_1\cdot p_3) - 2m^2\}]$
$\nu_1 + \overline{\nu}_1 \to e^- + e^+$	$32G_F^2[\{(p_1\cdot p_4)(p_2\cdot p_3)+$ $(p_1\cdot p_3)(p_2\cdot p_4)-$ $m^2(p_3\cdot p_4)\}(C_V^2 + C_A^2)+$ $(C_V^2 - C_A^2)m_e^2\{(p_1\cdot p_2) - 2m^2\}]$
$\nu_1 + \overline{\nu}_1 \to \nu_i + \overline{\nu}_i$	$16G_F^2[(p_1\cdot p_4)(p_2\cdot p_3)+$ $(p_1\cdot p_3)(p_2\cdot p_4)$ $-m^2(p_3\cdot p_4)]$

We parametrise the momenta of all particles in terms of the parameter $z =$

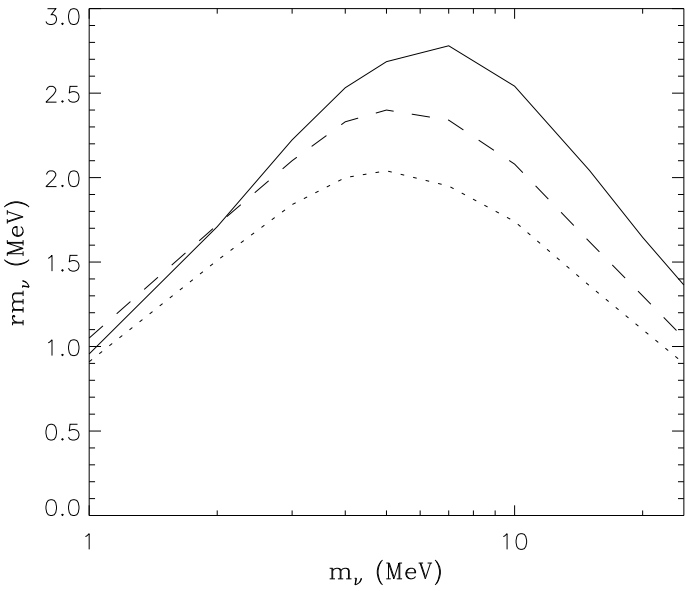

Figure 6.1: The relic number density of massive τ neutrinos normalised to a massless species times mass, rm_ν. The solid curve is calculated using the full Boltzmann equation and all interactions. Dotted and dashed curves are adopted from [57] and [58].

p_ν/T_γ, and use a grid of 25 points to cover the range in z. The system of equations is then evolved in time by a Runge-Kutta integrator, giving us the distribution function of each particle species, as well as the scale factor R, as a function of photon temperature. By doing it this way, we have the advantage that we know the specific distribution functions for all neutrino species, whereas a treatment using the integrated Boltzmann equation has to make an assumption of kinetic equilibrium, giving only a rough approximation to the true distribution functions.

Fig. 6.1 shows the final relic density of ν_τ before decay becomes important. rm_ν is defined as $rm_\nu = m_\nu n_\nu/n_\nu(m=0)$. We have compared our results to those of Kolb *et al.* [57] and Dolgov and Rothstein [58], who use the integrated Boltzmann equation. For small masses, it is not important whether we use the integrated or the full Boltzmann equation. The reason is that the neutrino decouples before annihilation really commences, therefore the treatment of the annihilation terms is not very important. But for higher masses our results exceed those obtained in earlier investigations. This is to be expected since our

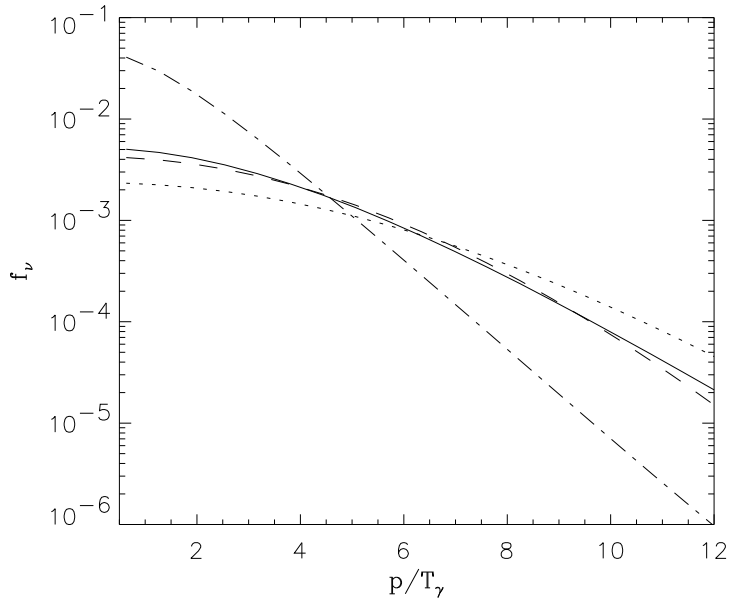

Figure 6.2: The distribution of τ neutrinos of mass 15 MeV at a photon temperature of 0.92 MeV. The solid curve includes all possible interactions whereas the dashed-dotted curve only includes annihilations. The dotted curve is a kinetic equilibrium distribution with the same number density as that of the solid curve and $T = T_\gamma$, whereas the dashed curve has the same number- and energy densities as the solid, with T and μ adjusted accordingly.

inclusion of the full neutrino spectra should reduce the annihilation of neutrinos as discussed below, thereby permitting more τ neutrinos to survive. Thus, the inclusion of spectral distortions leads in fact to a strengthening of previous limits on MeV neutrinos from the integrated Boltzmann equation. However, for very high masses there is still a difference between our result and those of Kolb *et al.* [57] and Dolgov and Rothstein [58]. At first one should expect the results to converge because at high masses the deviations from equilibrium are expected to be small because of the effectiveness of elastic scatterings. However, the calculations of Refs. [57] and [58] use Boltzmann statistics for all particles. This means that Pauli Blocking of final states is neglected, increasing the annihilation rate and giving a smaller final abundance. Our results appear to agree well with those of Fields *et al.* who also use Fermi statistics although a direct comparison is not possible.

In Fig. 6.2 we show the distribution of a 15 MeV ν_τ. The difference between

the distributions with and without scattering interactions is striking. If only annihilations are taken into account, the high momentum states are almost empty, because they cannot be refilled. On the other hand, the low momentum states are highly populated, because they annihilate more slowly and cannot be scattered away. That this should be so can be seen directly from the thermally averaged annihilation cross section for heavy Majorana neutrinos. In case of non-relativistic neutrinos the cross section for pair annihilation into massless species is [57]

$$\langle\sigma|v|\rangle_{\rm M} = \frac{G_{\rm F}^2 m^2}{2\pi}\sum_i (C_{V_i}^2 + C_{A_i}^2) 8\beta^2/3, \tag{6.4}$$

where β is the relative velocity of the incoming particles and the summation index i runs over all annihilation channels. The annihilation cross section is therefore strongly increasing with neutrino kinetic energy and thus the high momentum states annihilate more quickly. Therefore, calculations based on the full Boltzmann equations without scattering underestimate the annihilation rate [59]. Our neutrino distribution functions now differ less from kinetic equilibrium than found in [61]. Deviations by a factor of 2 appear frequently when compared to a kinetic equilibrium distribution, $f_\nu = [\exp((E-\mu)/T)+1]^{-1}$, with the same number density and $T = T_\gamma$, as often assumed, whereas the distribution is close to that of a kinetic distribution with T and μ determined by the number- and energy densities.

The resulting ν_e and ν_μ distributions are significantly heated relative to the standard case with a massless ν_τ. For eV-mass ν_μ or ν_e this changes the present day contribution to the cosmic density to $\Omega_\nu h^2 = \alpha m_\nu/93.03$eV with $\alpha = 1$ for a massless ν_τ, and α =1.10(1.13), 1.09(1.14), 1.03(1.05), 1.01(1.02) for $\nu_e(\nu_\mu)$ for m_{ν_τ} =5, 10, 15, 20 MeV (h is the Hubble-parameter in units of 100km s^{-1} Mpc^{-1}). Later decay of ν_τ can further increase the value of α.

Furthermore, the ν_e and ν_μ distribution functions become non-thermal, because the pairs created by annihilation of τ neutrinos cannot thermalise sufficiently before the electron and muon neutrinos decouple completely. This non-thermality can have a significant effect on the production of light elements, especially ^{4}He, because the n-p converting reactions depend not only on the energy density of neutrinos, but also on the specific form of the distribution function for ν_e, which enters in the n-p conversion rate integrals. Overall, the increase in the cosmic expansion rate due to the extra energy density in τ- (and massless) neutrinos, which increases ^{4}He-production, is to some extent compensated by a decrease in neutron-fraction due to the change in the n-p rate integrals. Notice also that for tau neutrino masses below 1 MeV there is very little effect from ν_e heating since almost no tau neutrinos annihilate before weak freeze-out. For very large masses the effect is again small. The reason here is that although there is a significant non-thermal contribution to the ν_e distribution from ν_τ annihilations this is washed out because the electron neutrinos stay in thermodynamic equilibrium with the photon plasma until long after the annihilations of ν_τ have ceased. The biggest effect is in the intermediate regime

where ν_τ annihilations cease roughly at the same time as the electron neutrinos drop out of equilibrium. Also, one should note that at low tau neutrino masses ΔN_{eq} found from our approach is roughly the same as that found from bulk heating. The difference between bulk heating and our approach is that bulk heating neglects residual annihilations of tau neutrinos after weak decoupling For low tau neutrino masses the produced electron neutrinos have energy not much above Q, the proton-neutron mass difference. Therefore they do not disturb the neutron-proton ratio very much. On the other hand, for large m_{ν_τ} the electron neutrinos have energy much larger than Q. Now, since the absorption cross section at high energy is the same on neutrons and protons and there are much fewer neutrons present, the end result is that more neutrons are produced. This again produces more helium and therefore these residual annihilations go in the direction of positive ΔN_{eq}. For very large masses the effect disappears because there are so few of these residual annihilations that they do not effect BBN at all.

6.2 Mass Limits

In order to derive mass limits on ν_τ we need to calculate the predicted abundances of the different light elements and compare them with observations. To do this, we have changed the nucleosynthesis code of Kawano [47] to incorporate a massive Majorana τ neutrino. As previously mentioned, we assume that decay has no effect during nucleosynthesis ($\tau \geq 10^3$s). Note that we not only have to change the energy density of the τ neutrino, but also the energy density in massless neutrinos, as well as the specific distribution function, f_{ν_e}, of electron neutrinos in the nucleosynthesis code.

Fig. 6.3 illustrates the consequences for Big Bang nucleosynthesis in terms of the equivalent number of massless neutrinos, N_{eq}, needed to give a similar production of ^{4}He at a baryon-to-photon ratio $\eta = 3 \times 10^{-10}$. The revised results with and without inclusion of the change in the ν_e number density are in fine agreement with recent results based on the integrated Boltzmann equation by Fields, Kainulainen, and Olive[12]. Including also the actual shape of the ν_e distribution to some extent compensates for the effect on the energy density, a result also found by Dolgov, Pastor, and Valle[60, 63], though we disagree by several equivalent neutrino species with the total N_{eq} found in [58], and to some extent also with the differential changes in N_{eq} quoted in [60]. We note, that a small, overall increase in N_{eq} due to these effects was estimated in a footnote in [57]. This agrees with our results for large m_{ν_τ}.

In conclusion our results show that no MeV τ-neutrino with mass in the region between $\simeq 0.1$ MeV and the the experimental upper limit of 24 MeV and lifetime longer than the timescale of nucleosynthesis is permitted unless more than 4 equivalent massless neutrino flavours can be accomodated by nucleosynthesis observations. Currently there is a lot of controversy as to the value of N_{eq} allowed by nucleosynthesis. As discussed in Chapter 3, there appears to be a consensus that the maximum allowed value is definitely not larger than 4.

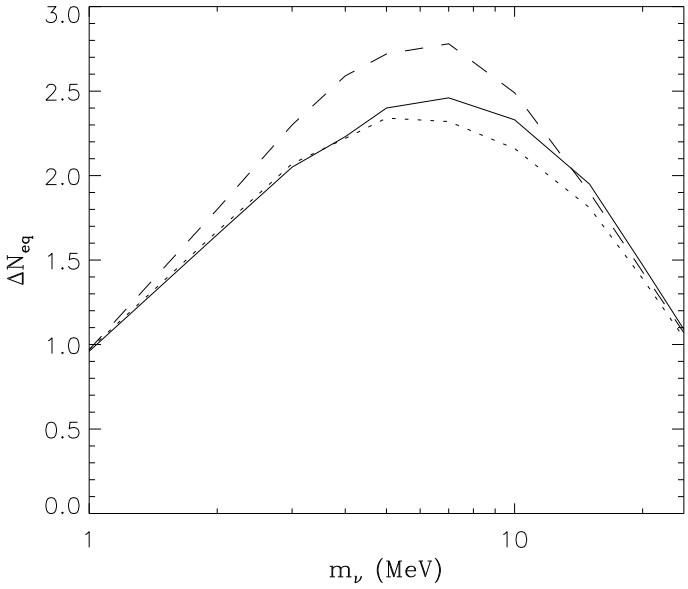

Figure 6.3: Equivalent number of massless neutrinos, shown as $\Delta N_{\rm eq} = N_{\rm eq} - 3$. The dashed curve is without heating of ν_e, the dotted with only the electron neutrino number density changed, and the solid curve with the full distribution of ν_e.

This means that we can fairly safely say that a tau neutrino with mass larger than a few tenths of an MeV is not allowed by Big Bang nucleosynthesis if its lifetime is longer than 10^3 s.

Chapter VII

Decaying τ Neutrinos in BBN

The contents of this chapter have been submitted to Phys. Rev. D.

In the last chapter we discussed the impact of a massive but stable tau neutrino on nucleosynthesis. From cosmology, we have the well known limit on stable low mass ($m \leq$ GeV) neutrinos [36]

$$\Omega_\nu h^2 = \frac{g_\nu}{2} \frac{m_\nu}{93.03\text{eV}}, \tag{7.1}$$

using a present photon temperature of 2.736 K. h is the dimensionless Hubble constant and Ω is the cosmological density parameter. $g_\nu = 2$ for one flavour of neutrino and antineutrino. Since observations demand that $\Omega_\nu h^2 \leq 1$ [36], we have a mass limit on any given stable neutrino [1]. Thus, any neutrino with mass in the range 100 eV - 24 MeV is necessarily unstable. In Chapter 4 we discussed in some detail the possible generic types of neutrino decay. First of all there is the standard model decay $\nu_i \rightarrow \nu_j e^+ e^-$ if the mass is larger than $2m_e$ and the mixing angle between the two neutrinos is different from zero. A flavour changing neutral current can also lead to the decay $\nu_i \rightarrow \nu_j \overline{\nu_j} \nu_j$. There can also be other more exotic modes of decay, for example decay via emission of scalars or pseudo-scalars. This decay mode is generic for example in the majoron models of neutrino mass.

The effect of such unstable tau neutrinos on nucleosynthesis have been investigated many times in the literature [40, 59, 64–68], the most recent investigations being those of Dodelson, Gyuk and Turner [40] and Kawasaki *et al.* [59, 68]. Dodelson, Gyuk and Turner have performed a detailed study of several possible decay modes in the context of non-relativistic decays, whereas Kawasaki *et al.* have performed a calculation using the full Boltzmann equation for the decay mode $\nu_\tau \rightarrow \nu_\mu \phi$. In all cases it is found that it is possible to change significantly the primordial abundances via decay of the tau neutrino.

[1] Note that this relation changes slightly if the heating of neutrinos from e^+e^- annihilation is included as discussed in Chapter 5.

In the present paper we focus on the decay

$$\nu_\tau \to \nu_e \phi, \tag{7.2}$$

where ν_τ is assumed to be a Majorana particle and ϕ is a light scalar or pseudoscalar particle. This differs from the decay $\nu_\tau \to \nu_\mu \phi$ in that it includes an electron neutrino in the final state. Since ν_e enters directly into the weak interactions that interconvert neutrons and protons this decay can potentially alter the outcome of nucleosynthesis drastically. Indeed the non-relativistic results of Dodelson, Gyuk and Turner indicate that the primordial helium abundance, Y_P, can be changed radically, either increasing or decreasing Y_P depending on the mass and lifetime of the tau neutrino.

Now, in the last few years, evidence has been gathering that the standard picture of the way light nuclei are formed in the early Universe may be facing a crisis [8]. The main point is that helium is overproduced relative to the other light nuclei so that the standard theoretical predictions are only marginally consistent with the observational results [8]. Other measurements of the primordial helium abundance do yield somewhat higher values [18], and the unknown systematical errors both in observations and in chemical evolution calculations may, however, be larger than presently assumed so that it is perhaps premature to talk of a real "crisis" for Big Bang nucleosynthesis.

Our approach will not be so much to discuss the specific limits from nucleosynthesis since these are still quite uncertain as it will be a discussion of the differences between our way of solving the Boltzmann equations and those previously used. Nevertheless, in light of the possibility that some new element is missing from the standard nucleosynthesis calculations we think that it is important to try and find methods of changing the nucleosynthesis predictions by including plausible new physics in the calculations. One possible way of doing this is to include a massive and unstable tau neutrino.

In order to obtain good fits to the observational data it is, as just mentioned, necessary to lower the helium abundance somewhat compared to the other light nuclei. This can be achieved by having relatively low mass tau neutrinos decay while they are still relativistic or semi-relativistic. However, this is exactly the region where the non-relativistic formalism breaks down because it assumes a delta function momentum distribution of the decay products and neglects inverse decays. It is therefore of significant interest to investigate this decay using the full Boltzmann equation in order to calculate abundances in this parameter region.

In the present chapter we calculate the expected primordial abundances for a tau neutrino mass in the range 0.1 - 1 MeV. In Sec. 7.1 we describe the necessary formalism needed for this calculation. In Sec. 7.2 we discuss our numerical results. Sec. 7.3 contains a description of our nucleosynthesis calculations compared to the observational data and finally Sec. 7.4 contains a summary and discussion.

7.1 Necessary formalism

As usual the basic formalism is the one described in chapter 2, namely that of the Boltzmann equation. Again, since we only consider 2-particle interactions like $1 + 2 \to 3 + 4$, $C_{\rm weak}$ can be written as in Eq. (2.29).

Since we are only looking at Majorana neutrinos the decay terms are quite simple. Since there is almost no net lepton number in the early Universe the Majorana neutrino is effectively an unpolarised species. However, this means that there can be no preferred direction in the rest frame of the parent particle. Therefore the decay is necessarily isotropic in this reference frame. The decay terms in this case were given in Chapter 2 as

$$C_{\rm dec}[f_{\nu_\tau}] = -\frac{m_{\nu_\tau}^2}{\tau m_0 E_{\nu_\tau} p_{\nu_\tau}} \int_{E_\phi^-}^{E_\phi^+} dE_\phi \Lambda(f_{\nu_\tau}, f_{\nu_e}, f_\phi) \tag{7.3}$$

$$C_{\rm dec}[f_{\nu_e}] = \frac{g_{\nu_\tau}}{g_{\nu_e}} \frac{m_{\nu_\tau}^2}{\tau m_0 E_{\nu_e} p_{\nu_e}} \int_{E_{\nu_\tau}^-}^{E_{\nu_\tau}^+} dE_{\nu_\tau} \Lambda(f_{\nu_\tau}, f_{\nu_e}, f_\phi) \tag{7.4}$$

$$C_{\rm dec}[f_\phi] = \frac{g_{\nu_\tau}}{g_\phi} \frac{m_{\nu_\tau}^2}{\tau m_0 E_\phi p_\phi} \int_{E_{\nu_\tau}^-}^{E_{\nu_\tau}^+} dE_{\nu_\tau} \Lambda(f_{\nu_\tau}, f_{\nu_e}, f_\phi), \tag{7.5}$$

where $\Lambda(f_{\nu_\tau}, f_{\nu_e}, f_\phi) = f_{\nu_\tau}(1 - f_{\nu_e})(1 + f_\phi) - f_{\nu_e} f_\phi (1 - f_{\nu_\tau})$, $m_0^2 = m_{\nu_\tau}^2 - 2(m_\phi^2 + m_{\nu_e}^2) + (m_\phi^2 - m_{\nu_e}^2)^2/m_{\nu_\tau}^2$. τ is the lifetime of the heavy neutrino and g is the statistical weight of a given particle. We use $g_{\nu_\tau} = g_{\nu_e} = 2$ and $g_\phi = 1$, corresponding to $\phi = \overline{\phi}$. This assumption is not significant to the present investigation. Furthermore we shall assume that the masses of ν_e and ϕ are effectively zero during nucleosynthesis.

The integration limits are given by

$$E_{\nu_\tau}^\pm(E_i) = \frac{m_0 m_{\nu_\tau}}{2m_i^2}[E_i(1 + 4(m_i/m_0)^2)^{1/2} \pm (E_i^2 - m_i^2)^{1/2}] \tag{7.6}$$

and

$$E_i^\pm(E_{\nu_\tau}) = \frac{m_0}{2m_H}[E_{\nu_\tau}(1 + 4(m_i/m_0)^2)^{1/2} \pm p_{\nu_\tau}] \tag{7.7}$$

where the index $i = \nu_e, \phi$.

These Boltzmann equations are then solved together with the Friedmann equation and the equation of energy conservation as discussed in Chapter 2.

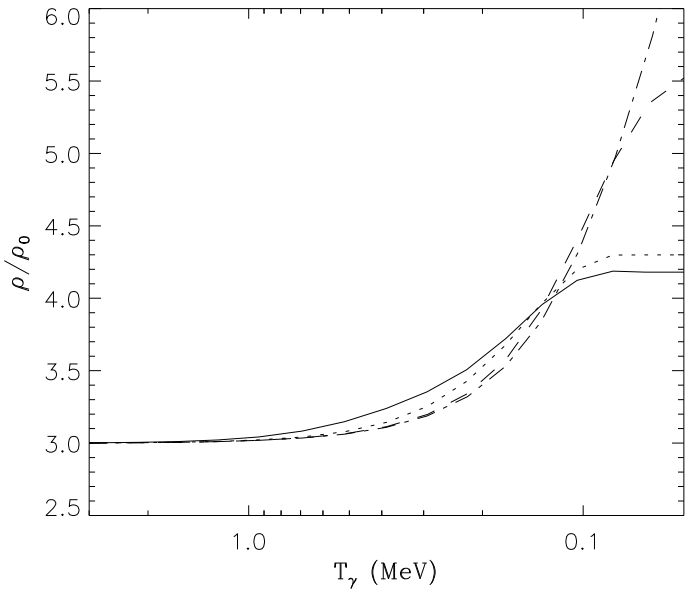

Figure 7.1: The electron neutrino distribution at asymptotically low temperature (after complete decay) in units of the distribution of a standard massless neutrino. The tau neutrino mass is 0.5 MeV. The full line is for $\tau = 1$ s, the dotted for $\tau = 10$ s, the dashed for $\tau = 100$ s and the dot-dashed for $\tau = 1000$ s.

7.2 Numerical Results

We have solved the Boltzmann equation for the evolution of distribution functions together with the energy conservation equation , Eq. (2.10), and the Friedmann equation, Eq. (2.3). Specifically we have solved for masses of 0.1-1 MeV and lifetimes larger than 0.1 s.

In Fig. 7.1 we show the evolution of energy density in neutrinos and the pseudoscalar particle for a tau neutrino mass of 0.5 MeV. The energy density evolves quite differently in the different cases. Since the energy density in a non-relativistic species only decreases as R^{-3} compared to R^{-4} for relativistic particles the rest mass energy of the tau neutrino will dominate completely at late times if it is stable. If it decays the rest mass energy is transferred into relativistic energy so that the total energy density no longer increases relative to that of a single standard massless neutrino species. This difference is clearly seen between different tau neutrino lifetimes.

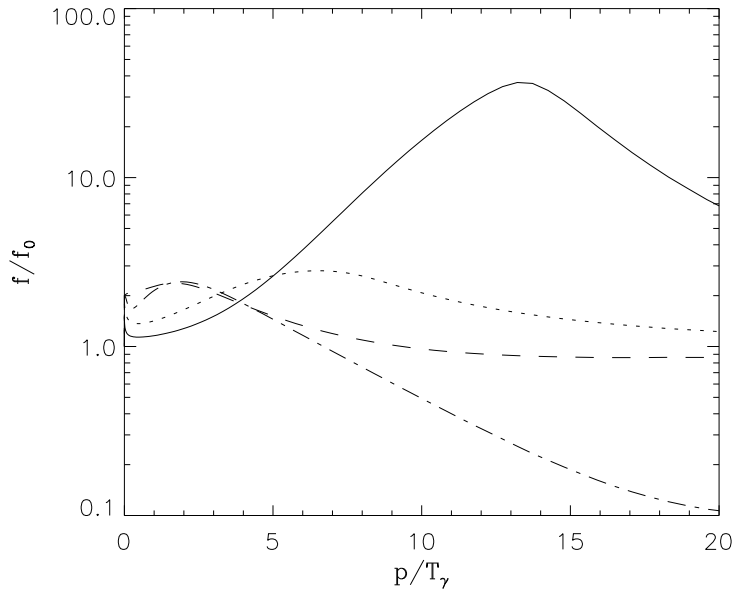

Figure 7.2: The electron neutrino distribution at asymptotically low temperature (after complete decay) in units of the distribution of a standard massless neutrino. The tau neutrino mass is 0.5 MeV. The full line is for $\tau = 1$ s, the dotted for $\tau = 10$ s, the dashed for $\tau = 100$ s and the dot-dashed for $\tau = 1000$ s.

In Fig. 7.2 we show the spectral distribution of the electron neutrino for a tau neutrino mass of 0.5 MeV and different lifetimes. To understand this plot better we can define a "relativity parameter", μ, for the decay

$$\mu_{\nu_\tau} \equiv \frac{m_{\nu_\tau}^2 \tau_{\nu_\tau}}{9\mathrm{MeV}^2\mathrm{s}}. \tag{7.8}$$

A particle shifts from relativistic to non-relativistic at a temperature of roughly $T \simeq m/3$. When the Universe is radiation dominated

$$\frac{t}{1\mathrm{s}} \simeq \left(\frac{T}{1\mathrm{MeV}}\right)^{-2}. \tag{7.9}$$

Therefore, if the decay is relativistic,

$$\tau < t(T = m/3) \simeq \frac{9m^{-2}}{\mathrm{MeV}^{-2}}\mathrm{s}. \tag{7.10}$$

Thus, if $\mu_i < 1$ the decay is relativistic, whereas if $\mu_i > 1$ it is non-relativistic. For lifetimes of 1, 10, 100 and 1000 s the relativity parameters are respectively 0.028, 0.28, 2.78 and 27.8. For non-relativistic decays the decay neutrino distribution assumes a rather narrow shape coming from the delta function energy distribution. For very short lifetimes the decay installs an equilibrium between ν_e, ν_τ and ϕ because of rapid inverse decays. This can lead to a significant depletion of high momentum electron neutrinos as also noted by Madsen [67] who treated this case of very short lifetimes using equilibrium thermodynamics.

7.3 Nucleosynthesis Effects

In order to estimate the effect on nucleosynthesis, we have employed the nucleosynthesis code of Kawano [47], modified in order to incorporate a decaying neutrino. This includes taking into account the changing energy density as well as the change in electron neutrino distribution.

A decaying tau neutrino can affect nucleosynthesis in several different ways. Firstly, the cosmic energy density ρ is changed. Since the cosmic expansion rate is given directly in terms of this energy density via the Friedmann equation, Eq. (2.3), it is also changed. It is a well known fact that increasing the energy density leads to an earlier freeze-out of the n-p conversion and therefore produces more helium [36], whereas decreasing the energy density decreases the helium fraction. This is the effect discussed by Kawasaki *et al.* [68], namely that an MeV neutrino decaying into sterile daughter products while still relativistic or semirelativistic can actually decrease the cosmic energy density thereby decreasing the helium abundance.

However, there is also another another effect stemming from the change in electron neutrino temperature. Since the electron neutrino enters directly into the n-p processes this can be called a "first order" effect and is potentially much more important than the "second order" effect of changing the energy density. This effect of change in the electron neutrino temperature has already been discussed by several authors in the context of non-relativistic decays [40, 64].

If the decay is non-relativistic, the energy of a produced electron neutrino is $m/2$. If this energy is significantly above the energy threshold for the two processes

$$p + \overline{\nu_e} \rightarrow n + e^+ \tag{7.11}$$

and

$$p + \overline{\nu_e} + e^- \rightarrow n, \tag{7.12}$$

the decaying tau neutrinos will act to produce more He [40, 64]. The reason is that the absorption cross section at high energies is the same on neutrons and protons. Since there are many more protons present than neutrons, more neutrons will be produced. In the end this leads to a higher helium fraction. However, if the mass of the decaying neutrino is below this threshold the produced electron neutrinos will stimulate the conversion of neutrons into protons

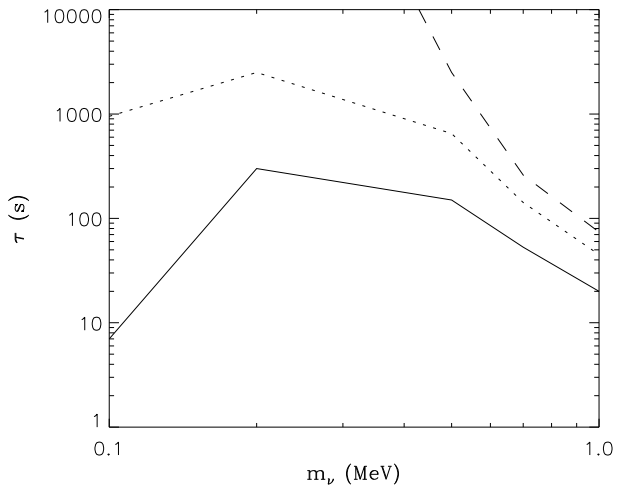

Figure 7.3: Helium abundance contours as a function of tau neutrino mass and lifetime for a baryon-to-photon ratio, η, of 3×10^{-10}. The full line is $Y_P = 0.20$, the dotted is $Y_P = 0.22$ and the dashed is $Y_P = 0.24$. The value in the standard model for this η is $Y_P = 0.2389$.

thereby actually decreasing the He abundance. This effect then competes with the rest mass effect which increases Y_P.

If the decay is relativistic the electron neutrinos are produced at roughly thermal energies. Effectively this amounts to increasing the electron neutrino temperature. This in turn leads to a decrease in helium production. If the decay takes place at high temperatures it is because beta equilibrium is kept for a longer time, whereas if the decay takes place at temperatures below the threshold for proton to neutron conversion it still leads to lower helium abundance because an increase in the electron neutrino temperature stimulates the conversion of neutrons to protons over the inverse reaction.

In Fig. 7.3 we show contour lines for the helium abundance as function of neutrino mass and lifetime. It is seen that helium can be significantly suppressed relative to the standard case if the lifetime is short enough and increased if the mass and lifetime are both high. If the mass and lifetime are both sufficiently high the helium abundance is instead increased. Notice also that even for small masses of the order 0.1 MeV the helium abundance can be changed significantly compared to the standard value for rather a large range of lifetimes.

Our Fig. 7.3 should be compared with for example the results of Terasawa and Sato [64] or Dodelson, Gyuk and Turner [40] obtained using non-relativistic theory. The most straightforward comparison is with Figs. 2b and 3b in Ref.

[64]. For long lifetimes the difference is quite small as would be expected since this is the non-relativistic limit. However, for short lifetimes the difference is significant. For very short lifetimes, our calculated He abundance is larger than that of Terasawa and Sato. The reason is that if one uses the full Boltzmann equation in this case, decays and inverse decays will bring the particle distributions into equilibrium as discussed in Sec. 7.2. Thus, if one keeps on going to shorter and shorter lifetimes nothing new happens since it is already decay in equilibrium. Therefore our curve for He flattens out instead of decreasing for very short lifetimes. For somewhat longer lifetimes our He abundance is on the other hand smaller than that found by Terasawa and Sato. The reason here is that the decay produces a peak of very low momentum electron neutrinos and that these states are not upscattered because the weak interactions have already frozen out. In the end this produces a somewhat colder electron neutrino distribution than would have been obtained using non-relativistic theory and therefore predicts less helium. This low momentum peak can be seen in Fig. 7.2 for the example of a 0.5 MeV τ neutrino. For non-relativistic decays this peak disappears because low momentum states are not energetically accessible. In essence our predicted curve for the He abundance is therefore much flatter at short or intermediate lifetimes than what one would obtain using the non-relativistic formalism. For very long lifetimes our calculation fits fairly well with that obtained by Terasawa and Sato as could be expected.

In Fig. 7.4 we show the abundance of D, ^{3}He and ^{7}Li for a specific example of m = 0.5 MeV. We see that the abundances of these elements only change by relatively small amounts even for great variations in neutrino lifetime. Thus, the main effect of the decay is to lower the helium abundance while leaving the other abundances more or less unchanged.

The calculated abundances for different masses and lifetimes are compared with observational limits. Unfortunately there is a great deal of controversy connected with these. However, since our main emphasis is on the differences between our approach to solving the Boltzmann equations and the non-relativistic approximations previously used, and not so much on the specific nucleosynthesis limits to tau neutrino mass and lifetime we will not go into too much detail regarding this point. For ^{4}He we use the value calculated by Hata *et al.* [8] of

$$\mathrm{Y}_P = 0.232 \pm 0.002 \pm 0.005. \tag{7.13}$$

For deuterium the situation is somewhat complicated. From measurements in the local interstellar medium one can obtain a deuterium abundance of [8]

$$\mathrm{D/H} \simeq 1.6 \times 10^{-5}, \tag{7.14}$$

which can be viewed as a lower limit to the primordial abundance. However, some recent results from QSO absorption systems seem to indicate a primordial value much higher than this [19]

$$\mathrm{D/H} \simeq 1.9 - 2.5 \times 10^{-4}. \tag{7.15}$$

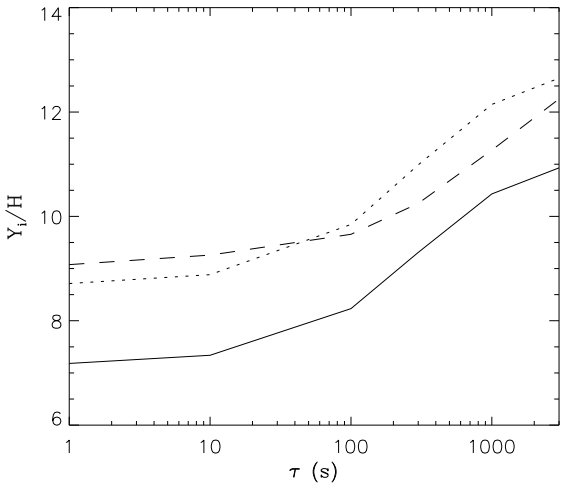

Figure 7.4: The abundance of D, ^{3}He and ^{7}Li as a function of tau neutrino lifetime. The curves have been calculated for $m = 0.5$ MeV and $\eta = 3 \times 10^{-10}$. The full line shows (D/H)/10^{-5} the dashed shows ((D+^{3}He)/H)/10^{-5} and the dot-dashed shows (^{7}Li/H)/10^{-11}.

Other similar observations yield much lower values, closer to the local one [22]. In light of the controversy of using deuterium results from these measurements, we use the locally obtainable lower limit in the present paper. From evolution arguments one can also obtain an upper limit to the primordial D+^{3}He abundance of [70]

$$(\mathrm{D} + {}^3\mathrm{He})/\mathrm{H} \leq 1.1 \times 10^{-4}. \tag{7.16}$$

Finally for the abundance of ^{7}Li we use a bound of

$${}^7\mathrm{Li/H} = 1.4 \pm 0.3^{+1.8}_{-0.4} \times 10^{-10} \tag{7.17}$$

obtained by Copi, Schramm and Turner [49].

Altogether these are the observational values which the theoretical predictions should be able to reproduce. In the standard model the theoretical predictions are only marginally consistent with observations because helium is overproduced compared to the other light nuclei. In our scenario this problem is resolved by having the tau neutrino decay during nucleosynthesis into an electron neutrino final state.

In Fig. 7.5 we show the allowed region of lifetime versus mass for the tau neutrino using the above constraints. In all the mass interval from 0.1-1 MeV it is possible to obtain a fit to the observed abundances. Note however, that

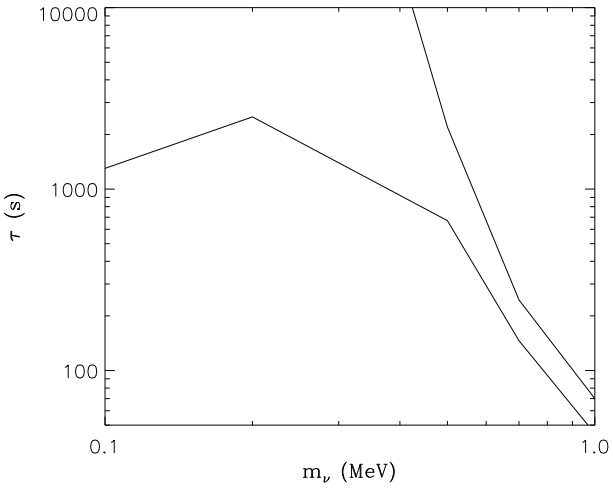

Figure 7.5: Allowed region of tau neutrino mass and lifetime. The allowed region is between the two full lines.

for masses in the high end of this region a fit can only be obtained in a very narrow lifetime interval. This is because of the very steep dependence of Y_P on the lifetime in this region. For lower masses a good fit can be obtained in a broad region of lifetimes.

Another important fact is that since the helium abundance is lowered without disturbing greatly the other abundances, the upper and lower bound on the baryon-to-photon ratio, η, is now given essentially only by the limits coming from D, ^{3}He and ^{7}Li. This also means that a relatively high value for η can be accommodated, about 6×10^{-10}, coming from requiring that ^{7}Li should not be overproduced.

In Fig. 7.6 we show the allowed region of η_{10} as a function of tau neutrino lifetime for three different masses. We have also plotted the upper and lower limits to η_{10} from the standard calculation.

7.4 Conclusion

We have studied the decay of a relatively low mass tau neutrino into an electron neutrino and a scalar or pseudoscalar particle using the full Boltzmann equation. It was found that the primordial helium abundance, Y_P, can change drastically compared to the standard value. This is in concordance with the findings of previous authors who used a non-relativistic treatment [40, 64]. Our actual

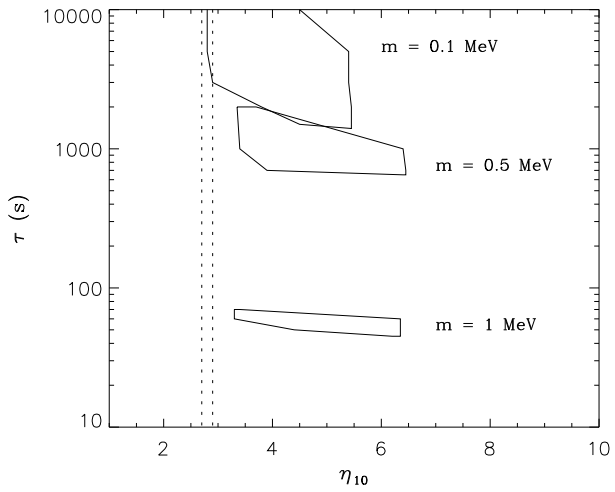

Figure 7.6: Allowed regions of $\eta_{10} \equiv 10^{10} \times \eta$ for different tau neutrino masses and lifetimes. The regions inside the full lines are allowed regions. The vertical dotted lines show the consistency interval for η_{10} in the standard model for our chosen observational constraints.

numerical values differ significantly from those previously obtained by use of non-relativistic formalism, but the general trend is the same, namely that low mass neutrinos decaying while relativistic or semi-relativistic lower the helium abundance.

The decay we have studied differs completely from the $\nu_\tau \rightarrow \nu_\mu \phi$ decay studied by Kawasaki *et al.* [59, 68] because the electron neutrinos directly affect the weak reaction rates that interconvert neutrons and protons. Only if much more reliable estimates of the primordial abundances are developed will it be possible to discern between the two different decay modes.

Our aim has mainly been to discuss the differences between using the full Boltzmann formalism and using the non-relativistic approximation in doing these calculations. We have not done very detailed statistical analysis in order to obtain strict nucleosynthesis limits.

However, it was shown that a good fit to the observed primordial abundances can be achieved for a large range of different masses and lifetimes. Given the possibly large unknown systematical errors in the observations and chemical evolution models it is perhaps too early to talk of a real crisis for Big Bang nucleosynthesis. However, once the observational bounds become more strict there might very well turn out to be such a crisis.

In light of this possible discrepancy between observed and predicted abun-

dances we still feel that it is important to explore possible ways to change the light element abundances via plausible introduction of new physics. The tau neutrino decay into an electron neutrino final state is just such a possibility.

Perhaps one should also finally note that even if the helium abundance turns out to have been significantly underestimated a tau neutrino decay of the type we have discussed can still make nucleosynthesis predictions fit the observations, but for completely different values of mass and lifetime.

Chapter VIII

Neutrino Lasing

Essentially all of this chapter has appeared as the paper *A Cosmological Three Level Neutrino Laser*, Phys. Rev. D **55**, 4571 (1997).

In this chapter we wish to proceed further with a detailed discussion of neutrino decays in the early Universe. As discussed in detail in Chapter 4, there are several possible decay modes, for example the simple radiative decay $\nu_2 \to \nu_1 + \gamma$ or the flavour changing neutral current weak decay $\nu_2 \to \overline{\nu}_1 \nu_1 \nu_1$. Another possibility is the decay

$$H \to F + \phi, \tag{8.1}$$

where H is a heavy neutrino, F is a light neutrino and ϕ is a light scalar particle (for example the majoron). It is not essential that the boson should have spin 0, but it simplifies calculations significantly. All of these decay modes have been investigated in an early Universe context [71]. We choose to focus on the last decay type in order to investigate some very interesting non-equilibrium effects that pertain to this decay. It turns out that under the right circumstances the heavy neutrino will decay by stimulated decay into F and ϕ instead of just decaying thermally. This runaway process leads to the formation of a very low momentum component of the scalar particle, ϕ, while the rest are in an almost thermal distribution. The scenario has been described by Madsen [67] and subsequently in more detail by Kaiser, Malaney and Starkman [16, 72], the idea being that the ϕ particle could make up the dark matter in our Universe. One of the currently favoured models of structure formation is the so-called Mixed Dark Matter (MDM) model [73]. This is essentially a Cold Dark Matter (CDM) model, but with a small matter content of Hot Dark Matter (HDM) that lessen the fluctuations on small scales. The ϕ particles could fit both roles, the cold component acts as cold dark matter and the thermal component as hot dark matter.

There are, however, several problems with this scenario. First of all, the favoured mixed dark matter models consist of roughly 5% baryons, 25% HDM

and 70% CDM. If there is too much HDM, structure formation will be affected so as to produce too little clustering on small scales (if normalised to COBE data). The simple scenario of Refs. [16, 67, 72] predicts only about 35% CDM and 60% HDM, which is incompatible with the observed structure [74].

We develop further this model and in Sec. 8.1 we list the relevant equations for calculating the particle distribution functions resulting from the decay. In Sec. 8.2 we describe a new way of producing neutrino lasing that is very similar to an atomic 3-level laser. Here it is possible to achieve lasing without invoking new neutrinos and to increase the CDM fraction, which however still remains well below 70%. Sec. 8.3 contains a description of the numerical results from our investigation of this 3-level model and, finally, Sec. 8.4 contains a discussion of the possible consequences of this type of decays as well as a discussion of various astrophysical limits on them. From this discussion it will become clear that lasing decays are most likely to take place after the epoch of nucleosynthesis ($T \simeq 1 - 0.1\mathrm{MeV}$). Of course they are also required to take place before matter-radiation equality ($T \simeq 1\mathrm{eV}$) if the bosons are to act as ordinary MDM.

8.1 The Basic Scenario

As previously we use the Boltzmann equation, Eq. (2.27), to follow the evolution of the different species as the Universe expands and cools. We shall assume that the term C_{coll} can be neglected, but possible limitations to this assumption will be discussed later. For simplicity we assume that the decay is isotropic in the rest-frame (see, however, Refs. [16, 72] for a discussion of the case of anisotropic decays).

The decay terms are then given by Eqs. (2.38), (2.39) and (2.40).

$$C_{\mathrm{dec}}[f_a] = -\frac{m_a^2}{\tau m_0 E_a p_a} \int_{E_\phi^-}^{E_\phi^+} dE_\phi \Lambda(f_a, f_F, f_\phi), \tag{8.2}$$

$$C_{\mathrm{dec}}[f_F] = \frac{g_a}{g_F} \frac{m_a^2}{\tau m_0 E_F p_F} \int_{E_a^-}^{E_a^+} dE_a \Lambda(f_a, f_F, f_\phi), \tag{8.3}$$

$$C_{\mathrm{dec}}[f_\phi] = \frac{g_a}{g_\phi} \frac{m_a^2}{\tau m_0 E_\phi p_\phi} \int_{E_a^-}^{E_a^+} dE_a \Lambda(f_a, f_F, f_\phi), \tag{8.4}$$

where $\Lambda(f_a, f_F, f_\phi) = f_a(1-f_F)(1+f_\phi) - f_F f_\phi (1-f_a)$, $m_0^2 = m_a^2 - 2(m_\phi^2 + m_F^2) + (m_\phi^2 - m_F^2)^2/m_a^2$. τ is the lifetime of the heavy neutrino and g is the statistical weight of a given particle. We use $g_a = g_F = 2$ and $g_\phi = 1$, corresponding to $\phi = \overline{\phi}$ [1]. The integration limits are

$$\begin{aligned} E_a^\pm(E_i) \quad = \quad & \frac{m_0 m_a}{2m_i^2}[E_i(1 + 4(m_i/m_0)^2)^{1/2} \pm \\ & (E_i^2 - m_i^2)^{1/2}], \end{aligned} \tag{8.5}$$

[1] All calculations may be redone using $g_\phi = 2$. The changes are not very significant and tend to lessen the lasing effect described below [67, 72].

and

$$E_i^{\pm}(E_a) = \frac{m_0}{2m_a}[E_a(1+4(m_i/m_0)^2)^{1/2} \pm p_a], \tag{8.6}$$

where the index $i = F, \phi$.

For non-relativistic decays, $E_\phi \simeq m_H/2 \gg T$. This means that the resulting fraction of low momentum bosons is vanishing because they are kinematically inaccessible. However, for relativistic decays this is not the case. Here the minimum boson energy is roughly $E_\phi^- \simeq \frac{1}{2}p_H[2m_\phi^2/m_H^2 + \frac{1}{2}m_H^2/p_H^2] \ll E_H$ which can be seen from Eq. (2.42). This corresponds to bosons being emitted backwards relative to the direction of motion of the parent particle. In relativistic decays it is thus possible to access very low energy boson states. This is essential for the phenomenon described below.

Something very interesting can happen if there is initially an overabundance of H over F. To see this, let us look at the structure of the decay term for the boson Eq. (2.40). Following Ref. [72] we make the following rough approximation, $1 + f_\phi \simeq f_\phi$. The decay term then reduces to

$$C_{\rm dec}[f_\phi] = \frac{2m_H^2}{\tau m_0 E_\phi p_\phi} f_\phi \int_{E_H^-}^{E_H^+} dE_H[f_H - f_F]. \tag{8.7}$$

If $f_H > f_F$ this indicates an exponential growth of f_ϕ. This effect has been called neutrino lasing because it is very similar to normal lasing, the overabundance of H over F corresponding to a population inversion. Exactly as in a laser, the process saturates when $f_H = f_F$. The remaining neutrinos will then decay to an almost thermal ϕ distribution as they go non-relativistic [2].

Note that in all our actual calculations we use a zero initial abundance of bosons before the decay commences. This is not essential for the lasing phenomenon, but the final fraction of cold bosons is decreased if there is an initial thermal population (In Ref. [72] it was assumed that the bosons decoupled prior to the QCD phase transition so that their number density was depleted by a factor of 8 relative to the other species).

The effect will be larger for low momentum states because of the $(E_\phi p_\phi)^{-1}$ term. This means that if the low momentum states are accessible, the bosons will cluster in these states and produce something similar to a Bose condensate. For this to happen it is a necessary condition that the decay is relativistic, because otherwise no low momentum states can be accessed.

This phenomenon was first investigated in Refs. [16, 67, 72]. However, Ref. [67] used a somewhat different approach, namely equilibrium thermodynamics, where the decays can lead to the formation of a true Bose condensate. In the above scenario, following Refs. [16, 72], no assumption of equilibrium has to be made.

[2] Note that as mentioned we have only considered isotropic decays, but as mentioned in Ref. [72] even if the decay is fully polarised and the bosons are emitted backwards, there will only be a rather small increase in the number of low momentum bosons. If the bosons are preferentially emitted in the forward direction there will be no lasing. Refs. [16, 72] have good discussions of these polarisation effects.

8.2 The 3-Level Laser

It was assumed in Refs. [16, 72] that F is a hitherto unknown neutrino that decouples prior to the QCD phase transition (for example a right handed component of one of the known neutrinos). This is the only way of achieving lasing in the above 2-level decay. However, it is actually possible to obtain lasing with only the three known neutrinos. The effect is somewhat similar to an atomic 3-level laser, where particles are pumped from the ground state to the top level. From there they decay rapidly to the lasing state and from the lasing state they decay by stimulated decay to the ground state. Exactly the same situation can occur for neutrinos if we have a three generation mass hierarchy, $m_{\nu_e} < m_{\nu_\mu} < m_{\nu_\tau}$ (the stable particles ν_e and ϕ are of course required to have masses below the cosmological limit for stable particles, $m < 30$eV, and can therefore be considered essentially massless in the calculations). Let us assume that we have the same generic decay mode as before. The possible majoron emitting decays are then [3]

$$\nu_\tau \to \nu_\mu + \phi \tag{8.8}$$

$$\nu_\tau \to \nu_e + \phi \tag{8.9}$$

$$\nu_\mu \to \nu_e + \phi. \tag{8.10}$$

We shall assume that the second decay mode, Eq. (8.9), is suppressed so that it is negligible relative to the first, Eq. (8.8). This assumption is not ruled out by the physical models described later.

If the decays are non-relativistic, nothing exciting happens and the decays are thermal. However, if all the decays are relativistic and the free decay of ν_τ proceeds much faster than that of ν_μ, then we can achieve lasing. The τ neutrino now functions as the top level in a normal laser, it feeds particles to the lasing state, ν_μ. Particles in this state then decay to the ground state, ν_e, by stimulated decay. The condition for the lasing process to work is that $f_{\nu_\mu} > f_{\nu_e}$, but because of the fast decay of the τ neutrino this is automatically fulfilled for a large temperature range between m_{ν_τ} and m_{ν_μ}.

Let us for the moment assume that the ν_τ decays completely before ν_μ begins to decay. It is then easy to see why the amount of lasing increases if ν_τ has decayed relativistically. We now start with a non-thermal distribution of muon neutrinos. If ν_τ decays while still relativistic, the distribution of ν_μ will be significantly colder than thermal. If we again look at the structure of Eq. (8.7), we see that for n_H given, the integral increases if the distribution of H gets colder because of the p^2 factor in the number density integral. This means that the relativistic decay to muon neutrinos enhances the lasing from ν_μ to ν_e. The effect is opposite if the ν_τ decay is non-relativistic, and the lasing diminishes or disappears completely. Fig. 8.1 shows the momentum distribution of the light neutrino after complete decay of the heavy neutrino. We see exactly that the

[3] We choose to focus alone on the majoron decays. In principle there might be other relevant decay modes as mentioned previously.

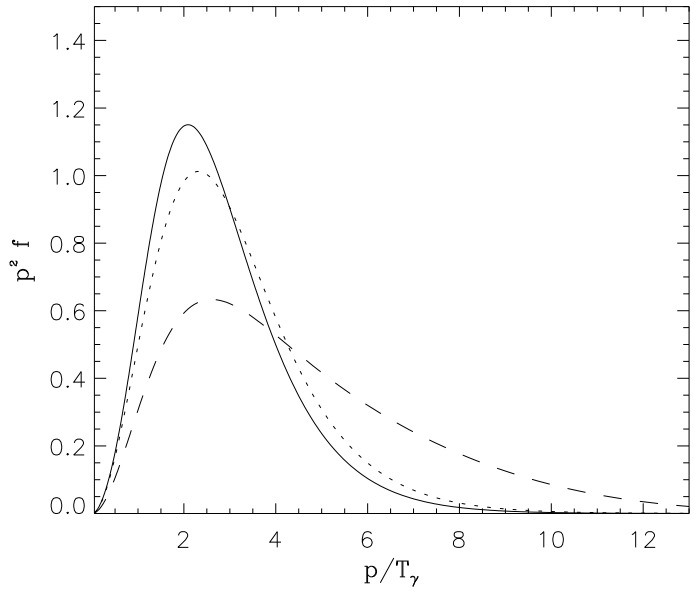

Figure 8.1: The distribution function of the light neutrino, F, after complete decay of the heavy neutrino, H, for different lifetimes of the heavy neutrino using specifically $m_H = 2$MeV, $m_F = 0.2$MeV and $m_\phi = 0.005$MeV. The full curve is for $\tau_H = 0.2$s, the dotted for $\tau_H = 1$s and the dashed for $\tau_H = 20$s.

light neutrino distribution gets colder if the decay is relativistic and hotter if it is non-relativistic. Of course, it is always a necessary condition for lasing to occur that ν_μ decays relativistically because otherwise it cannot populate low momentum boson states at all.

8.3 Numerical Results

We have investigated numerically the behaviour of this 3-level decay for different parameters by solving explicitly the coupled Boltzmann equations. Our numerical routine uses a grid in comoving momentum space and evolves forward in time using a Runge-Kutta integrator. The time evolution of the scale factor, R, and the photon temperature, T_γ, are found by use of the energy conservation equation $d(\rho R^3)/dt + pd(R^3)/dt = 0$ and the Friedmann equation $H^2 = 8\pi G\rho/3$.

In Fig. 8.2 we show an example of the number density evolution of the different involved particles. It is seen that in a large temperature interval, the ν_μ number density is slightly higher than that of ν_e. This leads to a very fast

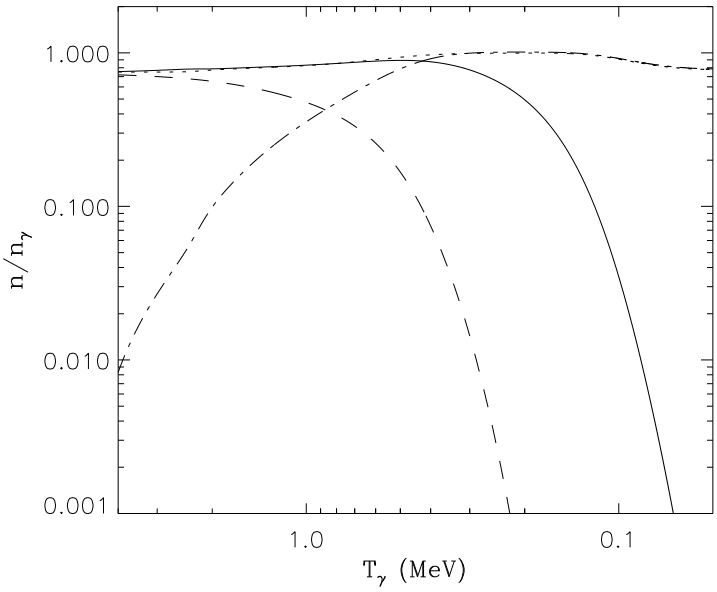

Figure 8.2: The evolution of number density for the different involved particles. The full curve is ν_μ, the dotted ν_e, the dashed ν_τ and the dot-dashed ϕ. The parameters used are $m_{\nu_\tau} = 2\text{MeV}$, $m_{\nu_\mu} = 0.5\text{MeV}$, $m_\phi = m_{\nu_e} = 0.005\text{MeV}$ and $\tau_{\nu_\tau} = 0.2\text{s}$, $\tau_{\nu_\mu} = 1.0\text{s}$.

growth of the boson number density and is identified with the region where lasing takes place. The final number density of ϕ and ν_e are the same because of neutrino number conservation (neglecting a possible small initial abundance of ϕ) because even though the ν_e abundance starts out higher, three ϕ's are produced for every two ν_e.

Since both ν_e and ϕ are almost massless there are essentially four free parameters in our equations. The first is the mass scale, defined for example by the τ neutrino mass. This mass scale is unimportant for the shape of the spectra (this is only true if the decays take place below the weak decoupling temperature $T_{\text{dec}} \simeq 2.3\text{MeV}$. If the free decay temperature is larger than T_{dec} the ϕ distribution will quickly thermalise. Only well below T_{dec} can the non-equilibrium lasing proceed, but now with an initial thermal ϕ distribution. In our numerical work we choose that the free decay temperature to be lower than the decoupling temperature). In Fig. 8.3 we show an example of changing the normalisation (m_{ν_τ}) by a factor of two. This leads to an almost identical final

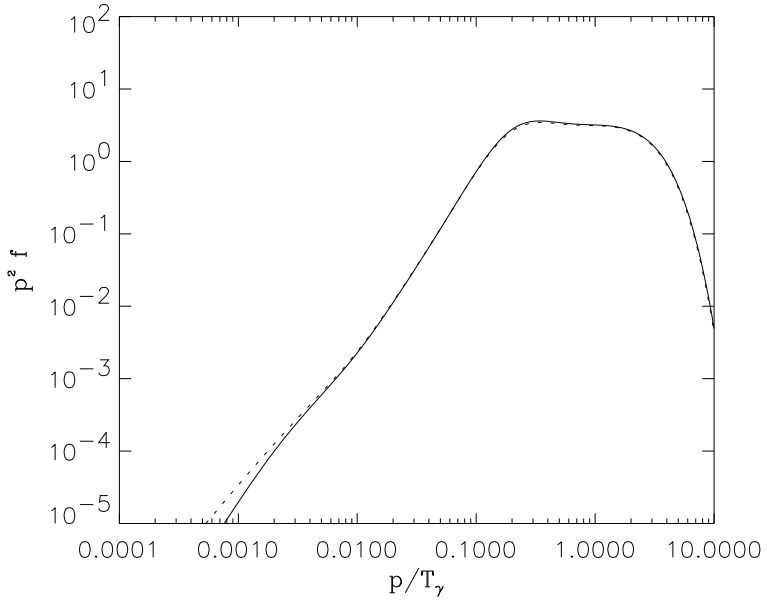

Figure 8.3: Final boson distribution for two different decay models. The full curve is for the parameters $m_{\nu_\tau} = 2\text{MeV}$, $m_{\nu_\mu} = 0.5\text{MeV}$, $m_\phi = m_{\nu_e} = 0.005\text{MeV}$ and $\tau_{\nu_\tau} = 1.125\text{s}$, $\tau_{\nu_\mu} = 18\text{s}$. The dashed curve is for $m_{\nu_\tau} = 1\text{MeV}$, $m_{\nu_\mu} = 0.25\text{MeV}$, $m_\phi = m_{\nu_e} = 0.0025\text{MeV}$ and $\tau_{\nu_\tau} = 4.5\text{s}$, $\tau_{\nu_\mu} = 72\text{s}$. Note that although we have chosen values for m_{ν_e} and ϕ which is orders of magnitude larger than the experimental/cosmological limit, this does not influence the results as long as the values are small compared to all other relevant masses and temperatures.

boson distribution. The other three parameters are

$$\alpha_{\nu_\tau} \equiv \left(\frac{m_{\nu_\tau}}{3\text{MeV}}\right)^2 \left(\frac{\tau_{\nu_\tau}}{1\text{s}}\right) \tag{8.11}$$

$$\alpha_{\nu_\mu} \equiv \left(\frac{m_{\nu_\mu}}{3\text{MeV}}\right)^2 \left(\frac{\tau_{\nu_\mu}}{1\text{s}}\right) \tag{8.12}$$

$$\beta \equiv \frac{m_{\nu_\mu}}{m_{\nu_\tau}}. \tag{8.13}$$

The first two parameters describe how relativistic the free decays of the particles are. A thermal particle shifts from relativistic to non-relativistic at a

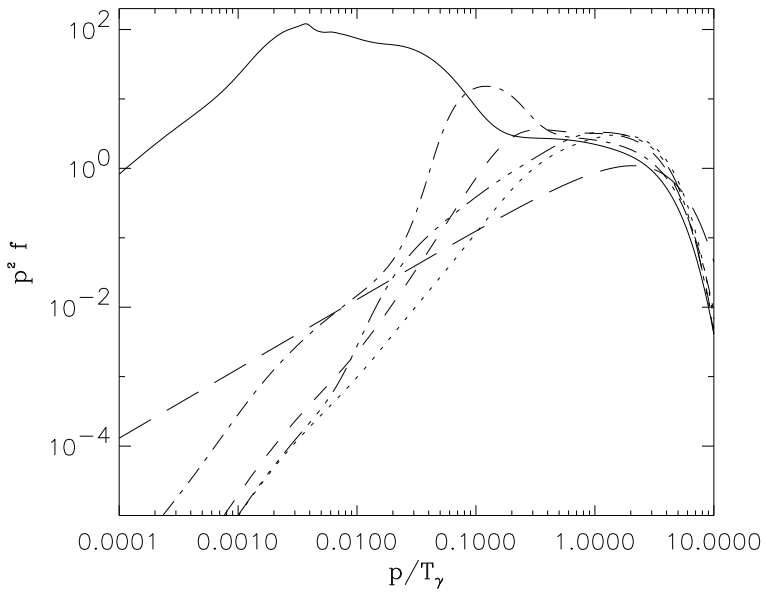

Figure 8.4: The momentum spectrum of ϕ after complete decay for different decay parameters. The full curve is $\alpha_{\nu_\tau} = 0.09$, $\alpha_{\nu_\mu} = 0.01$ and $\beta = 0.15$. The dotted is for $\alpha_{\nu_\tau} = 1$, $\alpha_{\nu_\mu} = 1$ and $\beta = 0.25$. The dashed is for $\alpha_{\nu_\tau} = 0.5$, $\alpha_{\nu_\mu} = 0.5$ and $\beta = 0.25$. The dot-dashed is for $\alpha_{\nu_\tau} = 1$, $\alpha_{\nu_\mu} = 0.03$ and $\beta = 0.25$. The dot-dot-dot-dashed is for $\alpha_{\nu_\tau} = 0.09$, $\alpha_{\nu_\mu} = 1$ and $\beta = 0.25$. The long-dashed is a thermal Bose distribution with the same number density.

temperature of roughly $T \simeq m/3$. When the Universe is radiation dominated

$$\frac{t}{1\mathrm{s}} \simeq \left(\frac{T}{1\mathrm{MeV}}\right)^{-2}. \tag{8.14}$$

Therefore if the decay is relativistic

$$\tau < t(T = m/3) \simeq \left(\frac{m}{3\mathrm{MeV}}\right)^{-2} \mathrm{s}. \tag{8.15}$$

Thus, if $\alpha_i < 1$ the decay is relativistic, whereas if $\alpha_i > 1$ it is non-relativistic. The third parameter is just the dimensionless ν_μ mass.

Fig. 8.4 shows the final boson distribution after complete decay for several different choices of decay parameters (for comparison we have also shown a thermal Bose distribution with the same number density). It is seen that in order to get a large fraction of cold particles, we need to have $\alpha_{\nu_\tau} \ll 1$ and

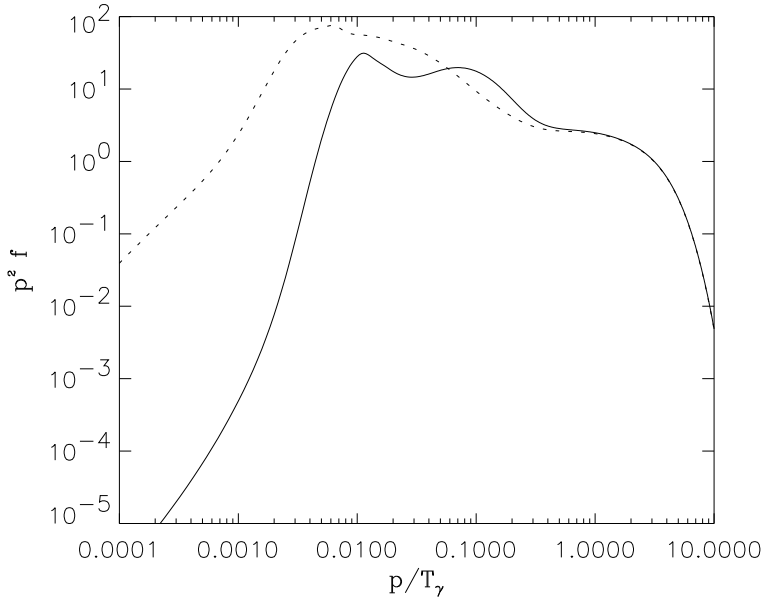

Figure 8.5: Final momentum distribution of ϕ. The full curve is for $\alpha_{\nu_\tau} = 0.09$, $\alpha_{\nu_\mu} = 0.03$ and $\beta = 0.25$. The dotted curve is for $\alpha_{\nu_\tau} = 0.09$, $\alpha_{\nu_\mu} = 0.03$ and $\beta = 0.15$.

$\alpha_{\nu_\mu} \ll 1$. The reason for this was described in the previous section. Fig. 8.5 shows the effect of changing the relative mass of the two heavy neutrinos. We see here that to get a large cold fraction we also need to have $m_{\nu_\mu}/m_{\nu_\tau} \ll 1$. This is also understandable if we look at the allowed momentum range of the produced bosons from Eq. (2.42)

$$\frac{p_\phi^-}{T_\gamma} = \frac{1}{2}(1-\beta^2)\left[\sqrt{\frac{p_{\nu_\tau}^2}{T_\gamma^2} + \frac{m_{\nu_\tau}^2}{T_\gamma^2}} - \frac{p_{\nu_\tau}}{T_\gamma}\right]. \tag{8.16}$$

If β is close to one we can get very cold bosons. This means that the bosons will tend to cluster in low momentum states, but because of energy conservation we get a very hot ν_μ distribution. On the other hand, if $\beta \to 0$, then the lowest boson states are unaccessible and we get instead a colder ν_μ distribution. This in turn leads to more lasing in the lasing state and even though the fraction of cold bosons coming from the initial ν_τ decay gets smaller, this is more than compensated for by the larger fraction coming from the ν_μ decay. This is indeed why the cold fraction increases when β decreases.

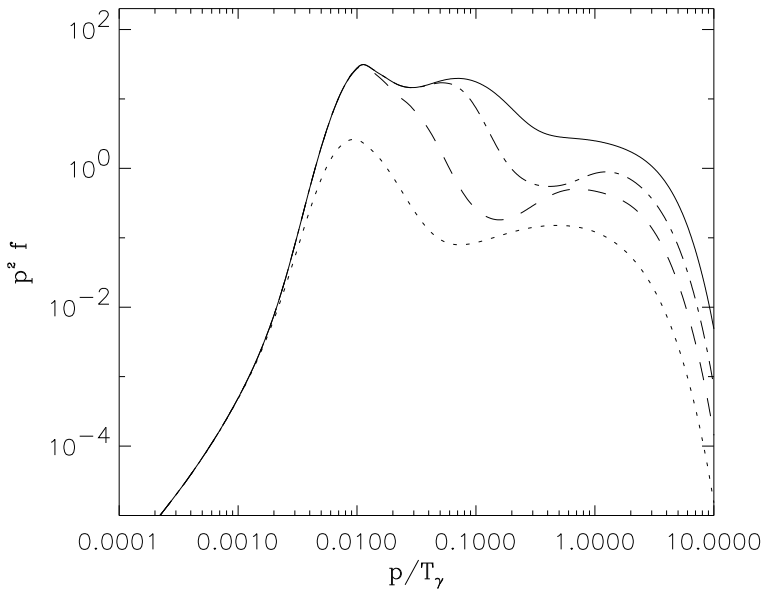

Figure 8.6: The temperature evolution of the ϕ-distribution. The decay parameters are $\alpha_{\nu_\tau} = 0.09$, $\alpha_{\nu_\mu} = 0.03$ and $\beta = 0.25$. The dotted curve is at $T_\gamma = 2.3$MeV, the dashed at $T_\gamma = 1.1$MeV and the dot-dashed at $T_\gamma = 0.5$MeV. The full curve is the final distribution after complete decay.

Thus, if we want to study the region of parameter space with possible interest for structure formation scenarios we have essentially limited ourselves to the region of ultrarelativistic decays with a large mass difference between the two heavy neutrinos. It is also interesting to follow the evolution of the boson distributions with temperature to see how the different states populate. Fig. 8.6 shows the temperature evolution of the boson distribution for the decay parameters $\alpha_{\nu_\tau} = 0.09$, $\alpha_{\nu_\mu} = 0.03$ and $\beta = 0.25$.

The minimum possible boson energy at a given temperature is given by Eq. (8.16), where instead of ν_τ we use ν_μ and for β we use 0. An approximate lower limit can be calculated by setting $p_{\nu_\mu}/T_\gamma = 3$, corresponding roughly to the mean value from a normal thermal distribution. This lower limit is an increasing function with decreasing temperature and indicates roughly the momentum where the distribution "decouples" (decoupling here means that the states are kinematically inaccessible) at a given temperature. For the model shown in Fig. 8.6 we get $p_\phi^-/T_\gamma = 0.0039, 0.017, 0.081$ for photon temperatures of 2.3, 1.1 and 0.5 MeV. We see that the lower limit at a given temperature

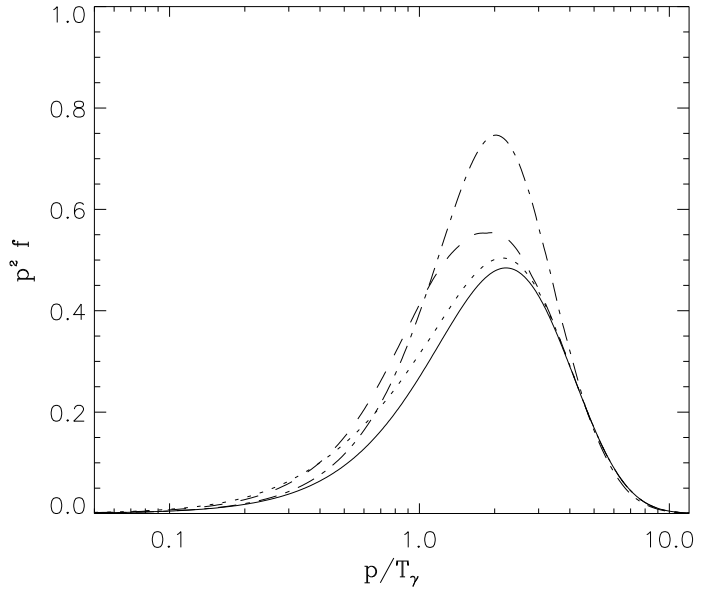

Figure 8.7: The temperature evolution of the ν_μ distribution. The decay parameters are as in Fig. 8.6. The full curve is the initial thermal ν_μ distribution. The dotted curve is at $T_\gamma = 2.3$MeV, the dashed at $T_\gamma = 1.1$MeV and the dot-dashed curve is at $T_\gamma = 0.5$MeV.

corresponds roughly to the momentum where the distribution decouples. Of course the lower limit will always be somewhat higher than the actual decoupling point, but it helps to understand the evolution of the spectra. Fig. 8.7 shows the corresponding evolution of ν_μ. We see the before mentioned effect of ν_τ decay producing a cold ν_μ distribution and thereby enhancing lasing.

However, even in the case where the decays are ultrarelativistic and the mass ratio small, the fraction of cold bosons is only moderate. For example in the case where $\alpha_{\nu_\tau} = 0.09$, $\alpha_{\nu_\mu} = 0.01$ and $m_{\nu_\mu}/m_{\nu_\tau} = 0.15$, the fraction of bosons with $p_H/T_\gamma < 0.3$ is only 44%. If the boson was to act as the dark matter in our Universe, a much larger fraction would be needed. Note, however, that even if the obtainable cold fraction is too small, it is comparable with or larger than that obtained in the model of Refs. [16, 67, 72]. Furthermore, it is achieved without invoking an unknown neutrino state.

8.4 Discussion

We have developed further the scenario originally proposed in Refs. [16, 67, 72] by introducing a physically different way of obtaining neutrino lasing. However, this model still suffers from one of the same shortcomings that the original model did, namely that it is impossible to achieve sufficiently large fractions of cold bosons for structure formation.

An interesting consequence of the 3-level decay is that the number density of electron neutrinos is increased by a factor of almost three relative to the standard case. If the decay takes place before or during Big Bang Nucleosynthesis (BBN), then it can significantly change the outcome because the electron neutrinos are very important for the neutron to proton conversion reactions. The higher than usual number of electron neutrinos will tend to keep equilibrium longer than in the standard case, meaning that less neutrons survive to form helium. The helium abundance will then be lower than in the standard case. Furthermore, the ratio of low energy electron neutrinos is significantly higher than normal. This favours the neutron to proton reaction because of the mass difference between the neutron and the proton and leads to the opposite effect of the one described by Gyuk and Turner [75], where a massive τ neutrino decays to electron neutrinos, thereby enhancing the neutron fraction and allowing a very high baryon density without violating the BBN constraints. However, in their scenario, the decaying neutrino is non-relativistic and the resulting electron neutrinos therefore have very high energy (the opposite of our case).

Decays producing lasing effects are, however, not likely to take place during BBN. The reason is that neutrinos are kept in equilibrium by the weak reaction until roughly $T \simeq 2$MeV. All neutrino distributions are then of equilibrium form and no lasing will take place. If the mass of any of the heavy neutrinos is of the same order or larger than this temperature, we will essentially have a non-relativistic decay after decoupling, but this will not produce lasing. Thus, the heaviest neutrino in our scenario must be substantially lighter than 2 MeV, thus making it improbable that it should decay during BBN. In general neutrino decays affecting BBN may well take place, but then they will not produce lasing effects. Therefore we have not treated this case in the present paper.

If we turn to more specific physical models, the most natural candidate for the light scalar particle, ϕ, is the majoron. There exist several majoron models, all of them designed to explain the very small neutrino masses compared to the other fermions. In the simplest models, the decay $\nu_2 \to \nu_1 + \phi$ is forbidden at tree level [77], making the lifetime too long to be of interest. However, there are more complicated models where the lifetime can be short. In the simplest case the majoron couples to the neutrino via a Yukawa interaction

$$\mathcal{L} = i\frac{g}{2} J \overline{\nu^c}_1 \gamma_5 \nu_2 + \text{h.c.} \tag{8.17}$$

From this generic interaction several limits to the coupling strength, g, and therefore to the lifetime can be derived. For example neutrinoless double β

decays give an upper limit on g of roughly 10^{-4} [76]. Other limits can be derived from the neutrino signal of SN1987A [11], but as mentioned in Ref. [11], it is very difficult to get a clear picture of the current limits. A coupling constant of 10^{-4} gives a restframe decay lifetime of [77]

$$\tau = \frac{32\pi}{g^2 m_2} > 10^{-5}\mathrm{s} \times \left(\frac{m_2}{1\mathrm{eV}}\right)^{-1}. \tag{8.18}$$

This limit is rather weak and leaves open a large region of parameter space for relativistic decays in the early Universe. Note that for our model to work the decay $\nu_\tau \to \nu_e$ must be suppressed. This corresponds to the coupling $g_{\tau e}$ being very small compared to the other coupling constants.

Finally, we have assumed that the scattering and annihilation reactions between neutrinos and majorons are weak compared with the decay reaction. If, as we have assumed, the decay is not forbidden at tree level this is the case because the scattering and annihilations all are of order g^4, whereas the decays are of order g^2. Were the annihilation and scattering reactions to be important we would not obtain any cold bosons because the low momentum states would not be decoupled. Therefore, it is absolutely necessary that the decays are stronger than the scattering and annihilation reactions. Note, that even if the decay is of order g^2 and the scattering and annihilation g^4 the decay rate will be damped by a factor $\gamma^{-1} = m/E$ which can be very large if the decay is extremely relativistic. Thus, in the limit of $\gamma \to \infty$ we have to account for scatterings and annihilations, but γ would have to be extremely large because of the very small value of g.

As far as the neutrino masses are concerned, they are naturally explained by see-saw models. Then only the left handed components participate in the interactions because of the very large mass of the right handed components. The possible Majoron decays are then exactly

$$\nu_i(L) \quad \to \quad \nu_j(L) + \phi \tag{8.19}$$

$$\nu_i(L) \quad \to \quad \overline{\nu}_j(R) + \phi \tag{8.20}$$

as required in our lasing model.

In conclusion, what we have shown is that it is possible to generate large non-equilibrium effects, even starting from identical neutrino distributions. Very few "fine-tunings" are necessary in order to achieve lasing. Thus, these effects may be present many places in early Universe physics, both because the decay types are generic and because the early Universe is an inherently non-equilibrium environment. This was also noted in Ref. [16], but our specific model shows that the relevant range of models is much larger than originally thought. It is therefore of considerable interest to search for other physical scenarios where the lasing process (and other similar non-equilibrium processes) may be effective.

Chapter IX

Conclusions

In the present work we have discussed in detail the effects of neutrinos on primordial nucleosynthesis. Neutrinos are important in several ways for the way in which nucleosynthesis proceeds. First of all they contribute to the cosmic energy density which in turn controls the expansion rate of the Universe. Furthermore the electron neutrinos directly enter the weak conversion rates between neutrons and protons. Since neutrinos influence nucleosynthesis in such a strong way, primordial nucleosynthesis can be used as an effective probe of neutrino physics.

Starting out with physics entirely within the standard model we have performed a detailed calculation of the effect of neutrinos on nucleosynthesis. This calculation was described in Chapter 5. The point is that, contrary to the usual assumption, neutrinos have not decoupled completely from the cosmic plasma when the electrons and positrons annihilate. Therefore they share to some degree the entropy transfer that takes place from the $e^{\pm}$ plasma to the other species. This heats up the neutrino distribution relative to a totally decoupled species and influences nucleosynthesis. The change is minute but nevertheless important if one wants to build a very accurate nucleosynthesis code. This type of calculation has been performed before, but our approach differs by the fact that we use the full set of Boltzmann equations without any approximations. We have found a somewhat smaller neutrino heating effect than the previous state-of-the-art calculation done by Dodelson and Turner [41]. Since our calculation was performed, new results have appeared by Dolgov, Hansen and Semikoz [51] that confirm our results. They have used the same approach as us, but with higher numerical precision.

Going beyond the standard model we have looked at neutrinos that are massive but with lifetime much longer than the timescale for nucleosynthesis. This was done in Chapter 6. Nucleosynthesis limits on massive neutrinos turn out to be complementary to limits obtainable in laboratories and used together they exclude a neutrino mass above $\simeq 0.2$ MeV if the neutrino lifetime is longer than $\simeq 10^3$ s. Again our approach differs from earlier calculations in that we use the full Boltzmann equations. It does turns out, however, that our results

do not differ widely from those obtained by Fields, Kainulainen and Olive [12] who used the integrated Boltzmann equation, but included the correct Fermi statistics for all neutrino species.

Since any neutrino with mass above the cosmologically safe limit of roughly 100 eV must be unstable with lifetime shorter than the Hubble time, it is natural to discuss the possibility of neutrinos decaying during nucleosynthesis. Neutrino decays can be split into a few generic types. Especially there is a difference between the case where decay products interact electromagnetically and the case where they are "invisible". There exist very strong limits on the first type of decay, making it extremely unlikely that these decays should play any role during BBN. However, this is not the case for the second type of decay. Such decays have been discussed in detail, most recently by Dodelson, Gyuk and Turner [40]. However, their approach is to use the integrated Boltzmann equation in a non-relativistic approximation. For neutrinos decaying sufficiently late, when they have already become non-relativistic, this is a very good approximation. For relativistic or semi-relativistic decays this not the case. Here one needs to study the full Boltzmann equation since there can be significant deviations from kinetic and chemical equilibrium. This has been done previously for the very simple decay $\nu_\tau \to \nu_\mu \phi$ by Kawasaki *et al.* [59, 68]. In Chapter 7 we presented the calculation for the case of of $\nu_\tau \to \nu_e \phi$, which is much more complicated because the decay product electron neutrinos enter into the conversion process between neutrons and protons, as previously mentioned. In our calculation we have found significant quantitative differences between our calculation and those performed with the non-relativistic approximation. We have also discussed the possibility that a low mass tau neutrino decaying with short lifetime to an electron neutrino final state can bring nucleosynthesis predictions into better agreement with observations.

Lastly we have looked at a neutrino process which is somewhat more exotic, namely that of neutrino lasing. The fundamental idea was originally introduced by Madsen [67] who studied a possible stimulated decay of some neutrino species into a neutrino plus scalar particle final state. If this stimulated decay proceeds in equilibrium it gives rise to the possibility of forming a Bose condensate of the decay product bosons. This could potentially be very interesting for models of structure formation in the early Universe. The reason is that both cold and hot dark matter is apparently needed to fit observations of the present day large scale structure. By having the above mentioned stimulated decay, some of the bosons are in a Bose condensate whereas the rest are in a thermal distribution. If this boson has a small mass it can act as both cold and hot dark matter, thereby explaining these mixed dark matter models with only one new particle. The problem is, however, that only a relatively small fraction of the bosons end up in the condensate, roughly 35%, whereas a fraction closer to 70% is needed to fit observational data. The scenario was calculated through in more detail using Boltzmann equation formalism by Starkman, Kaiser and Malaney [16]. They found that a true Bose condensate does not form, but that instead there will be a peak of very low momentum bosons in a "pseudo-condensate". The fraction

of particles in this low momentum peak is roughly the same as that found by Madsen for the equilibrium decay; that is, much too small to be interesting for structure formation.

We have developed a new scenario for the lasing decay using only equilibrium initial distributions. The trouble for the original scenario was that an initial population inversion is needed between the heavy and light neutrino. Otherwise the stimulated decay is never initiated and the final distribution is thermal. Originally this population inversion was invoked by having the light neutrino decouple very early (prior to the QCD phase transition) so that its abundance would be diluted by the entropy released in the subsequent phase transition. However, if there is a three neutrino mass hierarchy we have shown that it is possible to achieve lasing with just the three known neutrino species. In this scenario the heaviest neutrino acts as the pumping level in a normal three level laser, whereas the next species in the hierarchy is the actual lasing level. When the heaviest species decays while still relativistic it produces a population inversion between the first and second generation so that a lasing mechanism occurs naturally. We have presented thorough calculations of this scenario in Chapter 8. It was found that the amount of cold bosons produced is not much higher than in the original scenario so that the model is still not viable as an explanation of mixed dark matter. However, it does show that the range of models where the lasing phenomenon can occur is much larger than originally thought.

In conclusion, the present work has presented detailed calculations of some of the physical mechanisms that can take place during or close to the era of Big Bang Nucleosynthesis. It was found that neutrinos play a very important role for the evolution of our Universe, and that cosmological observations can therefore be used to probe neutrino physics in regions that terrestrial experiments cannot reach. However, there are still significant problems, for example the observational determinations of the primordial abundances are still quite uncertain. This again means that primordial nucleosynthesis is still not at a sufficient level of precision that one may start discussing constraints on fine-points in the input physics. This issue will hopefully be resolved in the coming few years as the observations of for example QSO absorption systems are improved. By determining the deuterium abundance accurately one should be able to pin down the baryon-to-photon ratio very precisely so that firm predictions can be made for the abundance of the other light elements. We should then be in a position to really start testing the physical composition of the Universe at an age of seconds using Big Bang nucleosynthesis.

Finally, a few words should perhaps be said about a possible new approach to determining the fundamental cosmological parameters, namely from the measuring of small scale anisotropies in the cosmic microwave background. This will be done within the next few years by two satellites, the American MAP and the European PLANCK (formerly known as COBRAS/SAMBA) missions.

According to expectations these should be able to perform a precision measurement of the fluctuation amplitude beyond the first Dopplerpeak, thereby

enabling an accurate determination of cosmological parameters like η, H, Ω etc. This would yield a value for η independent of nucleosynthesis arguments, so that the field of Big Bang nucleosynthesis would enter a new precision era by means of this external input.

Chapter X

Outlook

There are a number of issues which have not been addressed at all in the present work that may be very interesting for future work. The first is entirely within the standard model and deals with the precision to which one can really predict the helium abundance theoretically. During the past year or two, more and more emphasis has been put on the need to really understand the theoretical uncertainties in the nucleosynthesis calculations. This point is especially concerning when one looks at ^{4}He because this is probably the only light element where we can ever hope to measure the primordial abundance to sufficient accuracy. There are a number of uncertainties in the standard nucleosynthesis calculations that need to be addressed. This was first discussed by Dicus *et al.* [43] some 15 years ago and since then there has been an increasing number of calculations of these effects. Primarily, the error in the standard calculation comes from neglect of finite nucleon masses. The neutrino heating effect discussed in Chapter 5 is another example of a missing element. However, there are many more such fine-points, like medium effects etc. The normal calculation assumes that all processes proceed in vacuum which is of course not true. Many things are changed when physical processes occur in a dense medium, for example normally massless species like neutrinos and photons acquire an effective mass. Even though many of these effects are minute they are still interesting from a theoretical point of view and may improve our understanding of physics in the early Universe.

Another important issue is the possibility of neutrino oscillations during primordial nucleosynthesis. This is of course potentially important for massive neutrinos such as a heavy tau neutrino. Especially if electron neutrinos are involved in the oscillations, one can obtain quite large effects on nucleosynthesis.

Last, if we look at neutrino physics more generally it would also be very interesting to do studies of neutrinos in the supernova environment. This field is somewhat disjoint from neutrino physics in the early Universe; however, many of the techniques applied are similar. Also, what we can learn from studying neutrinos in supernovae is in many ways complementary to what one can learn from neutrino physics in the early Universe. For this reason this type of study is

a very interesting future prospect. In many ways the supernova environment is not nearly as well understood as the early Universe. Supernova physics couples a lot of complicated phenomena together in an almost intractable way and processes such as the transport of neutrinos in a very dense medium are not well understood from a theoretical perspective. Thus, a lot of work remains to be done in this field. For instance, presently the precise mechanism that leads to the visible supernova blast instead of complete collapse to a black hole is not understood, but is believed to be connected with the way neutrinos propagate through the medium surrounding the young neutron star.

Acknowledgements

There are a great number of people to whom thanks are due. First of all I wish to thank my thesis supervisor Jes Madsen for his guidance during the years and for making me choose this field of work by being such an inspiring lecturer.

The help and guidance of Georg Raffelt has been invaluable and he also made possible my stay at the Max Planck Institut für Physik in Munich for six months during 1997.

There are a number of people at the Institute of Physics and Astronomy whom I also wish to thank for interesting discussions and good company in general, my office mates Michael Christiansen and Georg B. Larsen as well as my other friends at the institute.

Del-B of my Ph.D. study has been financed by the Theoretical Astrophysics Center under the Danish National Research Foundation and they have also agreed to hire me after I have finished my Ph.D.

In the non-physics community I wish to thank my parents for all their support and especially my friend Jesper who has been very good at keeping me from doing physics all the time. Thanks also to all my other friends.

Appendix A

Mathematical Formalism

A.1 Dirac Matrices and Their Algebra

The Dirac matrices are defined from the Dirac equation for a free particle

$$(\gamma^\mu p_\mu - m)\psi = 0, \tag{A.1}$$

and they obey the commutation relations (Clifford algebra)

$$\{\gamma_\mu, \gamma_\nu\} = 2g_{\mu\nu}. \tag{A.2}$$

From these matrices one can define the a matrix, γ_5, as

$$\gamma_5 \equiv i\gamma_0\gamma_1\gamma_2\gamma_3, \tag{A.3}$$

where γ_5 obeys the relations

$$\gamma_5^2 = 1 \tag{A.4}$$

and

$$\{\gamma_5, \gamma_\mu\} = 0, \tag{A.5}$$

so that γ_5 is its own inverse and furthermore it anticommutes with all the other γ-matrices.

Several different representations are used for the Dirac matrices, depending on convenience in a given calculation. The standard choice is the Dirac representation where

$$\gamma_0 = \begin{bmatrix} I & 0 \\ 0 & -I \end{bmatrix} \qquad \gamma_i = \begin{bmatrix} 0 & \sigma_i \\ -\sigma_i & 0 \end{bmatrix}, \tag{A.6}$$

and

$$\gamma_5 = \begin{bmatrix} 0 & I \\ I & 0 \end{bmatrix}. \tag{A.7}$$

The matrices σ_i are the usual Pauli spin matrices defined as

$$\sigma_1 = \begin{bmatrix} 0 & 1 \\ 1 & 0 \end{bmatrix} \qquad \sigma_2 = \begin{bmatrix} 0 & -i \\ i & 0 \end{bmatrix} \qquad \sigma_3 = \begin{bmatrix} 1 & 0 \\ 0 & -1 \end{bmatrix}. \tag{A.8}$$

Other choices than the Dirac representation are possible, for example the chiral representation in which

$$\gamma_0 = \begin{bmatrix} 0 & -I \\ -I & 0 \end{bmatrix} \qquad \gamma_i = \begin{bmatrix} 0 & \sigma_i \\ -\sigma_i & 0 \end{bmatrix}. \tag{A.9}$$

In this representation γ_5 is

$$\gamma_5 = \begin{bmatrix} I & 0 \\ 0 & -I \end{bmatrix}. \tag{A.10}$$

There are many different such representations which may be chosen for convenience in a given situation.

Another quantity which is often important is the commutator between Dirac matrices

$$\sigma_{\mu\nu} = \frac{i}{2}[\gamma_\mu, \gamma_\nu], \tag{A.11}$$

which has the properties

$$\gamma_\mu\gamma_\nu = g_{\mu\nu} - i\sigma_{\mu\nu} \tag{A.12}$$

and

$$[\gamma_5, \sigma_{\mu\nu}] = 0. \tag{A.13}$$

A.2 Dirac Spinors

For free particles the solutions to the Dirac equation have the form of plane waves of positive and negative energy

$$\psi^+(x) = ue^{-ip\cdot x} \tag{A.14}$$
$$\psi_-(x) = ve^{ip\cdot x}, \tag{A.15}$$

where u and v are Dirac spinors that are themselves solutions to the Dirac equation

$$(\gamma_\mu p^\mu - m)u = 0 \tag{A.16}$$
$$(\gamma_\mu p^\mu + m)v = 0. \tag{A.17}$$

Explicitly these spinors are given by

$$u(\mathbf{p}, s) = \sqrt{E+m}\begin{bmatrix} \chi_s \\ \frac{\sigma\cdot\mathbf{p}}{E+m}\chi_s \end{bmatrix}, \tag{A.18}$$

$$v(\mathbf{p}, s) = \sqrt{E+m}\begin{bmatrix} \frac{\sigma\cdot\mathbf{p}}{E+m}\chi_s \\ \chi_s \end{bmatrix}, \tag{A.19}$$

where χ_s is a two-component spinor field. s is the helicity which can be $\pm 1/2$. Therefore the spinor χ_s can assume the values

$$\chi_+ = \begin{bmatrix} 1 \\ 0 \end{bmatrix} \qquad \chi_- = \begin{bmatrix} 0 \\ 1 \end{bmatrix} \tag{A.20}$$

This gives the normalisation

$$u_s^\dagger(\mathbf{p})u_{s'}(\mathbf{p}) = 2E\delta_{ss'} \quad (A.21)$$
$$v_s^\dagger(\mathbf{p})v_{s'}(\mathbf{p}) = 2E\delta_{ss'} \quad (A.22)$$
$$v_s^\dagger(\mathbf{p})u_{s'}(\mathbf{p}) = 0, \quad (A.23)$$

of the Dirac spinors.

A.3 Creation and Annihilation Operators

The fermion creation and annihilation operators ($f^\dagger$ and f) as well as the corresponding operators for antiparticles ($\overline{f}^\dagger$ and $\overline{f}$) are defined so as to obey the anti-commutation relations

$$\{f(\mathbf{p},s), f^\dagger(\mathbf{p}',s')\} = \delta_{ss'}\delta(\mathbf{p}-\mathbf{p}') \quad (A.24)$$
$$\{\overline{f}(\mathbf{p},s), \overline{f}^\dagger(\mathbf{p}',s')\} = \delta_{ss'}\delta(\mathbf{p}-\mathbf{p}'), \quad (A.25)$$

with all other anti-commutators being zero. The action of the creation and annihilation operators on physical states has the following effect

$$f(\mathbf{p},s)|\mathbf{p},s\rangle = |0\rangle \quad (A.26)$$
$$f^{\dagger(\mathbf{p},s)}|0\rangle = |(\mathbf{p},s)\rangle \quad (A.27)$$
$$\overline{f}(\mathbf{p},s)\overline{|\mathbf{p},s\rangle} = |0\rangle \quad (A.28)$$
$$\overline{f}^{\dagger(\mathbf{p},s)}|0\rangle = \overline{|(\mathbf{p},s)\rangle}, \quad (A.29)$$

where by $|0\rangle$ we mean the vacuum state.

Appendix B

Phase-space Integrals

This appendix shows how to reduce the integral in Eq. (2.29) from 9 to 2 dimensions. Except for the inclusion of mass terms, most of what can be found in this appendix was originally developed by Yueh & Buchler [78] for use in supernova calculations.

The collision integrals all have the form of Eq. (2.29). The innermost integral can be rewritten using the equality

$$\frac{d^3p_4}{2E_4} = d^4p_4\delta(p_4^2 - m_4^2)\Theta(p_4^0). \tag{B.1}$$

The integral over d^4p_4 is now done using the δ-function. Hereafter p_4 is fixed as

$$p_4^2 = p_1^2 + p_2^2 + p_3^2 + 2(p_1 \cdot p_2 - p_1 \cdot p_3 - p_2 \cdot p_3). \tag{B.2}$$

Now, the following angles are introduced

$$\cos\alpha = \frac{\mathbf{p_1} \cdot \mathbf{p_2}}{p_1 p_2} \tag{B.3}$$

$$\cos\theta = \frac{\mathbf{p_1} \cdot \mathbf{p_3}}{p_1 p_3} \tag{B.4}$$

$$\cos\alpha' = \frac{\mathbf{p_2} \cdot \mathbf{p_3}}{p_2 p_3} \tag{B.5}$$

$$= \cos\alpha\cos\theta + \sin\alpha\sin\theta\cos\beta.$$

Thus we obtain

$$d^3p_2 = p_2^2 dp_2 d\cos\alpha d\beta \tag{B.6}$$

$$d^3p_3 = p_3^2 dp_3 d\cos\theta d\mu. \tag{B.7}$$

The integration over $d\beta$ is carried out using the δ-function. We use that

$$p_4^2 - m_4^2 = f(\beta). \tag{B.8}$$

From the standard theory of δ-functions we use

$$\int d\beta\delta(f(\beta)) = \sum_i \int d\beta \frac{1}{\left|\frac{df(\beta)}{d\beta}\right|_{\beta=\beta_i}} \delta(\beta - \beta_i), \tag{B.9}$$

where β_i are the roots of $f(\beta) = 0$. The derivative is evaluated to

$$\frac{df(\beta)}{d\beta} = -2p_2p_3 \sin\alpha \sin\theta \sin\beta. \tag{B.10}$$

$\sin\beta_i$ is found as $\pm(1 - \cos^2\beta_i)^{1/2}$, where

$$\begin{aligned} \cos\beta_i &= \frac{2E_2E_3 - 2p_2p_3\cos\alpha\cos\theta - Q}{2p_2p_3\sin\alpha\sin\theta} \\ &\quad - \frac{(2E_1E_2 - 2p_1p_2\cos\alpha)}{2p_2p_3\sin\alpha\sin\theta} \\ &\quad + \frac{(2E_1E_3 - 2p_1p_3\cos\theta)}{2p_2p_3\sin\alpha\sin\theta}, \end{aligned} \tag{B.11}$$

and we have introduced $Q = m_1^2 + m_2^2 + m_3^2 - m_4^2$. The equation for $\sin\beta_i$ will have two solutions, one in the interval $[0, \pi]$, and one in the interval $[\pi, 2\pi]$. Since the r.h.s. of Eq. (B.9) is symmetric in β we can multiply by two and integrate over $[0, \pi]$. The limits on the integral $d\cos\alpha$ come from demanding that $\cos^2(\beta) \leq 1$. But this means that

$$(2p_2p_3 \sin\alpha \sin\theta \sin\beta)^2 \geq 0. \tag{B.12}$$

Notice, that this is the same as demanding that

$$\left(\frac{df(\beta)}{d\beta}\right)^2 \geq 0. \tag{B.13}$$

Finally we end up with

$$\int_0^{2\pi} d\beta\delta(f(\beta)) = 2\frac{1}{\left|\frac{df(\beta)}{d\beta}\right|_{\beta=\beta_i}} \Theta\left(\left|\frac{df(\beta)}{d\beta}\right|^2_{\beta=\beta_i}\right). \tag{B.14}$$

The derivative can be written as

$$\left|\frac{df(\beta)}{d\beta}\right|_{\beta=\beta_i} = \sqrt{a\cos^2\alpha + b\cos\alpha + c}, \tag{B.15}$$

where

$$a = p_2^2(-4\kappa + 8\epsilon) \tag{B.16}$$

$$b = p_2(p_1 - \epsilon/p_1)(8\gamma + 4Q + 8\epsilon) \tag{B.17}$$

$$\begin{aligned} c &= -4\gamma^2 - 4\gamma Q - Q^2 - 8\gamma\epsilon - 4Q\epsilon - 4\epsilon^2 \\ &\quad + 4p_2^2p_3^2(1 - \cos^2\theta), \end{aligned} \tag{B.18}$$

and we have introduced the following parameters in order to limit the amount of space required to write out the formulae

$$\begin{aligned} \gamma &= E_1E_2 - E_1E_3 - E_2E_3 && \text{(B.19)} \\ \epsilon &= p_1p_3\cos\theta && \text{(B.20)} \\ \kappa &= p_1^2 + p_3^2. && \text{(B.21)} \end{aligned}$$

Notice that Eqs. (B.16), (B.17) and (B.18) reduce to those of Yueh & Buchler [78] in the limit of zero masses.

Now, any one of the possible matrix elements only include products of 4-momenta. All the possible products of these momenta are calculated below:

$$\begin{aligned} p_1 \cdot p_2 &= E_1E_2 - p_1p_2\cos\alpha && \text{(B.22)} \\ p_1 \cdot p_3 &= E_1E_3 - p_1p_3\cos\theta && \text{(B.23)} \\ p_1 \cdot p_4 &= m_1^2 + (E_1E_2 - p_1p_2\cos\alpha) && \text{(B.24)} \\ &\quad -(E_1E_3 - p_1p_3\cos\theta) \\ p_2 \cdot p_3 &= (E_1E_2 - p_1p_2\cos\alpha) && \text{(B.25)} \\ &\quad -(E_1E_3 - p_1p_3\cos\theta) + Q/2 \\ p_2 \cdot p_4 &= (E_1E_3 - p_1p_3\cos\theta) + m_2^2 - Q/2 && \text{(B.26)} \\ p_3 \cdot p_4 &= (E_1E_2 - p_1p_2\cos\alpha) - m_3^2 + Q/2. && \text{(B.27)} \end{aligned}$$

Because all the above products are analytically integrable over $d\cos\alpha$, the integrals over this parameter can now be carried out by use of the fundamental relation

$$\int_{-\infty}^{\infty} \frac{dx}{\sqrt{ax^2+bx+c}}\Theta(ax^2+bx+c) = \frac{\pi}{\sqrt{-a}}\Theta(b^2-4ac) \qquad \text{(B.28)}$$

The step function comes from demanding that there be a real integration interval. This actually also insures that the roots of ax^2+bx+c are not outside the fundamental integration interval of $[-1,1]$, because the step function singles out the physical situations, where $d\cos\alpha$ can not be outside this interval. Integrating over $d\mu$ is no problem, as there is no dependency on this parameter. The final integration that can be done is the one over $d\cos\theta$. Any one of the possible products of momenta is analytically integrable over $d\cos\theta$. The solution of $b^2-4ac=0$ gives the integration interval. The solutions are

$$\begin{aligned} \cos\theta &= (-2\gamma - 2p_2^2 - Q && \text{(B.29)} \\ &\quad \pm 2p_2(2\gamma + p_1^2 + p_2^2 + p_3^2 + Q)^{\frac{1}{2}})/(2p_1p_3). \end{aligned}$$

If there is to be a real integration interval, both of these solutions must be real. The fundamental interval is of course $[-1,1]$, but the real limits are $\alpha = \sup[-1, \cos\theta_{\min}]$ and $\beta = \inf[1, \cos\theta_{\max}]$. There can only be a real integration interval if both α and β are real numbers and $\beta \geq \alpha$.

Note that there are seemingly two places where divergences occur in the collision integral. The first one is for $p_1 = p_3, \cos\theta = 1$, but in this case there is no problem because although the integrand becomes infinite it is integrably infinite [78]. The second place is for $p_1 \to 0$. To see what happens here, we have to go back to the fundamental integral, Eq. (B.28). If $p_1 \to 0$ then $a = -4p_2^2 p_3^2$, but then there can be no divergence, as p_1 no longer appears in any denominator. Clearly there is still the possibility of divergence if $m_1 \to 0$ also, because of the $1/E_1$ term. Fortunately it turns out that $b^2 - 4ac = 0$ if $m_1, p_1 = 0$, so that the rate becomes equal to 0 in this case, as it ought to be. Finally the collision integral can be written as

$$\begin{aligned} C_{\rm coll}[f] &= \frac{2}{(2\pi)^4}\frac{1}{2E_1}\int \frac{p_2^2 dp_2}{2E_2}\frac{p_3^2 dp_3}{2E_3} S \times \\ &\quad \Lambda(f_1, f_2, f_3, f_4) F(p_1, p_2, p_3)\Theta(A), \end{aligned} \tag{B.30}$$

where A is the parameter space allowed (that is, the space defined by requiring α, β real and $\beta \geq \alpha$). F is the matrix element integrated over $d\cos\alpha$ and $d\cos\theta$,

$$F(p_1, p_2, p_3) = \int \mid M \mid^2 d\cos\alpha d\cos\theta \tag{B.31}$$

Appendix C

English Resumé

The goal of the present work has been to investigate aspects of the interface between particle physics and cosmology. This field is one of the most promising in the whole area of modern physics, since in many cases the whole Universe can be used as a giant particle physics laboratory. We have focused on the particles called neutrinos and their importance in the early Universe. Neutrinos are weakly interacting spin-1/2 leptons, essentially equivalent to electrons except for the fact that they apparently do not possess either mass or electric charge. Three generations of neutrinos are known to exist, ν_e, ν_μ and ν_τ, corresponding to the charged leptons e, μ and τ. Since neutrinos interact so weakly, very little is actually known about them. They are extremely difficult to detect in the laboratory even though they are present in great abundance everywhere, being produced continuously by for example the Sun. For this reason, one must often turn to indirect means of studying neutrinos. One such possibility is to use the early Universe as a neutrino laboratory.

There is no *a priori* reason why neutrinos should be completely massless, and a large part of this thesis has been devoted to the study of massive neutrinos in cosmology. It turns out that neutrinos are intimately connected with the formation of light nuclei when the Universe was about 1 second old, the phenomenon usually referred to as Big Bang Nucleosynthesis (BBN). Studies of the outcome of BBN can therefore tell us a lot about the properties of neutrinos. Features that are completely unreachable in terrestrial laboratories.

The first four chapters of the thesis have been devoted to an introduction to the fundamental concepts needed. Chapter 1 is a general introduction, Chapter 2 contains a discussion of the evolution equations for the expansion of the Universe as well as a review of the Boltzmann equation, the fundamental transport equation relating different particle species in the early Universe. Chapter 3 reviews Big Bang Nucleosynthesis, both the theoretical and the observational aspects. In the theoretical section the influence of neutrinos and other particles on nucleosynthesis is discussed. In the observational part we look at how the different light element abundances are observed as well as discuss the problems connected with these observations. In Chapter 4 the physics of neutrinos is

discussed. We start out with the definitions of quantum neutrino fields and discuss the weak interactions of neutrinos, emphasising the similarities and differences of Dirac and Majorana neutrinos. In the final section neutrino decays are discussed, primarily the experimental constraints that exist on such decays.

In the next four chapters we proceed with a more specific discussion of neutrino physics in the early Universe. Chapter 5 contains a thorough calculation of the influence of massless standard model neutrinos on primordial nucleosynthesis. We find that the neutrinos distributions are heated slightly relative to the standard calculations because energy is transferred from electrons and positrons as these become non-relativistic and annihilate. Our calculation has been more careful than previous ones, taking into account the full quantum statistics of neutrinos. After our results appeared, new and numerically more precise results by Dolgov, Hansen and Semikoz have appeared that confirm our results.

Chapter 6 goes beyond the minimal standard model in that neutrinos are allowed to have mass. However, we still assume that they only possess standard model weak interactions and furthermore we assume their lifetime against decay to be sufficiently long not to have any effect on nucleosynthesis ($\tau \geq 10^3$s). Massive neutrinos affect primordial nucleosynthesis quite dramatically, mainly because their non-zero rest mass energy can come to dominate the cosmic energy density at temperatures below the rest mass. This again changes the cosmic expansion rate and generally leads to a strong increase in helium production. We find that tau neutrinos with mass larger than roughly 0.2 MeV are ruled out by combining our nucleosynthesis arguments with the laboratory mass limit of 24 MeV for the tau neutrino. This is consistent with previous results, but our treatment has included use of the full Boltzmann equation, following each momentum mode in time instead of the usual approach where one assumes scattering equilibrium for the involved neutrinos. Our calculations were performed for Majorana neutrinos only, but the limits can be expected to be roughly the same for Dirac neutrinos, also ruling out a massive Dirac neutrino if its rest mass is larger than roughly 0.2 MeV, still assuming a sufficiently long lifetime against decay.

In Chapter 7 we proceed to look at the possibility of neutrino decays during nucleosynthesis. This phenomenon has been discussed many times in the literature, but we look at one very interesting range in parameter space that has so far not been treated properly, namely that of a low mass tau neutrino decaying to an electron neutrino final state. For the last few years there have been some indication that the standard picture of BBN may be lacking something. The problem is that apparently too much helium is produced to be consistent with observations. A decay of the type we discuss can help solve this problem since it lowers the helium abundance from nucleosynthesis if the mass and lifetime of the decaying neutrino are both sufficiently low. Again, we have used the full set of Boltzmann equations as opposed to previous treatments. For the specific decay we look at, this is the only way to obtain sensible results because the decay does not necessarily install equilibrium in the particle distributions. We have found a large range of allowed neutrino decay lifetimes for masses in the range

0.1-1 MeV. As in the previous chapter we only looked at Majorana neutrinos because there are several additional complications for Dirac neutrinos.

Lastly, in Chapter 8 we have looked at a different aspect of neutrino physics in the early Universe. Here we study the possibility of making dark matter from neutrino decays. Dark matter is the generic term for the mass known to be present in the Universe, but not identifiable as normal baryonic matter. This matter is for example needed to produce the present day structure of the Universe, such as galaxies etc. It turns out that to be consistent with observations most of the dark matter should be in very heavy particles, called cold dark matter. However, a small fraction of light particles is needed, termed hot dark matter. Some years ago it was suggested by Madsen that this type of scenario could possibly be produced by stimulated decay of massive neutrinos to a final state containing some scalar particle. It turned out, however, that the relative fraction of cold and hot dark matter was wrong, most of the dark matter ended up in the form of hot dark matter. We have developed this scenario to a new model with more than one neutrino decay, but it still appears that too much hot dark matter is produced.

Bibliography

[1] G. F. Smoot *et al.*, Astrophys. J. Lett. **396**, L1 (1992).

[2] See for example R. Giovanelli and M. P. Haynes, in Annual Review of Astronomy and Astrophysics **29**, 499 (1991).

[3] G. Gamow, Phys. Rev. **70**, 572 (1946).

[4] Much more extensive information can be found in recent reviews such as H. Reeves, Rev. Mod. Phys. **66**, 193 (1994); R. A. Malaney and G. J. Mathews, Phys. Rep. **229**, 145 (1993); M. S. Smith, L. H. Kawano and R. A. Malaney, Astrophys. J. Suppl. **85**, 219 (1993).

[5] S. Burles and D. Tytler, Report no. astro-ph/9603070.

[6] K. A. Olive and D. Thomas, Astropart. Phys. **7**, 27 (1997).

[7] R.M. Barnett *et al.* (Particle Data Group), Phys. Rev. D **54**, 1 (1996).

[8] N. Hata *et al.*, Phys. Rev. Lett. **75**, 3977 (1995).

[9] J. Bernstein, *Kinetic Theory in the Expanding Universe*, Cambridge University Press (1988).

[10] S. Weinberg, *Gravitation and Cosmology*, John Wiley and Sons (1972).

[11] G. G. Raffelt, *Stars as Laboratories for Fundamental Physics*, University of Chicago Press (1996).

[12] B. D. Fields, K. Kainulainen, and K. A. Olive, Report no. hep-ph/9512321 (1995).

[13] R. V. Wagoner, in *Physical Cosmology* - Les Houches (1979), edited by R. Balian, J. Audouze and D. N. Schramm, Les Houches Summer School Proceedings Vol. 32, p. 395.

[14] P. Gondolo and G. Gelmini, Nucl. Phys. **B360**, 145 (1991).

[15] K. Kainulainen and A. D. Dolgov, Nucl. Phys. **B402**, 349 (1993).

[16] G. D. Starkman, N. Kaiser and R. A. Malaney, Astrophys. J. **434**, 12 (1994).

[17] K. A. Olive and G. Steigman, Astrophys. J. Suppl. **97**, 49 (1997).

[18] Y. I. Izotov, T. X. Thuan and V. A. Lipovetsky, Astrophys. J. Suppl. **108**, 1 (1997).

[19] A. Songaila *et al.*, Nature (London) **368**, 599 (1994).

[20] M. Rugers and C. J. Hogan, Astron. J. **111**, 2135 (1996).

[21] J. K. Webb *et al.*, Nature **388**, 250 (1997).

[22] D. Tytler, S. Burles and D. Kirkman, Report no. astro-ph/9612121.

[23] F. Spite and M. Spite, Astron. Astrophys. **115**, 337 (1982).

[24] P. Bonifacio and P. Molaro, Mon. Not. R. Astron. Soc. **847**, 285 (1997).

[25] see for example J. Bahcall, talk given at 18th Texas Symposium on Relativistic Astrophysics, Chicago IL, Report no. astro-ph/9702057.

[26] See for example T. K. Gaisser, Talk given at the 17th International Conference on Neutrino Physics and Astrophysics (Neutrino 96), Helsinki, Finland, Report no. hep-ph/9611301.

[27] C. Athanassopoulos *et al.*, Phys. Rev. Lett. **77**, 3082 (1996).

[28] K. Grotz and H. V. Klapdor, *The Weak Interaction in Nuclear, Particle and Astrophysics*, Adam Hilger 1990.

[29] K. Assamagan *et al.*, Phys. Rev. D **53**, 6065 (1996).

[30] D. Buskulic *et al.*, Phys. Lett. B **349**, 585 (1995).

[31] B. Kayser, F. Gibrat-Debu and F. Perrier, *The Physics of Massive Neutrinos*, World Scientific Lecture Notes in Physics - Vol. 25 (1989).

[32] D. Bailin and A. Love, *Introduction to Gauge Field Theory*, Adam Hilger 1986.

[33] R. Plaga, Report no. hep-ph/9610545 (1996); S. Hannestad, Report no. hep-ph/9701216 (1997); B. Kayser, Reoprt no. hep-ph/9703294 (1997); A. Hoefer, Report no. hep-ph/9705362 (1997); S. H. Hansen, Report no. hep-ph/9708359 (1997).

[34] see the paper by R. Plaga in Ref. [33].

[35] P. Vilain *et al.* (CHARM II collaboration), Phys. Lett. **B335**, 246 (1994).

[36] E.W. Kolb and M.S. Turner, *The Early Universe*, Addison Wesley (1990).

[37] P. J. E. Peebles, *Principles of Physical Cosmology*, Princeton University Press 1993.

[38] see for example A. L. Mellott and D. W. Sciama, Phys. Rev. Lett. **46**, 1369 (1981).

[39] see for example R. N. Mohapatra and P. B. Pal, *Massive Neutrinos in Physics and Astrophysics*, World Scientific Lecture Notes in Physics - Vol. 41 (1991).

[40] S. Dodelson, G. Gyuk and M. S. Turner, Phys. Rev. D **49**, 5068 (1994).

[41] S. Dodelson and M.S. Turner, Phys. Rev. D **46**, 3372 (1992).

[42] A. D. Dolgov and M. Fukugita, Phys. Rev. D **46**, 5378 (1992).

[43] D. A. Dicus *et al.*, Phys. Rev. D **26**, 2694 (1982).

[44] M. A. Herrera and S. Hacyan, Astrophys. J. **336**, 539 (1989).

[45] N. C. Rana and B. Mitra, Phys. Rev. D **44**, 393 (1991).

[46] S. Hannestad and J. Madsen, Phys. Rev. D **52**, 1764 (1995).

[47] L. Kawano, Report no. FERMILAB-Pub-92/04-A (1992) (unpublished).

[48] B.D. Fields, S. Dodelson, and M.S. Turner, Phys. Rev. D **47**, 4309 (1993).

[49] C. J. Copi, D. N. Schramm, and M. S. Turner, Phys. Rev. Lett. **75**, 3981 (1995).

[50] R. Cowsik and J. McClelland, Phys. Rev. Lett. **29**, 669 (1972).

[51] A. D. Dolgov, S. H. Hansen and D. V. Semikoz, Preprint no. TAC-1997-10, Report no. hep-ph/9703315.

[52] For recent reviews, see G. Gyuk and M. S. Turner, Nucl. Phys. B Proc. Suppl. **38**, 13 (1995); G. Gelmini and E. Roulet, Rep. Prog. Phys **58**, 1207 (1995).

[53] D. A. Dicus *et al.*, Phys. Rev. D **17**, 1529 (1978).

[54] E. W. Kolb and R. J. Scherrer, Phys. Rev. D **25**, 1481 (1982).

[55] R. J. Scherrer and M. J. Turner, Ap. J. **331**, 19 (1988).

[56] A. D. Dolgov, K. Kainulainen and I. Z. Rothstein, Phys. Rev. D **51**, 4129 (1995).

[57] E. W. Kolb *et al.*, Phys. Rev. Lett. **67**, 533 (1991).

[58] A. D. Dolgov and I. Z. Rothstein, Phys. Rev. Lett. **71**, 476 (1993).

[59] M. Kawasaki *et al.*, Nucl. Phys. **B419**, 105 (1994).

[60] A. D. Dolgov, S. Pastor, and J. W. F. Valle, Report no. hep-ph/9602233 (1996).

[61] S. Hannestad and J. Madsen, Phys. Rev. Lett. **76**, 2848 (1996).

[62] J. Bernstein, L. S. Brown and G. Feinberg, Phys. Rev. D **32**, 3261 (1985).

[63] In the published version of Ref. [48] the same effect will be accounted for, with very good agreement with our results (Kimmo Kainulainen, private communication).

[64] N. Terasawa and K. Sato, Phys. Lett. B **185**, 412 (1987).

[65] E. W. Kolb and R. J. Scherrer, Phys. Rev. D **25**, 1481 (1982).

[66] R. J. Scherrer and M. S. Turner, Astrophys. J. **331**, 19 (1988); R. J. Scherrer and M. S. Turner *ibid.* **331**, 31 (1988).

[67] J. Madsen, Phys. Rev. Lett. **69**, 571 (1992).

[68] M. Kawasaki, K. Kohri and K. Sato, Report no. astro-ph/9705148.

[69] S. Hannestad and J. Madsen, Phys. Rev. D **54** 7894 (1996).

[70] C. J. Copi, D. N. Schramm, and M. S. Turner, FERMILAB-Pub-94/174-A (1994).

[71] Recent treatments are M. Kawasaki, G. Steigman, and H.-S. Kang, Nucl. Phys. **B403**, 671 (1993); G. Gyuk and M. S. Turner, in *Neutrino 94*, Proceedings of the 16th International Conference on Neutrino Physics and Astrophysics, Eilat, Israel, edited by A. Dar *et al.* [Nucl. Phys. Proc. Suppl. **B 38**, 13 (1995)].

[72] N. Kaiser, R. A. Malaney, and G. D. Starkman, Phys. Rev. Lett. **71**, 1128 (1993).

[73] See for example A. Klypin, J. Holtzman, J. Primack, and E. Regös, Astrophys. J. **416**, 1 (1993).

[74] G. B. Larsen and J. Madsen, Phys. Rev. D **53**, 2895 (1996).

[75] G. Gyuk and M. S. Turner, Phys. Rev. D **50**, 6130 (1994).

[76] Z. G. Berezhiani *et al.*, Phys. Lett. **B 291**, 99 (1992).

[77] See for example C. W. Kim and A. Pevsner, *Neutrinos in Physics and Astrophysics*, Harwood Academic Publishers (1993).

[78] W. R. Yueh and J.R. Buchler, Astrophysics & Space Science, **39**, 429 (1976).